

Authors' response to the “Interactive comment on “A coastally improved global dataset of wet tropospheric corrections for satellite altimetry” by Clara Lazaro et al.”

Posted by Anonymous Referee #1

We would like to start by thanking Reviewer#1 for his/her valuable contribution, for the many useful suggestions and corrections, and for his/her constructive comments that led to the improvement of the quality of the manuscript. The main changes introduced in the manuscript following the comments and suggestions of the two Reviewers can be summarised as:

- Sections containing the Abstract and the Conclusions have been updated to accommodate the new results presented in the revised version of the manuscript.
- Some parts of the text have been moved to new sections or were rewritten/completed to be clearer and more informative.
- Figures 1 as well as figures 11, 12 and 13 have been updated, the latter to include the results for the comparison of the GPD+ WTC with the MWR-derived WTC, instead of that for the Comp WTC, following the concerns raised by Reviewer#2.
- Previous Figure 5 has been divided into Figures 7 and 8 and the geographic location of the Envisat tracks have been added, following the recommendation of Reviewer#1.
- New figures have been added to the revised version (Figures 2, 3 and 14).
- Tables 1 and 4 have been updated, the former to include more information, the latter in the sequence of the last update of the GPD+ database (performed to include more data for the recent missions).
- A new table (Table 2) has been added in the revised version.
- All figures and tables have been renumbered.
- Section 3.2 has been divided into sections 3.2.1 and 3.2.2 describing the global and the regional (coastal) results, respectively, and the text has been extended.
- Reference Vieira et al. (2019c) has been updated, since at the time of this revision it has already been published.
- Reference AVISO (2017) has been removed.
- Five new references (Bevis et al. (1994), Rudenko et al., (2017), Valladeau et al. (2015), Dinardo et al. (2020) and Escudier et al. (2017)) have been inserted in the revised version.

Our point-by-point responses to Reviewer#1 are presented below.

MAJOR COMMENTS

In this paper, the authors present a novel dataset of Wet Troposphere Correction (WTC) to correct the sea level anomaly (SLA) derived from satellite radar altimetry. The dataset is particularly important for coastal altimetry being well known that this correction is the most critical in the coastal zone. The new correction (known as GPD+)

computes the Water Path Delay (WPD) for all along-track altimeter points where the default correction (from onboard radiometer) is unusable. The method adopts an objective analysis approach to estimate WPD from a number of sources (coastal and island GNSS stations, satellites carrying microwave radiometers, valid on-board MWR measurements). The method is applied to all conventional missions and CryoSat-2. The validation of the dataset is made through statistical analysis of SLA and the metric used is the reduction of variance.

The author provide a clear description of the datasets apart details specified below in the minor comments. However, the validation of the dataset (that is the part of interest to users) is really poor in showing the improvements, in particular with reference to the coastal zone. The authors titled this paper “A coastally improved global dataset. . .”, unfortunately the reader does not see any zooming in the coastal zone.

R.: The paper’s aim was to present and describe the GPD+ WTC dataset/database. The authors’ intention was to show the improvement in the SLA description in the coastal zone when using the correction in global terms, therefore with no focus on a particular region. The authors refer two papers that show in detail the improvement in the SLA signal description in the coastal region (German Bight and the Indonesia Archipelago) when the GPD+ WTC is used. However, in response to the Reviewer’s comment, results for three coastal regions, selected on the one hand, due to the large number of available GNSS stations (North American and European coasts) and, on the other hand, due to the fact of being a challenging region for coastal satellite altimetry (Indonesia region), have been added to the revised version of the manuscript, as an attempt to show the potential of the GPD+ dataset along the coastal waters. Section 3.2.2 has been added in the manuscript to present these results.

The metric used is certainly appropriate for open ocean but not for the coastal zone. The results do not provide a clear measure of confidence of the dataset in these challenges area.

R.: The assessment of the performance of the GPD+ WTC dataset is made using statistical analyses of sea level anomaly variability. The reduction of SLA variance is a metric commonly used to assess the performance of a correction against its counterparts available in the altimetry products accessible to the user. The larger the SLA variance reduction, the better the correction, since its application will lead to an SLA whose variability is more likely to be due to oceanic conditions than to the error in the correction(s). The metric is used to assess the performance of the dataset and not to validate it. Observations adequate to validate the GPD+ WTC dataset over coastal regions are not of sufficient quantity and quality. The vertical distribution of water vapour in the troposphere can be obtained using data from a network of radiosondes. However, datasets from radiosondes possess undesirable inhomogeneities (e.g., vertical range, vertical resolution, temporal regularity, poor continuity), have poor spatial coverage, particularly over coastal zones, and are not collocated with altimeter measurements. Therefore, completeness of observations lacks in these regions.

For these reasons, the authors also performed an assessment of the GPD+ WTC performance using GNSS observations, as explained in Section 3.1 of the manuscript. Former Figure 7 (now Figure 10) illustrates the results, showing that the RMS of the differences GNSS-MWR increases when approaching the coast. On the contrary, the RMS of the differences GNSS-GPD+ decreases and this result is thought to be a clear indicator of the performance of the GPD+ correction.

All plots are global and some plots globally averaged when quantities are showed as a function of distance. Instead, the reader expects to see a selection of relevant coastal regions in the world, based e.g. on bibliography (i.e. areas where users already applied coastal altimetry) or peculiar characteristics (e.g. authors mentioned Indonesia).

R.: The main objective of this paper is to present the GPD+ WTC database to users of the Geophysical or Level 2 altimetry products, i.e., users mainly interested in ocean applications yet wishing to extend their analysis to the coastal regions. Therefore, the authors had opted to show the results for the latest Envisat reprocessing (which have not been published yet), summarised globally and to refer previous published results that have used GPD+ and focused on particular regions (Handoko et al., 2017; Dinardo et al., 2018). However, in response to the reviewer's comments, we have extended the Results section and provided some results for the three coastal regions already referred. Section 3.2.2 has been included in the revised manuscript.

Moreover, the testing in the coastal zone has to be at 20Hz being the available re-tracked products at this rate. The RADS product is fine for open ocean studies but not in the coastal zone.

R.: The rate of the altimetry measurements is not a limitation to the GPD+ methodology. In the scope of a current research project in which the University of Porto (UPorto) is involved, the GPD+ methodology will be used to estimate the WTC for the coastal (and inland water) zone for CryoSat-2 and Sentinel-3 missions. The outcome of this project will be a GPD+ WTC product at high rate (20 Hz), intended to be used for applications over the coastal zone (i.e., no ocean values included for distances larger than ~100 km off the coast) and over inland waters. However, the GPD+ WTCs presented in this manuscript have been computed to be incorporated in altimetry products providing observations at 1 Hz, the rate still most used by the altimetry community databases. They are intended for users who want to have a consistent and continuous WTC correction, from open ocean to coasts (and polar regions as well). The correction can be extended to the coast since a valid WTC value is provided for the first along-track measurement over land. Users can therefore use this measurement to interpolate the valid GPD+ WTC up to the coast, for the location and time instant of the 20 Hz data. Moreover, as the onboard radiometer data are not available at a higher than 7 Hz rate, neither these data nor the third-party data have enough resolution to be provided at 20 Hz. Therefore, and for the time being, the strategy for those users who want to focus on coastal zones, would be to interpolate these 1-Hz data to the location and time instant of the 20 Hz data.

For high-frequency MWR, expected in the future, high-rate WTC are definitely advisable, and the authors intend to exploit this possibility. A sentence has been added to the "Conclusions".

Also the metrics has to be different, as in the coastal zone we can use tide gauges as an independent measure of SLA. Therefore, by changing the wet troposphere (default vs GPD+) in the altimetry formula, absolute differences of SLA along the track would show the distance of the coast at which noise increases in the specific region. Comparisons with TGs would show the improvements in terms of statistical indicators (correlation and rms error).

R.: Some analyses previously performed by the authors seem to indicate that comparison with tide gauges is not the best way to validate the WTC, because the differences between altimetry and tide gauges are large when compared to the SLA variability due to different WTC. For this reason, in this paper, the analysis suggested by the reviewer has been performed using GNSS data. Former Figure 7 (Figure 10 in the revised version) shows an

independent comparison between GNSS-derived and MWR-derived WTC, function of distance from coast, for the newly reprocessed Envisat data. This result yields the distance from coast at which this contamination appears. This distance depends on the altimetric mission, due to their different footprint sizes and different MWR retrieval algorithms, varying from 10 to 30 km. For Envisat, this distance is 30 km. This assessment provided us the distance from coast at which an MWR measurement is expected to be contaminated by land. This means that the GPD+ methodology does not use MWR-derived WTC in the last 30 km to the coast, even if they are not flagged as invalid by other rejection criteria, to prevent land contamination in the GPD+ estimates.

We believe that the assessment with GNSS, together with the SLA variance analysis, are clear and sufficient indicators of the GPD+ performance.

Having said that there are other important remarks that I would like to highlight.

First, the authors are discussing a product at 1 Hz, when users need a product at 20 Hz in the coastal zone. So this product after publishing would not be usable for the typical non expert coastal users.

R.: As previously said, these products contain a consistent and continuous WTC correction at 1 Hz rate. Improved criteria have been established in the GPD+ methodology for each mission (e.g. criteria derived from statistical analyses to detect measurements contaminated by ice, land, rain and outliers, based not only on the information available on the points for which a GPD+ estimation is being computed, but also on the information available for neighbouring points) and applied to detect valid/invalid MWR measurements, besides the criteria based on the flags provided in the GDR/RADS/PEACHI products. Moreover, the correction has been calibrated against the SSM/SSM radiometers, ensuring the long-term stability of the GPD+ WTCs.

As previously mentioned, the correction has been provided continuously over ocean and coastal regions, precisely to be used by non-expert users, working over ocean but wanting to extend their analysis to the coastal regions, without discarding altimeter measurements in the coastal zone as would happen when relying on MWR-derived measurements to compute SLA. As already explained, the correction provided at 1 Hz can be interpolated to 20 Hz data by expert users with enough accuracy. As explained before, this is due to the characteristics of current on-board radiometers.

Typical non expert coastal users who are not able to perform this interpolation procedure and in the absence of MWR data in the coastal strip can rely on a Numerical Weather Model (NWM) derived WTC. However, anomalies in the NWM-derived WTCs have been found in the Envisat FMR V3.0, which are corrected in the GPD+ processing. A sentence clarifying this has been added to the text: "Anomalies in this field have been found, with the field out of limits in a set of points, most of them concentrated on certain passes. This is due to the fact that this correction has been computed from 3D model fields at the altimeter measurement altitude. Therefore, whenever the altimeter-derived surface height is not set (NaN value), the corresponding Model WTC will also be NaN. As our goal is to be able to provide continuous WTC, without data gaps, this field is unsuitable for use in the GPD+ estimations.". Moreover, as described in this manuscript, NWM-derived WTC are not able to describe the small-scale variability of this field yet.

Second, I also see insufficient the strategy of showing results related to only one missions. As multi-mission approach is essential in the coastal zone to have more coverage in space and time, the reader expects to see the validation extended to all missions.

R.: The primary scope of this paper is the dissemination of the GPD+ database fostering its use among as many people as possible, since in the authors' opinion the GPD+ database is of sufficient quality for both expert and non-

expert users. Therefore, the paper focuses mainly on the data description and their usage, and for this reason the Earth System Science Data (ESSD) journal has been chosen. The authors have tried to show the added value of the correction using the results for the newly recomputed Envisat FMR V3.0 data, not yet published before. Results for other missions have been already published by the authors in papers of more scientific nature (cf. references e.g. Fernandes et al. (2015) for results regarding reference and ESA missions, Fernandes and Lázaro (2016) for results for CryoSat-2 and GFO, Fernandes and Lázaro (2018) for Sentinel-3). These works are cited in the manuscript leading the readers to the reference list. The GPD+ WTC are available for all altimetry missions in the UPorto database, except for Sentinel-3A/B as their development is still on course and can therefore be chosen for a multi-mission approach.

Third, one important input for the estimation of an improved WTC in the coastal zone is the presence of GNSS station. The authors provide poor information about distribution in space and time. There is just one figure related to Envisat showing the number of GNSS stations over mission time. The authors have to add same figures for the other missions. Moreover, a map has to add concerning the geographical distribution (areas well covered and areas where no GNSS stations are available. These figures are important for the users that after zooming in their coastal regions of interest can perceive the space and time coverage.

R.: Figure 1 shows the number of GNSS stations used as input in the GPD+ algorithm, function of time. This information does not depend on the mission and therefore one single figure suffices to illustrate that the later the period of the mission, the larger the number of available GNSS stations. Figure 1 has been remade to include information for the whole satellite altimetry era, so the reader can more easily understand this and the Envisat period (2002-2012) is shaded in the figure.

However, the reviewer is right in indicating that the geographical location of the GNSS stations could be of interest to the reader and a new figure (Figure 2) has been added to the revised version of the manuscript.

In summary, the paper in the actual version fails to convince the reader that in the coastal zone the new correction cannot be immediately exploited by users (because not at 20 Hz) and that misses a thorough validation in selected coastal areas of investigation (i.e. zooming locally where the user would use SLAs). Therefore, the paper calls for significant revision in order to fill the gaps in term of exploitability of the product and validation of the correction in the coastal zone.

R.: The authors consider that the Reviewer's comments have undoubtedly improved the paper and therefore are thankful for his/her contribution. The authors expect to have satisfactorily responded to the critiques and/or suggestions raised by the Reviewer.

MINOR COMMENTS

Pg 1, abstract: "The results are presented with vague sentences (e.g. GPD+ WTC is the most effective. . .). The reader expects here to see quantitative results that show the improvement with reference to the state-of-the-art and discussion of these results. In the present version, the abstract is substantially an introduction to the dataset that should be the core with more details, e.g., distance from the coast, etc..

R.: The ESSD journal encourages the submission of manuscripts describing original research datasets that use can be considered beneficial to Earth system sciences. Therefore, the authors focused on the description of the GPD+ dataset. However, the abstract has been rewritten according to the reviewer's suggestion and quantitative results have been added.

Pg. 1, rows 13-14, “SLA dataset over open ocean accurate to the centimetre-level”: The authors in the previous sentences refer to sea level rise (which means mm/yr error level). The reader might be confused with cm level accuracy that is generally a target for oceanography. Moreover, accuracy is not enough for trends, there is also a need of “stability”, and here it is the case of wet tropo not drifting over time. Please rephrase properly

R.: Lines 8 to 14 of the abstract have been rephrased and moved to Section 2.1.4 (Radiometer Calibration), to simplify the Abstract (since new information has been added to describe quantitative results, following the Reviewer’s suggestion) and because this information is relevant to understand the need for performing the inter-calibration of the radiometers.

Pg. 2, row 44, “with a centimetre-level radial error”: Please provide reference where it is demonstrated.

R.: The following reference has been added:

S. Rudenko, K. Neumayer, D. Dettmering, S. Esselborn, T. Schöne and J. Raimondo, "Improvements in Precise Orbits of Altimetry Satellites and Their Impact on Mean Sea Level Monitoring," in *IEEE Transactions on Geoscience and Remote Sensing*, vol. 55, no. 6, pp. 3382-3395, June 2017, doi: 10.1109/TGRS.2017.2670061.

Pg. 2, row 44, “precise SSH”: You used “accurate” before. It depends on what you refer, e.g., global mean sea level requires accuracy; fronts requires precision, etc.)

R.: The suggestion has been accepted and the word “precise” has been replaced by “accurate”.

Pg. 2, row 55, “Chelton et al. (2001).”: please refer to recent bibliography (Satellite altimetry over oceans and land surfaces (Detlef Stammer & Anny Cazenave Editors), Earth observation of global changes book series, CRC Press Taylor & Francis, London, UK, 670 pp, doi:10.1201/9781315151779, 2017).

R: Chelton et al. (2001) is still an important reference. The following reference has been added:

Escudier, P., Ablain, M., Amarouche, L., Carrère, L., Couhert, A., Dibarboure, G., Dorandeu, J., Dubois, P., Mallet, A., Mercier, F., Picard, B., Richard, J., Steunou, N., Thibaut, P., Rio, M.-H., and Tran, N.: Satellite radar altimetry: principle, accuracy & precision, in: *Satellite Altimetry Over Oceans and Land Surfaces*, edited by: Stammer, D. and Cazenave, A., CRC Press Taylor & Francis, London, UK, 670 pp, doi:10.1201/9781315151779, 2017

Pg. 3, row 67, “as large as 2.3 ± 0.2 m”, is this cited in Fernandes et al. 2014? If not, please provide reference.

R.: Yes, these values are given in Fernandes et al. (2014).

Pg. 3, row 67-68, “calculated with millimetre-accuracy, provided the surface atmospheric pressure is known at each location”: as we are talking about coastal zone, the authors have here to specify that pressure has to be known at surface level. This pressure is generally retrieved from coarse models that can fail in steep coastal regions.

R.: For oceanic coastal points, the DTC must be computed at sea level from sea level pressure data. If the DTC is provided in the altimetric products at the level of the model orography, as is usually the case, which can depart significantly from sea level at coastal zones, then the value of the dry tropospheric correction should be corrected as described in Fernandes et al. (2013a) (cited in this manuscript). In the same paper, it is also shown that current models are accurate enough to compute the DTC with this accuracy, including the coastal zones, provided adequate procedures are adopted.

The sentence “calculated with millimetre-accuracy, provided the surface atmospheric pressure is known at each location” has been changed to “over the ocean it can be calculated with millimetre-accuracy, provided the sea level atmospheric pressure is known at each location”.

Pg. 3, row 69, “dry and wet tropospheric corrections (negative values)”: why negative ? please explain.

R.: The measured distance between the satellite and the sea surface, or altimeter range R_{obs} , is computed from the following equation, neglecting atmospheric refraction:

$$R_{obs} = c \frac{\Delta t}{2}$$

where c represents the velocity of light in vacuum and Δt is the two-way travel time of a radar pulse between the satellite antenna and the sea surface. The velocity of the altimeter pulses is reduced in a refractive medium as the atmosphere. Therefore, when the signal passes through the troposphere, the propagation velocity of the altimeter pulses is smaller than c . This means that the R_{obs} computed from equation above will be longer than the true range. To correct for this overestimation in the measured range, both the DTC and the WTC are negative.

Pg. 3, row 70, “DPD and WPD to the corresponding absolute values”: What do you mean with “absolute”? what is the difference between DTC and DPD, WTC and WPD?

R.: Following the previous answer, we can define the effect of the troposphere on the altimeter signals, which appears as an extra delay in the measurement of the signal traveling from the satellite to receiver, as the tropospheric path delay, which can be divided into the dry and wet components, called the dry path delay (DPD) and the wet path delay (WPD), respectively. Each delay component contributes to an error (path length) in the measured distance that must be corrected for. The corrections needed to consider these delays – the dry tropospheric correction (DTC) and the wet tropospheric correction (WTC) – have therefore the same magnitude as the DPD/WPD and the opposite (negative) sign, and must be subtracted from the range estimated assuming the free-space value for the speed of light.

Hereupon, the term “absolute” is used to refer to the modulus of the DTC and WTC.

Pg. 3, row 73-74, “possessing an absolute value less than 0.50 m.”: Please specify how 0,50 is estimated. Please also specify the meaningful of “absolute” vs “relative”.

R.: As explained in the previous response, the term “absolute” is used to refer to the modulus of the corrections, which are negative.

In the computation of the water vapour range correction, passive microwave estimates of columnar water vapour from satellite radiometers are used. The maximum value of 50 cm for the wet path delay is known from decades of observations from satellite passive microwaves (e.g., Special Sensor Microwave/Imager (SSM/I) on board the United States Air Force Defense Meteorological Satellite Program (DMSP) satellites). Considering the global dynamic range of columnar water vapor, 0.5–7 g cm⁻², the wet tropospheric path delay varies from 3 to 45 cm, with standard deviations covering the range from 3 to 6 cm. A very thorough description of the underlying theory and principles of the wet tropospheric correction estimation can be found in:

Chelton, D. B., Ries, J. C., Haines, B. J., Fu, L. L., Callahan, P. S.: Satellite Altimetry. In Satellite Altimetry and Earth Sciences: A Handbook of Techniques and Applications; Fu, L.L., Cazenave, A., Eds.; Academic: San Diego, CA, USA; Volume 69, 1–131, 2001.

Pg. 3, row 73, “Contrasting”: Maybe you mean “in opposite”

R.: Accepted and changed.

Pg. 3, row 79-86, “Radiometers .. 12 km”: please explain the different impact of the three radiometers on the retrieved measurements, e.g. with reference with data quality. Are there differences in the coastal zone in retrieving data ?

R.: According to the literature, and as mentioned in the paper, radiometer footprints depend on instrument and frequency. So, footprint size is the key factor in the coastal zone. In addition to the known footprint of each radiometer and according to several analyses performed by the authors (e.g., Fernandes et al., 2015, Fernandes and Lázaro, 2016) land contamination for these missions occurs at distances from coast less than 15 km, while for ESA’s missions, T/P and GFO, this value is around 30 km. All this information is given in the paper.

Pg. 3, row 88, “precise modelling”: I think the word “modelling” is confusing. WTC can be derived from models too. However, here we are talking about “observations”.

R.: The suggestion has been accepted. The word “modelling” has been replaced by “estimation”.

Pg. 3, row 91, “flagged as invalid, being therefore discarded, or non-existent due to several reasons.”: The sentence is vague. Why data are flagged invalid? What is the criteria used ? What re the reasons for missing data ? please explain

R.: The reasons why the microwave measurements are flagged as invalid in the coastal zones are given in the sentences that follow the referred one. In the coastal region, the measurements of the MWR are in general contaminated by land, due to the large diameter of the footprint of the instrument. The WTC retrieval algorithms are based on sea surface emissivity conditions, which is valid only for open-ocean conditions since surface emissivity can be highly variable when the coastal land contribute to the returning signal. This cause a failure of the algorithms that retrieve the WTCs from the onboard microwave radiometer measurements, resulting in their absence. Also, the algorithms can retrieve the WTCs but their values are considered invalid and are, therefore, flagged by the retrieval algorithms. The invalid WTC values are exemplified in red in Figures 7 and 8 (former Figure 5). If used, invalid SLA values would consequently be obtained. For those altimeter points for which the MWR-derived WTC values are missing, no SLA values can be computed unless the user decides to use WTC values from the model. The estimation of the WTC in these points that has been made possible by GPD+, therefore allowing the computation of SLA, is one of the advantages of the methodology.

Pg.4, row 96, “surface emissivity”: Coastal zone has also non homogeneous scattering due to variable waves, winds, surfactant streaks, etc. Are they influencing the retrieval of a valid measurement?

R.: The microwave radiation measured by an on-board MWR, expressed as brightness temperature, corresponds to the sum of three contributions: atmosphere, surface and the cosmic background. Regarding the surface contribution, it depends on the surface temperature and emissivity properties. All WTC retrieval algorithms are based on sea surface emissivity models, so they do not consider the very strong (emissivity higher than 0.9) and variable non-ocean radiation. The problem of the non-homogeneous scattering as mentioned by the reviewer appears in the altimeter (active sensor) measurements. Any surface (different from calm waters) induces a non-homogeneous scattering, influencing the retrieval of altimeter measurements.

Pg. 4, row 105, “is to describe and grant access”: The access to a dataset cannot be an aiming of a paper. I think the authors have to reformulate clearly the main goal of this paper that is presenting and validating a dataset and then elucidate specific single objectives

R.: The sentence has been rewritten.

Pg. 4, rows 111-115, “The main objective”: Objectives have to be stated in the introduction. Also description of sections has to be moved in the introduction.

R.: The authors are here stating the main objective of the methodology and not of the study itself. To avoid any confusion to the reader, this sentence has been rewritten. The description of the sections has been moved to the Introduction, as suggested by the Reviewer.

Pg. 4, row 118, “GNSS network of stations”, please provide a map of GNSS stations used so the reader can appreciate the global coverage

R.: Figure 2 has been added to the manuscript as suggested.

Pg. 4, row 123, “This way”, please add “In”

R.: Accepted and changed.

Pg. 5, row 118, “this way are given at station height”. The GPS stations are over land. So you measure the column at land point. It is not clear to me (and probably to most of not expert people) how this value is extrapolated to the ocean

R.: The handling of the GNSS observations is described in Section 2.1.1. After the computation of the GNSS-derived WTC, at the level of the station height, the WTC are reduced to sea level, the quantity of interest for satellite altimetry, using the height reduction procedure (exponential decay with height) proposed by Kouba (2008), cited in this paper. This height reduction is fully described in e.g. Fernandes et al. (2013a, 2015).

Pg. 6, row 156, “In fact, GPD+ is an upgrade from the GPD methodology”: Please better clarify differences between GPD and GPD+. Apparently you say that GPD+ was for coastal zone but now global. Is the reason related to CryoSat-2 ? as it has no radiometer onboard.

R.: The GPD methodology was developed to compute the WTC only for coastal points, where WTCs derived from the on-board MWR are usually invalid. In its former version, the GPD methodology used as input GNSS-derived WTCs and valid MWR measurements only. Later, the methodology was updated to estimate the WTC for CryoSat-2. Since this mission does not possess an on-board MWR, it was necessary to estimate the WTC not only for coastal regions, but also for open ocean. To do this, the GPD methodology was improved to use data from the scanning imaging radiometers, which are available over coastal regions as well as open ocean, as another input data source. This later version was called GPD Plus (GPD+).

The sentence has been rephrased for clarity:

“In fact, GPD+ is an upgrade from the GPD methodology, which was developed to compute the WTC only for coastal points, relying only on GNSS and valid on-board MWR measurements. Motivated by the need to compute an improved correction for CS-2, the SI-MWR data set was included and the focus of the correction extended to open ocean.”.

Pg. 5, row 158-164: as you provide a table it is redundant here to report names of the mission. It is important to add space and time resolution of single MWR sensors in the table. A matrix has to be added showing the MWR sensors available for each altimetry mission. Again, this is an important figure for the reader. Some comments about substantial differences between sensors should be recalled here from cited references

R.: We believe the information concerning the data providers for the different SI-MWR missions should be kept in the paper, however the spatial and time resolutions of the SI-MWR missions have been added to Table 1 as requested. Since the number of SI-MWR sensors varies with time, a figure showing their availability along time for each satellite altimetry mission has been added (current Figure 3). Also, a sentence summarizing the main differences between the data types has been added to the manuscript:

“Two types of TCWV products have been used: Level-2 swath products in HDF-EOS2 format (near real time products, 14-15 orbital swaths per day available for each instrument) from all data sources except RSS, and Level-2 gridded products (two grids per day, each containing the ascending/descending passes) in binary format from RSS.”.

Pg. 5, row 173-176, “It is known that, in addition to TCWV, WPD also depends on temperature. Expressions such as Eq. (3) account for an implicit modelling of this dependence. Fernandes et al. (2013b) have shown that this expression leads to similar results as those obtained by adopting formulae that make use of explicit values of atmospheric temperature given e.g. by an NWM.” The reader might not understand what you mean here with “Implicit” and “explicit” values. Please show examples of comparisons with WTC derived from NWP in open ocean and in coastal zone.

R.: The WTC can be calculated from using the expression given in Bevis et al. (1994), given below:

$$WTC = - \left(0.101995 + \frac{1725.55}{T_m} \right) \frac{TCWV}{1000}$$

where T_m is the weighted mean temperature of the atmosphere. This expression shows that the WTC explicitly depends on the temperature. Equation (3) given in the manuscript does not depend explicitly on temperature as the former. The results requested by the Reviewer are given in Fernandes et al. (2013b), which show that, after sensor inter-calibration, crucial to guarantee datasets consistency, the WTC derived from both methods are equivalent, with differences within ± 2 mm. This result has been added to the manuscript and the following sentence has been included in the revised manuscript:

“The authors show that after sensor inter-calibration, a crucial step to guarantee datasets consistency, the WTC derived from both methods are equivalent, with differences within ± 2 mm.”.

Also, the reference Bevis et al. (1994) has been added to the manuscript to direct the reader to the appropriate literature, in case of interest:

Bevis, M., Businger, S., Chiswell, S., Herring, T.A., Anthes, R.A., Rocken, C., Ware, R.H. (1994), GPS Meteorology – Mapping Zenith Wet delays onto precipitable water. *Journal of Applied Meteorology*, 33, 379-386.

Pg. 6, row 179-180, “We recall that the WTC is the symmetric of the wet path delay and the quantity of interest in satellite altimetry” Please rephrase and specify what you mean with “symmetric”

R.: The term “symmetric” has been replaced by “absolute value” and the sentence referred by the Reviewer has been rewritten as: “It is recalled that the WPD is the absolute value of the WTC, the quantity of interest in satellite altimetry.”.

Pg. 6, row 180, “RA data necessary to compute”, Please specify the sources you used for corrections, orbit, MSS, etc.

R.: The models and corrections used to derive the SLA datasets are provided in the altimetric products (RADS and Envisat FRM V3.0). To derive these datasets, used to analyse the SLA variance reduction, the same corrections and models are kept unchanged except the WTC. In other words, an SLA dataset is computed using a set of selected models and corrections and the WTC from ERA, then another SLA dataset is computed using the same models and corrections and the MWR-derived WTC, and so on. We do not consider necessary to enumerate all the models and corrections used to generate the SLA datasets, since these SLA datasets have been generated only to perform the statistical assessment, i.e., have been used only as a mathematical tool.

Following the Reviewer’s comment, however, the following sentence has been introduced in the revised version of the manuscript:

“The criteria to select valid SLA are those recommended in the literature and adopted in the standard RADS processing (Scharroo et al., 2012, cited in this manuscript) and include: application of thresholds for all involved fields (satellite orbit above reference ellipsoid, altimeter range, all range and geophysical corrections), altimeter ice and rain flag (whenever set) and SLA within $\pm 2\text{m}$.”

Pg. 7, row 191, “Threshold values used in this criterion depend on the RA mission”: Please specify thresholds

R.: The threshold values are specified in the text that follows the referred sentence (lines 193-196). Values of 30 and 15 km have been set for ESA missions, GFO and T/P, and for the Jason series of satellites and SARAL, respectively.

Pg. 7, row 194, “at distances from coast”: The authors use some editing criteria. I am curious to know what happens when tracks are parallel to the coast, but also some situations, e.g., Indonesia where the altimeter crosses successive land segments due to presence of closest islands.

R.: The distance that is inspected by the algorithm is the distance from the point to the closest land point. If a track is parallel to the coast and the distance from its point to the coast is less than the threshold value, all points will be flagged as invalid by the methodology, even if they are not flagged as invalid in the original products. This guarantees that non-flagged invalid MWR-derived WTCs contribute to the estimations.

Pg. 7, row 203, “number of 18 Hz measurements to compute the 1 Hz”: is the global product at 1 Hz (i.e. around 7 km spaced for all missions)? While in open ocean it makes sense, I am bit skeptical the coastal zone might benefit from this product if not provided at 18/20 hz. It has been demonstrated that we need high resolution data in the coastal zone (and in fact waveforms are retracked at that rate and SLAs computed at that rate). Otherwise, the user will not be able to exploit the product.

R.: As already explained, the GPD+ WTC database has been computed for GDR products, which are used by most non-expert users. Over open ocean regions, the MWR-derived WTC is the best choice to account for the wet path delay in the altimeter measurements, and this correction is usually available in these regions. Users that want to extend the use of these products in the coastal zone must rely on model-derived WTC since the former is usually invalid or absent in the coastal zone. Discontinuities may therefore occur between both corrections. The GPD+ WTC, which preserves the valid MWR-derived WTC over open ocean and improves the WTC estimation in the coastal region, has the advantage of being a continuous correction in the transition open ocean/coastal zone. As already explained, expert users can interpolate the GPD+ WTC for the location and epoch of the high-rate altimeter

measurements, benefiting this way of an improved WTC in coastal zones. To prevent the loss of points when interpolating to 20 Hz points, in addition to ocean points, the WTC for the closest land point, computed at sea level, is included as explained in the manuscript. Provided the necessary funding is allocated, the GPD+ WTC can be computed for high-rate altimetry products.

In the revised version of the paper, results highlighting the improvement in the Envisat SLA datasets when the GPD+ WTC is used in coastal regions have been added. A summary of the results for the other missions have been included in the revised manuscript. The readers are advised to refer to the cited references from the authors.

Pg. 7, row 203-204, "For approximately 10% of all oceanic points": What do you mean with "oceanic domain ? Does it include coastal zone ? at which distance ? The value seems for Envisat only. What about the other missions?

R.: This percentage is computed using all points over ocean with valid SLA values (i.e., along-track points with all available corrections but the MWR-derived WTC, which is computed using GPD+), including coastal regions. The values given in the manuscript are typical for ESA's missions. Results for other missions have been added in the conclusions section:

"The percentage of recovered points when GPD+ is applied in place of the baseline MWR-derived WTC, depends on instrument type, band of latitudes covered by the mission (which determines the extent of ice contamination) and instrument performance. For all ESA missions (ERS-1, ERS-2, Envisat, Sentinel-3) and SARAL, possessing 2-band radiometers and measuring up to latitudes $\pm 81.2^\circ$, the percentage of recover data is similar to that of Envisat, in the range of 7% - 15% of the SLA valid points of each cycle. For the reference missions, measuring only up to $\pm 66.7^\circ$ and already possessing an improved WTC near the coast (all except T/P), this percentage is smaller, from 2 to 4%. For T/P, these values are from 4% to 7%, larger in the second half of the mission. For GFO, measuring up to $\pm 72.0^\circ$, the percentage is similar to that of TP. Exceptions occur for various missions over periods of instrument malfunction, when the percentage of recovered points can be considerably larger, up to 100%, as it happens for Envisat and GFO."

Pg. 8, row 220, "parameters have been obtained for Envisat": Please provide parameters for all missions

R.: The calibration parameters for all satellite altimetry missions possessing an MWR are now provided in Table 2. Subsequent tables have been renumbered.

Pg. 8, row 240, "For all satellite missions but CryoSat-2 and for each along-track point deemed as invalid": The sentence is unclear, please rephrase

R.: The sentence has been rewritten to: "For the altimetry missions carrying an on-board MWR (all but CryoSat-2), a GPD+ WTC estimate is calculated for all along-track points with an MWR-derived WTC deemed as invalid, using valid WTC observations from different sources at the nearby location and within a time interval, defined by the spatial and temporal radiuses of influence used in the computation."

Pg. 9, row 275, "50 km from the ocean": The setting of this value has to ne justified

R.: The justification has been included: "To prevent the loss of points when interpolating to 20 Hz points, in addition to ocean points, the closest point over land is included, provided it is within a distance less than 50 km from the ocean. This guarantees that observations over ocean necessary to compute the WTC for this location are still

available within the radiuses of influence centred on the point. The WTC estimated for the closest points over land are also estimated at sea level.”.

Pg. 9, row 278, “Figure 4 gives an example of the GPD+ WTC for Envisat’s cycle 12”. I don’t understand the message of this figure. The upper map is substantially unreadable. The lower map is not providing information as the reader would like. Moreover, one cycle per one mission would be only for visual purposes. There is no comments in the paper. The reader expects quantitative results about the improvement.

R.: Figure 4 is presented to show, as an example, the availability of the GPD+ WTC globally (Panel (a)). Panel (b) shows the correction over ocean only, to be used in satellite altimetry. The idea is to show the global coverage, and therefore one of the advantages, of the GPD+ WTC. This explanation is given in lines 278-279 of the original manuscript.

Pg. 10, row 289, “respectively, are provided at 1 Hz.”. Previously, the authors mentioned 20 Hz. People using the product in the coastal zone need 20 hz data. I don’t understand the utility of publishing a product that then in practice it is not usable from coastal zone users (who are not experts in altimetry). The authors refer to RADS that cannot be considered a “coastal altimetry product”. In my opinion, the authors have to satisfy the user requirements if they want to publish this dataset.

R.: We believe that the GPD+ WTC satisfies the requirements of the users who want to base their analyses on the GDR/RADS products. In what concerns the availability of the GPD+ WTC for coastal purposes only, please refer to previous answers.

Pg. 11, row 315-318: “For results concerning algorithm.”: The reader is confused here and reminded to previous paper. Indeed, the reader wants to see statistics of all missions here with the application of the algorithm described here. The authors have to add relevant statistics of all missions.

R.: We would like to emphasise that the purpose of this paper is not to describe in detail the results for all missions as that has already partly been done in previous papers. Moreover, a paper with an exhaustive description of the results for all missions would necessarily be very long and tedious. Here, we believe the focus should be on the benefits of using these products. Therefore, we detail the results for Envisat, not presented before, and provide a summary of the results for all other missions in the conclusions.

Pg. 11, row 320, “The GPD+ WTC is here compared to the ECMWF Reanalysis WTC”: This kind of comparison make sense in open ocean but not in the coastal zone. The authors provide a title “A coastally improved global dataset. . . .”. They clearly state previously that models fail in the coastal zone and now they use for validation.

R.: Actually, the authors assessed the performance of the GPD+ WTC by comparing it with those WTC available to the users in the altimetry products, to show the improvement attained when the GPD+ WTC is used in the SLA datasets generation, instead of using the MWR- or NWM-derived WTCs. The word “validation” has therefore been changed to “assessment” throughout the text whenever it was used incorrectly.

Pg. 11, row 335, “Figure 5 shows the GPD+ WTC for some Envisat tracks”: The reader expects to see the map showing where the passes are located and identification of the segments where the new corrections improves. The discussion of Figure 5 is not provided. The plots have to be commented in relation to the places touched over ground.

R.: Figure 5 has been divided into Figures 7 and 8 and now includes the geographical coverage of the selected tracks, as we agree with the Reviewer that this information is necessary. The discussion of these figures has been included.

Pg. 11, row 340, “interesting results”: please remove being subjective

R.: The sentence has been rewritten.

Pg. 11, row 346, “most of these points are located at high latitudes and in coastal regions”: This statement is not demonstrated in the figure. The authors expects to see zooming in coastal regions to see improvements.

R.: Results for three different coastal regions have been added in the revised version of the manuscript.

Pg. 11, row 361, “for the whole Envisat mission”: the authors have to provide th same figure for the other missions too

R.: We have already explained that it is not possible to present detailed results for all missions, neither it would be relevant to repeat results already published before.

Similar figures for most missions (T/P, Jason-1, Jason-2, ERS-1, ERS-2, Envisat, GFO and SARAL) are provided in Vieira et al. (2019) and in Fernandes and Lazaro (2018) for Sentinel-3 (both cited in the paper). The following sentences have been introduced in the paper:

“For other missions, results have been presented in Vieira at al. (2019) and in Fernandes and Lázaro (2018) and are summarised here. For the 2-band radiometers, land contamination on the MWR observations occurs for points at distances from coast smaller than 25-30 km (ERS-1 and ERS-2), 20-25 km (Sentinel-3) and 15-20 km (GFO and SARAL), the latter in agreement with the smaller radiometer footprint of the SARAL MWR. Similar analysis shows that land contamination is observed up to 25-30 km from the coast for T/P and Jason-1 and up to 20-25 km for Jason-2 and Jason-3. These numbers are function both of the instrument footprint size and of the efficiency of the criteria used to detect valid/invalid MWR observations, since in these plots only MWR values that passed all validation criteria, except for the distance from coast, have been used. In summary, for each mission, these analyses show the distances from coast up to which the MWR observations are contaminated by land and must be discarded. Moreover, they also show that GPD+ is efficient in removing this effect.”.

Pg. 12, row 369, “The results are shown in Fig. 7”. The authors state the product is at 1 Hz (7 km) and in the plot show values at less than 5 km

R.: Figure 7 (now Figure 10) shows the RMS of WTC differences in bins of distance from coast. While along-track points are separated by 7 km, the points closest to land can be at any distance from the coast, even at distances less than 5 km.

Pg. 13, row 393-395, “Therefore, three SLA datasets of collocated along-track points were derived using the same standard corrections (Sect. 1) but the WTC, which can be the Composite correction present in AVISO CorSSH L2P products (Comp), the GPD+ or the ERA Interim WTCs.”. This comparison makes sense only in the open ocean and not in the coastal zone (0-50 km)

R.: The GPD+ WTC has been compared with the other WTCs available in the altimeter products provided by RADS, GDR, PEACHI and AVISO for use in both open-ocean and coastal regions. The Comp WTC is the result of the methodology developed by AVISO, to improve the WTC in the coastal region, therefore we consider that the comparisons shown are reasonable. However, following the concerns of Reviewer#2, who were right pointing out that the Composite WTC available at the time of our analysis in AVISO products has not been computed using this new Envisat FMR V3.0, we decided to show in the revised version of the manuscript the assessment of the GPD+ WTC by comparing it with the ERA- and MWR-derived WTCs, which are the actual corrections provided in these products. Therefore, Section 3 has been rewritten accordingly.

Pg. 13, row 406, "Fig.8a": Fig. 8c si not commented in the text. Moreoer, there is a strange behavior around cycle 95

R.: Figure 11 has been changed to include a new panel (b) the number of points used in the MWR and GPD+ WTCs, since it is different from the number of points used in the comparison with ERA (shown in panel (d) of the same figure). This is explained in the manuscript. Reference to both panels (b) and (d) of Figure 11 (previous Figure 8) have been added in the text.

In October 2010, a new orbit configuration (30-day repeat cycle) for Envisat was implemented, corresponding to a change from Envisat Phase b to Phase c. As a consequence, a large amount of data was lost in the period corresponding to cycles 94 and 95. This information has been added in the revised paper.

Authors' response to the "Interactive comment on "A coastally improved global dataset of wet tropospheric corrections for satellite altimetry" by Clara Lazaro et al."

Posted by Anonymous Referee #2

We would like to start by thanking the Reviewer for his or her careful reading of our manuscript and for taking the time to assess it.

The main changes introduced in the manuscript following the comments and suggestions of the two Reviewers can be summarised as:

- Sections containing the Abstract and the Conclusions have been updated to accommodate the new results presented in the revised version of the manuscript.
- Some parts of the text have been moved to new sections or were rewritten/completed to be clearer and more informative.
- Figures 1 as well as figures 11, 12 and 13 have been updated, the latter to include the results for the comparison of the GPD+ WTC with the MWR-derived WTC, instead of that for the Comp WTC, following the concerns raised by Reviewer#2.
- Previous Figure 5 has been divided into Figures 7 and 8 and the geographic location of the Envisat tracks have been added, following the recommendation of Reviewer#1.
- New figures have been added to the revised version (Figures 2, 3 and 14).
- Tables 1 and 4 have been updated, the former to include more information, the latter in the sequence of the last update of the GPD+ database (performed to include more data for the recent missions).
- A new table (Table 2) has been added in the revised version.
- All figures and tables have been renumbered.
- Section 3.2 has been divided into sections 3.2.1 and 3.2.2 describing the global and the regional (coastal) results, respectively, and the text has been extended.
- Reference Vieira et al. (2019c) has been updated, since at the time of this revision it has already been published.
- Reference AVISO (2017) has been removed.
- Five new references (Bevis et al. (1994), Rudenko et al., (2017), Valladeau et al. (2015), Dinardo et al. (2020) and Escudier et al. (2017)) have been inserted in the revised version.

We have responded to all the comments and suggestions raised by the Reviewer as follows.

The paper presents a dataset of wet tropospheric correction applicable to altimetry and the methodology used to product it. The wet tropospheric correction is one of the correction applied to the altimeter range to compute the Sea Level Anomaly. The WTC is traditionnaly provided by on board microwave radiometer, measuring in appropriate frequencies bands to correct for the excess path delay. The estimation of the WTC from the MWR measurements can be degraded by extreme rains events, ice surface, land contamination in coastal areas,

instrument malfunctions. The author proposes a method named GPD+ that intend to improve the MWR-based WTC of operational processing, or propose a correction for mission without MWR on-board (Cryosat-2). The method consists first in the filtering of the invalid WTC estimation from the operational product and second, by the estimation based on the objective analysis using external data such as GNSS data, MWR Imaging data (providing water vapour), Numerical Weather Prevision model (ECMWF, ERA interim). The method is applied to almost all conventional missions.

The dataset used for the algorithm is rather well defined. The section about the GNSS dataset lack a discussion about the coverage of this network. Although the paper states otherwise, GNSS stations don't seem to be distributed globally over the globe.

R: The GNSS stations used in the methodology belong to several international GNSS networks (IGS, EPN, SuomiNet); some stations from national networks have also been used by the authors (e.g., in Indonesia, German Bight, etc.). The Reviewer is right saying that GNSS stations providing atmospheric products are not well distributed over the globe. The authors only say that GNSS stations all over the world are used, provided their atmospheric products are made available to users.

The section about the Imaging radiometer seems more dedicated to the filtering step of the method than to the description of the input dataset itself and the added value of this dataset.

R: By filtering step the reviewer may refer to the calibration step. This is a very relevant step, as it is important to ensure that the corrections are stable in time and do not introduce spurious trends in the SLA. In the revised version, information about the SI-MWR products have been inserted as well as the added value of this dataset.

The NWP dataset is slightly described, and lack a discussion of the difference between ERA Interim and ECMWF. The paper don't say if one mission can be covered by only one model or if two are needed, if there is a bias between the two models that shall be corrected. Also the paper stated that NWM data are provided as output from GPD+ for northernmost latitudes, but the method to adjust the model to measurements is not clearly defined (is it a simple bias computed over each cycle?).

R: As ECMWF operational model has undergone several updates, this model does not have the same accuracy over time. For example, the RMS of the differences between MWR-derived WTC and NWM-derived WTC, in points with valid MWR values, is in the range 1.2-1.4 cm after 2004. Before that date, the RMS of differences increases as we go back in time, reaching 2.8-3.0 cm in 1995. On the contrary, ERA Interim is fairly uniform, with RMS of WTC differences with respect to the MWR WTC in the range 1.2-1.4 cm, including the period of the first altimeter decade. For this reason, for all missions with data before 2004 (T/P, Jason-1, ERS-1, ERS-2, Envisat and GFO), ERA Interim is used in GPD+, while for the most recent missions the Operational model is adopted. More details can be found in Legeais et al. (2014), cited in this manuscript. A sentence clarifying this has been added in the revised version of the paper.

The question concerning the adjustment of the WTCs derived from the model and GPD+ is addressed below.

The algorithm is well described and the workflow provides a clear overview of the processing. The method is assessed for Envisat only in this paper. The paper introduces Full Mission Reprocessing (FMR v3.0) but compare GPD+ dataset to the Composite Correction extracted from L2P products issued from an older reprocessing (FMR v2.1). According to the L2P product handbook available on AVISO, there is no composite correction in the L2P

products, only MWR-derived correction. This point must be clarified. In the validation section, both corrections (MWR-based and composite) are used for comparisons. It is difficult to follow which version of the Envisat MWR-based correction is used for the generation of the GPD+ and which one is compared to the GPD+.

R.: The Composite correction has been developed also aiming at getting a WTC with validity extended up to the coast. According to personal communication of colleagues from CLS, the AVISO products usually adopt this correction. However, it is difficult to find a proper reference for this product. Moreover, the Reviewer is right when states that the MWR-derived WTC used to generate the Composite WTC is different from the one provided in FMR V3.0 dataset.

Therefore, in the revised manuscript we dropped the comparison with the Composite WTC for Envisat. Now, GPD+ WTC is compared with both the ERA-derived WTC and the MWR-derived WTC (from Envisat V3.0), the latter therefore has replaced the comparison with the Composite correction. In the present comparisons between GPD+ and MWR, the points for which the MWR observations are not set (NaN values) or are out of the limits of the WTC range (-50 cm to 0 cm) in the GDR products, have been discarded from the analysis. This has been clarified in the paper.

The number of 30% of invalid WTC data over ocean for Envisat is stated but not justified.

This number seems quite high.

R.: This question is addressed below.

Moreover, the criteria to select valid SLA points is not discussed. The paper shall define the criteria of validity of the SLA. The L2P products provide a validity flag that could be used.

R.: The following sentence has been introduced:

“The criteria to select valid SLA are those recommended in the literature and adopted in the standard RADS processing (Scharroo et al., 2012, cited in this manuscript) and include: application of thresholds for all involved fields (satellite orbit above reference ellipsoid, altimeter range, all range and geophysical corrections), altimeter ice and rain flag (whenever set) and SLA within $\pm 2\text{m}$.”.

The comparison of GPD+ with GNSS is more a validation of the method than a performance assessment. This section can gain in clarity in the method used for this comparison. GNSS data are not independent of GPD+ data. Is the GNSS data cited in this section also used in the generation of the GPD+ dataset (data from another network for example)? In the first sections, one of the criteria for rejection of MWR-based correction is the distance to coast, but it is not clear if this criteria is used in this section. The fact that the method is not clear makes the figure 7 difficult to understand.

R.: As stated in the paper (line 353 of original manuscript), GNSS data are not independent from the GPD+ WTC, as they have been used in their computation. Nevertheless, the analysis of the root mean square (RMS) value of the GNSS-derived and GPD+ WTC differences, function of distance from coast, is valuable to inspect the correction in coastal regions since it allows us to derive a threshold value of the distance to coast where the radiometer correction starts to become invalid (even if not flagged as invalid in the original GDR). Once this threshold value is obtained, it can and should be used in the GPD+ algorithm. This has been done for the Envisat FMR V3.0 used in this paper (more details are given below). The authors have detailed the methodology used in this comparison in the revised paper.

The paper provides a performance assessment (and not accuracy) of the section 3.2 using analyses of Sea Level Anomaly variances. In this section, the author compares the composite correction which is not part of the L2P products to the GPD+ correction. The method used is to select all valid SLA points, and for the points with the composite outside limits or invalid, the ERA interim WTC value is used. These points shall be discarded from the analysis as they do not represent a fair comparison with the MWR-based correction as the use of the model correction will degrade it.

R.: As stated before, the assessment with respect to the Composite WTC has been replaced by the corresponding comparison with the MWR-derived WTC. Since in this comparison we cannot assess the performance of the GPD+ WTCs in the points where these corrections are not set, we have now removed these points from the analyses. We believe that the assessment of the GPD+ through comparison with the model WTC is important for the users, who must rely on model data when the correction from the on-board radiometer is invalid/absent.

The previous sections have already shown that the GPD+ retrieves some invalid points.

R.: The GPD+ methodology retrieves a WTC estimate for all points with an invalid MWR-derived WTC. In the absence of observations (valid MWR-, GNSS- and SI-MWR-derived WTCs), the GPD+ output is the first guess (ERA Interim WTC) adjusted to the valid MWR-derived WTCs, as explained here. Therefore, all GPD+ estimates are valid. The GPD+ products provide a flag identifying the model-derived WTCs.

The color scales for figure 9 is not well chosen and is difficult to read.

R.: In Figure 9 (now Figure 12), blueish colours have been chosen to show an improvement from the use of the GPD+ WTC in the computation of SLA, compared to the use of other WTC correction, while the yellow to red colours show a degradation of the SLA dataset when the GPD+ WTC is used. The green colour is used for differences around zero. Since this colour can be difficult to see in the colour scale, a note has been added to the caption of the figure.

Figure 10a shows a strong peak, with not physical values, for latitude around 50°N that is not explained in the paper.

R.: This comment is addressed below.

For this diagnosis, it is not stated if data cover open-ocean only, or ocean and coastal areas. Moreover the figure shows a reduction of the SLA variance from 200km up to the coast but it is difficult to see the improvement close to the coast.

R.: For the diagnoses described in the paper, global data have been used (please refer to former Figures 9 and 10 (Figure 12 and 13 of the revised paper), which show that data for the whole ocean, including coastal regions, have been used). This has been written clearly in the revised paper. The improvement in the closest 20 km to the coast can be as high as 3 cm² for the GPD+ and MWR-derived WTCs comparison and 1 cm² for the comparison with ERA. We believe that in both cases the improvement in SLA dataset is significant, by reducing the SLA error introduced by the WTC in a few centimetres.

Although the paper title is “A coastally improved global dataset”, there is no real focus on coastal areas. It is not stated clearly in the paper but it seems that the dataset is based on 1Hz data where 20Hz data are more adequate for studies on coastal areas.

R.: In response to the Reviewer's concern, results for three coastal regions selected, on the one hand, due to the large number of available GNSS stations (North American and European coasts) and, on the other hand, due to the fact of being a challenging region for coastal satellite altimetry (Indonesia region), have been added to the revised version of the manuscript, as an attempt to show the potential of the GPD+ dataset along the coastal waters. Section 3.2.2 has been added in the manuscript to present these results.

The rate of the altimetry measurements is not a limitation to the GPD+ methodology. In the scope of a current research project in which the University of Porto (UPorto) is involved, the GPD+ methodology will be used to estimate the WTC for the coastal (and inland waters) zone for CryoSat-2 and Sentinel-3 missions. The outcome of this project will be a GPD+ WTC product at high rate (20 Hz), intended to be used for applications over the coastal zone (i.e., no ocean values included for distances larger than ~100 km off the coast). However, the GPD+ WTCs presented in this manuscript have been computed to be incorporated in altimetry products providing observations at 1 Hz rate, still the most used by the altimetry community databases. They are intended for users who want to have a consistent and continuous WTC correction, from open ocean to coasts (and polar regions as well). The correction can be extended up to the coast since a valid WTC value is provided for the first along-track measurement over land. Users can therefore use this measurement to interpolate the valid GPD+ WTC up to the coast, for the location and time instant of the 20 Hz data. Moreover, as the onboard radiometer data are not available at a higher than 7 Hz rate, neither these data nor the third-party data have enough resolution to be provided at 20 Hz. Therefore, and for the time being, the strategy for those users who want to focus on coastal ones, would be to interpolate these 1-Hz data to the location and time instant of the 20 Hz data.

For high-frequency MWR, expected in the future, high-rate WTCs are definitely advisable, and the authors intend to exploit this possibility. A sentence has been added in the section with the conclusions.

Minor comments

Row 118: "GNSS network of stations distributed globally along the coastlines": GNSS stations don't seem to be distributed globally over the globe. A map could be added to show the position of the GNSS stations used for the generation of the dataset.

R.: Following the suggestion of the Reviewer, a figure showing the location of the coastal and island GNSS stations used in this study has been added in the revised version (Figure 2).

Row 195: "values of 15km have been used for Jason-1/2/3": 15km seems quite small for this series of MWR knowing that they measure at three frequencies, including a 18.7GHz with a large footprint. What is the reason for that?

R.: The quoted values refer to those used currently in the GPD+ processing. For the Jason series of satellites, a smaller value has been adopted since the WTC provided in their products are already improved in the coastal regions using the methodology developed by Brown (2010), cited in the text. However, the assessment of the MWR-derived WTCs through their comparison with GNSS-derived WTCs in the coastal zone has shown the existence of contaminated measurements for distances larger than 15 km off the coast. The result from this assessment for Envisat (30 km), shown in current Figure 10, has already been used in the GPD+ processing described in this paper. The same value was obtained for E1, E2 and GFO, which is the value in use in the GPD+

processing. For the reference missions (T/P, J1, J2 and J3), however, the assessment using GNSS data has shown land contamination up to 25 km off the coast. Therefore, the threshold value currently set (15 km) will be updated in the forthcoming GPD+ processing for these missions. For SARAL and Sentinel-3, the outcome of this assessment were thresholds of 15 and 25 km, respectively, that have been already implemented in GPD+. It should be emphasized that the distance from coast is a rejection criterion applied after a set of other criteria, such as the radiometer land flag, that, if efficient, should have already rejected land contaminated points. So, these distances must be large enough to ensure the rejection of contaminated points, but also conservative to avoid rejection of good MWR observations.

Row 201: Talking about Envisat data from latest reprocessing, the author states “30 % of the oceanic points have an invalid WTC value”: This seems quite a large number of invalid points when focusing on ocean surface only (with a valid SLA). From Figure 2, it does not look like one third of the points are invalid. How do you explain that number?

R.: Altimeter data are acquired along satellite tracks only, therefore at low latitudes the distance between adjacent tracks is maximum, with large diamond-shaped regions without altimeter points. Therefore, the quantity of points sampled by the altimeter varies with latitude, being maximum over polar regions where WTCs are usually invalid. Also, the points within a strip of width 30-50 km along the coasts have usually invalid WTCs. Additionally, as depicted in Figure 2 (now Figure 4), there are generally full tracks with invalid WTCs. The percentage of ocean points with invalid WTC for Envisat cycle 12 is 29.5%. The corresponding number when only points with valid SLA are selected is 10.9%. These figures have been added to the text.

Row 209: the author states “Data from the reference missions”. For a non-specialist audience, the author should explain which are the reference missions.

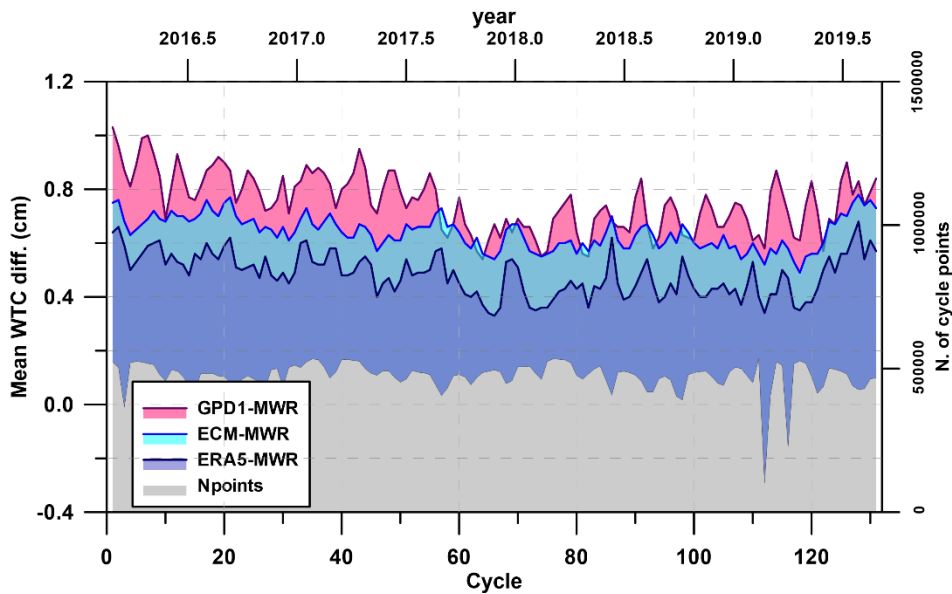
R.: The explanation has been added in the revised version of the manuscript.

Row 219: for the intercalibration processing, the difference at cross-over points with a time-lag of 180 minutes between reference missions and other altimetry missions are computed. Is that time span not too large for WTC ?

R.: As explained in Fernandes et al. (2013b), cited in the text, this value has been chosen to guarantee the existence of enough crossovers to perform the analysis i.e., it is the best compromise between the number of crossovers and the minimum time interval.

Row 229: “In addition, to reduce data discontinuities, : : .” : from this sentence it seems that a bias is computed between the MWR and the NWM correction for each cycle. What is the rationale for a simple bias? How is computed that bias?

R.: The bias is computed, for each cycle, as the mean difference between MWR and model WTC, for all points where the former correction has been considered valid. The rationale behind this comes from the observation that the differences between the WTC from MWR and that from models, in addition to the small scales observed in Figures 7 and 8 in the revised version, have long-wavelengths from yearly to decadal signals. See for example in the figure below, the mean cycle differences between Sentinel-3A (S3) MWR and ECMWF operational (cyan) and between S3 MWR and ERA5 (blue). Although these differences are small (only a few mm) the application of a mean bias per cycle helps to reduce these small discontinuities.



The method used to adjust the NWM-derived and GPD+ WTCs has been described in more detail in the revised version of the manuscript.

Row 274-275: "To prevent the loss of points when interpolating to 20 Hz points, in addition to ocean points, the closest land point is included, provided it is within a distance less than 50 km from the ocean." Can you clarify the processing here? what is the closest land point?

R.: This means that, for each track crossing a coastal zone, a GPD+ WTC at sea level estimate is also computed for the first altimeter measurement point located over land. This WTC estimate and the previous one over ocean, allow the user to perform the interpolation of the WTC field if high-rate data are to be used. The sentence has been rewritten to "To prevent the loss of points when interpolating to 20 Hz points, in addition to ocean points, the closest point over land is included, provided it is within a distance less than 50 km from the ocean. This guarantees that observations over ocean necessary to compute the WTC for this location are still available within the radiuses of influence centred on the point. The WTC estimated for the closest points over land are also estimated at sea level." to become more clearer to the reader.

Row 320: ""The GPD+ WTC is here compared to the ECMWF Reanalysis WTC (ERA Interim, GDR field mod_wet_tropo_cor_reanalysis_01) and with the WTC present in the AVISO CORSSH L2P products in July 2019 (AVISO, 2017). The latter dataset is usually called Composite Correction ". You state here that you compare the GPD+ to Composite correction, but latter (line 334). But according to the L2P products handbook (https://www.aviso.altimetry.fr/fileadmin/documents/data/tools/hdbk_L2P_all_missions_except_S3.pdf), there is no composite correction in these products. And latter, the author says that he used the field 'rad_wet_tropo_cor_sst_gam_01'. This point shall be clarified

R.: As stated before, the comparison with the Composite WTC has been removed.

The MWR-based correction used in the generation of the GPD+ Envisat files is the 'rad_wet_tropo_cor_sst_gam_01' field provided in Envisat FMR V3.0 GDR dataset, based on a five-input algorithm, according to reference:

Collecte Localisation Satellites (CLS). Surface Topography Mission (STM) SRAL/MWR L2 Algorithms Definition, Accuracy and Specification; S3PAD-RS-CLS-SD03-00017; CLS: Ramonville St-Agne, France, 2011.

Row 330: "Anomalies in this field have been found, with the field out of limits in a set of points, most of them concentrated on certain passes," : Do you mean that you found anomalies in the ERA interim product for WTC field?

R.: Yes, please see sentence below, added to the paper:

"Anomalies in this field have been found, with the field out of limits in a set of points, most of them concentrated on certain passes. This is due to the fact that this correction has been computed from 3D model fields at the altimeter measurement altitude. Therefore, whenever the altimeter-derived surface height is not set (NaN value), the corresponding model-derived WTC will also be NaN. As our goal is to be able to provide continuous WTC, without data gaps, this field is unsuitable for use in the GPD+ estimations."

Row 334: "The MWR-based correction used in the generation of these files" : Which files?

R.: The sentence has been rewritten in the revised version of the manuscript to make it clearer to the reader.

Row 342: The author found 30% of points with a rejected MWR-derived WTC. This figure seems quite large. It could be interesting to discuss that number and provides some insights of the repartition within the different causes. It seems this number is estimated over ocean. Does it include coastal regions? Which latitudes?

R.: The analysis is global, including coastal zones and the whole range of latitudes. This can be verified from Figure 2 (Figure 4 in the revised version), which shows an example of all points with invalid MWR-derived WTCs. This figure allows the reader to inspect the causes that led to the occurrence of all invalid WTCs. A sentence emphasizing that the reader, when analysing Figure 6 (Figure 9 in the revised version) can also refer to Figure 2 has been included. Moreover, the percentage of points contaminated due to each cause has been included in the text for Envisat cycle 12 (the same cycle used to generate Figure 2).

Row 362: "Only GPD+ estimates retrieved using observations are selected." Which observations? MWR? GNSS?

R.: WTC from along-track MWRs, SI-MWRs and GNSS stations are considered observations. The referred sentence has been rewritten as "Only GPD+ estimates retrieved using observations (valid MWR-, GNSS- and SI_MWR- derived WTCs) are selected, GPD+ estimates based on model have been discarded from this analysis."

Row 370-376: Methodology difficult to understand

R.: The authors have included a more detailed explanation of the methodology.

Row 381: "On the contrary": -> Moreover, Additionally ...

R.: The suggestion has been accepted.

Row 384: "Accuracy assessment" ==> Performance assessment

R.: The suggestion has been accepted.

Row 420: "third party data": what are those third-party data?

R.: Third-party data are WTC observations, other than those from the on-board MWRs. The explanation has been included in the manuscript, where the term is used for the first time.

Figure 5: b) and c) look quite similar with land/ice contaminated pass. Outliers are not obvious in c).

R.: In general, all tracks have land and ice contamination. We decided to keep both figures because the referred tracks cover different oceans and therefore show different WTC variability. This has been highlighted in the text. Also, the discussion of former Figure 5, which has been divided into figures 7 and 8 to add plots showing the geographical coverage as recommended by Reviewer#1, has been extended in the text. The caption of Figures 7 and 8 includes now a brief description of the issues in the MWR-derived WTC.

Figure 7: why is there an increase in the number of points for the GNSS-GPD+ comparison but not for the GNSS-MWR one?

R.: As the tracks gets closer to the coast, the MWR-derived WTC become invalid or are inexistent, therefore the number of valid MWR-derived WTC diminishes. The GPD+ methodology computes a WTC estimate for these along-track points, therefore allowing SLAs to be computed at these locations and epochs. Therefore, the number of valid WTCs in the coastal region increases, being this one of the advantages of the GPD+ methodology.

Figure 9: The green color cannot be seen on the color scale.

R.: The green colour is used for the SLA variance differences with values around zero. A note has been added in the caption of the figure to help the reader interpreting this result.

Figure 10: What is this peak around latitudes 50_N?

R.: The peak in latitudes 50°N is related to the large reduction in SLA variance when the GPD+ WTC is used instead of the Comp WTC or the MWR-derived WTCs. This can be seen in the original Figure 9, as dark blue pixels (GPD+ WTC performs better than Composite WTC or MWR-derived WTC) are found in the westernmost coastal regions of the oceanic basins (e.g., in the Gulf of Saint Lawrence or in the Sea of Okhotsk sea).

Summary of relevant changes included in the revised version of the manuscript

The main changes introduced in the manuscript following the comments and suggestions of the two Reviewers can be summarised as:

- Sections containing the Abstract and the Conclusions have been updated to accommodate the new results presented in the revised version of the manuscript.
- Some parts of the text have been moved to new sections or were rewritten/completed to be clearer and more informative.
- Figures 1 as well as figures 11, 12 and 13 have been updated, the latter to include the results for the comparison of the GPD+ WTC with the MWR-derived WTC, instead of that for the Comp WTC, following the concerns raised by Reviewer#2.
- Previous Figure 5 has been divided into Figures 7 and 8 and the geographic location of the Envisat tracks have been added, following the recommendation of Reviewer#1.
- New figures have been added to the revised version (Figures 2, 3 and 14).
- Tables 1 and 4 have been updated, the former to include more information, the latter in the sequence of the last update of the GPD+ database (performed to include more data for the recent missions).
- A new table (Table 2) has been added in the revised version.
- All figures and tables have been renumbered.
- Section 3.2 has been divided into sections 3.2.1 and 3.2.2 describing the global and the regional (coastal) results, respectively, and the text has been extended.
- Reference Vieira et al. (2019c) has been updated, since at the time of this revision it has already been published.
- Reference AVISO (2017) has been removed.
- Five new references (Bevis et al. (1994), Rudenko et al., (2017), Valladeau et al. (2015), Dinardo et al. (2020) and Escudier et al. (2017)) have been inserted in the revised version.

A coastally improved global dataset of wet tropospheric corrections for satellite altimetry

Clara Lázaro^{1,2}, Maria Joana Fernandes^{1,2}, Telmo Vieira^{1,2}, Eliana Vieira¹

5 ¹Faculdade de Ciências, Universidade do Porto, 4169-007 Porto, Portugal

² Centro Interdisciplinar de Investigação Marinha e Ambiental (CIIMAR/CIMAR), Universidade do Porto, 4450-208 Matosinhos, Portugal

Correspondence to: Clara Lázaro (clazaro@fc.up.pt)

10 **Abstract.** ~~Global mean sea level is a valuable proxy to understand climate change and how it operates, since it includes the response from various components of the climate system. Global sea level rise is accelerating, which is a concern for coastal areas management from medium to long term time scales. Satellite radar altimetry (RA) has been providing us information regarding the sea level anomaly (SLA) field and its space-time variability since the early 90s. As satellite orbit determination, reference surfaces (e.g., mean sea surface) and instrumental, range and geophysical corrections improved over the decades,~~
15 ~~the data from past missions were reprocessed subsequently, leading to an SLA dataset over open ocean accurate to the centimetre level.~~ The accuracy of satellite radar altimetry (RA)-~~altimetry~~ is known to deteriorate towards the coastal regions due to several reasons, amongst which the improper account for the wet path delay (WPD) can be pointed out. The most accurate WPDs for RA are derived from the on-board microwave radiometer (MWR) radiance measurements, acquired simultaneously as the altimeter ranges. In the coastal zone, however, the signal coming from the surrounding land contaminates
20 these measurements and the water vapour retrieval from the MWR fails. As meteorological models do not handle coastal atmospheric variability correctly yet, the altimeter measurements are rejected whenever MWR observations are absent or invalid. The need to solve this ~~altimetry-RA~~ issue in the coastal zone, simultaneously responding to the growing demand of data in these regions, motivated the development of the Global Navigation Satellite Systems (GNSS)-derived Path Delay (GPD) algorithm.

25 The GPD combines WPD from several sources through objective analysis (OA) to estimate the WPD or the corresponding RA correction accounting for this effect, the wet tropospheric correction (WTC), for all along-track altimeter points for which this correction has been set as invalid or is ~~absent~~not defined. The current GPD version (GPD Plus, GPD+) uses as data sources WPD from coastal and island GNSS stations, from satellites carrying microwave radiometers, and from valid on-board MWR measurements. The GPD+ has been tuned to be applied to all, past and operational, RA missions, with or without an on-board
30 MWR. The long-term stability of the WTC dataset is ensured by its inter-calibration with respect to the Special Sensor Microwave Imager (SSM/I) and SSM/I Sounder (SSM/IS). The dataset is available for TOPEX/Poseidon (T/P), Jason-1 and

Jason-2 (NASA/CNES), Jason-3 (NASA/EUMETSAT), ERS-1, ERS-2, Envisat and CryoSat-2 (ESA), SARAL/AltiKa (ISRO/CNES) and GFO (U.S. Navy) RA missions. The GPD+ WTC for Sentinel-3 ([ESA/EUMETSAT](#)) shall be released soon. The present paper describes the GPD+ database and its ~~independent validation assessment~~ through statistical analyses of Sea Level Anomaly (SLA) datasets, calculated either with GPD+, ECMWF ReAnalysis Interim (ERA Interim) model or MWR-derived WTCs. Global results, as well as results for three regions (North American and European coasts and Indonesia region), are presented for the recent ESA's Envisat Full Mission Reprocessing (FMR) V3.0. Overall, Global results show that the GPD+ WTC leads to a is the most effective in reducingreduction in the SLA variance of 1-2 cm² in the coastal zones, when used instead of the ERA WTC, which is one of the WTC available in these products and can be adopted when the MWR-

derived WTC is absent/invalid in the coastal regions, in particular for the ESA missions. The improvement of the GPD+ WTC over the ERA WTC is maximum over the tropical oceans, particularly in the Pacific Ocean, showing that the model-derived WTC is not able to capture the full variability of the WPD field yet. The statistical assessment of the GPD+ for the North American coast shows a reduction in SLA variance, when compared to the use of the ERA-derived WTC, of 1.2 cm², on average, for the whole range of distances from coast considered (0-200 km). Similar results are obtained for the European

coasts. For the Indonesia region, the use of GPD+ WTC instead of that from ERA leads to an improvement, on average, of the order of 2.2 cm² for distances from coast up to 100 km. Similar results have been obtained for the remaining missions, particularly for those from ESA. MoreoverAdditionally, GPD+ recovers ~~a the WTC for a~~ significant number of ~~measurements~~along-track altimeter points with missing or invalid MWR-derived WTCs, due to land, rain and ice contamination and instrument malfunctioning, which otherwise would be rejected ~~due to land, rain and ice contamination and instrument malfunctioning~~.

Consequently, GPD+ database has been chosen as the reference WTC in the Sea Level Climate Change Initiative (CCI) products; the GPD+ has also been adopted as reference in CryoSat-2 Level 2 Geophysical Ocean Products (GOP). Strategies to further improve the methodology, therefore enhancing the quality of the database, are also discussed. The GPD+ dataset is archived on the homepage of the Satellite Altimetry Group, University of Porto, publicly available at the repository https://doi.org/10.23831/FCUP_UPORTO_GPDPlus_v1.0 (Fernandes et al., 2019).

55 **1 Introduction**

Since the early 1990s, satellite radar altimetry (RA) missions have been observing the oceans, measuring global and regional mean sea level, as well as its change. Altimeters on board RA missions measure the sea surface height (SSH) by subtracting the measured altimeter range, the nadir-measured distance between the satellite and the sea surface, from the satellite altitude (H) above a reference ellipsoid of a terrestrial (geocentric) reference frame, currently known with a centimetre-level radial error ([Rudenko et al., 2017](#)). In the computation of ~~precise-accurate~~ SSH, a multitude of well understood effects must be properly considered: those that introduce errors in the measured range, e.g. atmosphere propagation delay, and those that induce SSH variability other than that under analysis over time, e.g. ocean tides and atmospheric pressure. Sea surface height

anomalies, or sea level anomalies (SLA), are computed subtracting a mean sea surface (MSS) from the corrected SSH measurements.

65 Range corrections are required to account for the delay the microwave pulses suffer, as they propagate through the atmosphere (ionospheric and tropospheric corrections, the latter including the effect of the neutral atmosphere) and for the interaction with the sea surface (sea state bias); geophysical corrections account for the sea level variability due to tides (ocean, solid earth and polar tides, as well as loading effects) and for the ocean's response to atmospheric pressure (dynamic atmospheric correction, a combination of a high-frequency signal with the low-frequency inverted barometric response of the ocean); if needed to
70 homogenize and inter-calibrate multi-mission data, the reference frame offset correction is applied, accounting for instrument-dependent effects and biases between missions (Fernandes et al., 2014). A detailed description of the corrections is given in Chelton et al. (2001) [and Escudier et al. \(2017\)](#).

This may be expressed as:

$$SLA = H - R_{corr} - MSS \quad (1)$$

75 where R_{corr} is the altimeter range (R) corrected for all instrument (ΔR_{inst}), range (ΔR_{range}) and geophysical (ΔR_{geoph}) effects:

$$R_{corr} = R + \sum(\Delta R_{range} + \Delta R_{geoph} + \Delta R_{inst}) \quad (2)$$

The quality of the SLA measurements has considerably improved over time, essentially because new models and corrections have become available, and satellite orbit determination as well as radar processing ~~has~~ [have](#) improved in absolute accuracy. This is particularly true over open ocean, where altimeter waveforms do not depart from the expected shape given by the
80 Brown model and geophysical and range corrections can be accurately estimated (Chelton et al., 2001; [Escudier et al., 2017](#); Fernandes et al., 2006).

The total tropospheric path delay for microwaves can be divided into two components, one depending only on the surface pressure, the hydrostatic term, and a remainder that mainly depends on water vapour abundance, commonly termed wet path delay (WPD) (Askne and Nordius, 1987). The dry tropospheric correction (DTC) accounts for the hydrostatic term that, despite
85 having an absolute value as large as 2.3 ± 0.2 m in the zenith direction at sea level, [over the ocean it](#) can be calculated with millimetre-accuracy, provided the [surface-sea level](#) atmospheric pressure is known at each location (Fernandes et al., 2014). From here onwards, the terms DTC and WTC are used to refer to the dry and wet tropospheric corrections (negative values), respectively, applied to RA measurements and, accordingly, DPD and WPD to the corresponding absolute values. The DTC computation can be carried out using sea level pressure fields given by numerical weather models (NWMs), as described e.g.
90 in Fernandes et al. (2013a). Ranges are corrected for the wet path delay through the wet tropospheric correction (WTC), possessing an absolute value less than 0.50 m ([Chelton et al., 2001](#)). ~~Contrasting~~ [In opposite](#) to the estimation of the DTC, the WTC retrieval requires the knowledge of the full water vapour and temperature profiles, which are known to be highly variable, both temporally and spatially (Dousa and Elias, 2014; Vieira et al., 2019a). Therefore, to properly account for the microwave propagation delay through the troposphere, RA missions carry aboard a passive microwave radiometer (MWR), nadir-looking

95 instruments capable of measuring both the water vapour and the cloud liquid water components of the wet path delay, from brightness temperatures in appropriate bands of the microwave spectrum.

Radiometers embarked on RA missions can be divided into two main groups (Steunou et al., 2014). Two-channel MWR, operating at frequencies 21–23.8 GHz, the primary water vapour sensing channel, and 34–37 GHz, carried by the European Space Agency (ESA) ERS-1, ERS-2 and Envisat, by ESA/EUMETSAT Sentinel-3, ~~and~~ by US Navy's mission Geosat Follow-
100 On (GFO) and by the joint Indian Space Research Organization (ISRO) and Centre National d'Études Spatiales (CNES) SARAL (Satellite with ARgos and ALtiKa) missions; three-channel MWR carried by NASA's missions TOPEX/Poseidon (T/P), Jason-1, Jason-2 and Jason-3, with an additional channel operating at 18–18.7 GHz. MWR footprints vary in the range of from 20 to 45 km, depending on the instrument and frequency except for the one embedded within SARAL's altimeter, for which the dual frequency radiometer has a footprint of diameter less than 12 km (Steunou et al., 2014).

105 Accurate measurements of the integrated amount of water vapour and cloud liquid in the atmosphere are achievable in open ocean, but difficult to perform in coastal regions where the precise modelling-estimation of the WTC is still challenging. Nearly a decade ago, the RA community started developing new algorithms and methodologies aiming at recovering altimetric data in the coastal region, leading to a more mature status of the emerging, at that time, field of coastal altimetry. Altimetric data in the closest 50 km away from the coast are usually flagged as invalid, being therefore discarded, or non-existent due to
110 several reasons. On the one hand, the shape of the waveforms no longer can be described by the Brown model and this is overcome using specific retracking techniques; on the other hand, the accurate modelling of some corrections is difficult. This is particularly true for the estimation of the wet path delay, and consequently of the WTC, since in coastal areas the measurements of the MWR are in general contaminated by land, in part due to the large diameter of its footprint. Also important, is the fact that the WTC retrieval algorithms are designed for open-ocean conditions, thus assuming surface
115 emissivity values only valid for the corresponding to open-ocean easeconditions; however, surface emissivity can be highly variable when the surrounding land surfaces contribute partially to the returning signal, causing a failure of the retrieval algorithms. Different strategies have been proposed in the last years to accomplish the estimation of the wet tropospheric correction in coastal areas, which are summarized in Cipollini et al. (2017). One of these is the GNSS (Global Navigation Satellite System) derived Path Delay (GPD) algorithm. The GPD was developed by the University of Porto (UPorto) in the
120 scope of the ESA's funded project COASTALT (Vignudelli et al., 2009) to estimate the WTC for correcting the altimetric data in the coastal European region. It has evolved over the last years reaching a mature status recently (GPD Plus, GPD+), with the global computation of a WTC dataset for all operational and past RA missions that has been adopted as reference to derive the ESA Climate Change Initiative Sea Level dataset (Quartly et al., 2017, Legeais et al., 2018).

With this article, it is aimed to inform GPD+'s current and potential new users about the content and the services that the
125 GPD+ database provides. The methodology, the input data sources and the supplied GPD+ products are presented and described. The WTCs provided in the GPD+ products have been assessed through various SLA variance statistical analyses, inspecting simultaneously the impact of the correction on sea level variability. Results are provided for the recently reprocessed and released Envisat Geophysical Data Records (GDR) V3.0 dataset, both globally and for three selected regions (North

American and European coasts and Indonesia region), aiming at showing the improvement in the description of the SLA field when the GPD+ WTC is adopted instead of the MWR- or ERA-derived WTCs provided in the Envisat GDR V3.0. A summary of the results for the remaining satellite altimetry missions is also provided. For more details concerning these results, readers may refer to Fernandes et al. (2015) and Fernandes and Lázaro (2016, 2018). To ensure the long-term stability of the GPD+ WTC, an important issue when trends in sea level change are calculated, the large set of radiometers used in this study have been previously inter-calibrated through the inter-comparison of the various datasets. The calibration parameters of this analysis are presented for all satellite altimetry missions. Additionally, strategies to further improve the methodology, aiming at enhancing the quality of the GPD+ products publicly available in the database, are shared.

The aim of this study is to describe and grant access to the GPD+ collection of WTCs for RA provided by UPorto (Fernandes et al., 2019). Results regarding the validation of this dataset are shown for the recently reprocessed and released Envisat Geophysical Data Records (GDR) V3.0 dataset, for which the GPD+ shows a substantial improvement in the computation of the SLA dataset over coastal and polar regions. For more results, readers may refer to Fernandes et al. (2015) and Fernandes and Lázaro (2016, 2018). This paper is organised in five sections. The input data are described in Sect. 2.1, the technical description of the algorithm is presented in Sect. 2.2, and the generated WTC database in Sect. 2.3. Section 3 describes the results obtained globally and for three zoomed-in regions, selected to show the performance of the database in coastal regions, and includes their discussion. Section 4 describes the availability of the GPD+ products. The conclusions are provided in Section 5.

2 The GPD+ algorithm and the GPD+ WTC database

The ~~main objective of the~~ GPD+ algorithm ~~is the estimation of~~ has been developed to estimate the WTC ~~overfor~~ coastal regions, where MWR-derived WPDs, if available, are usually ~~invalid-anomalous~~ values due to land contamination both in the altimeter and MWR observations. If uncorrected, this leads to a rejection of a large number of points in these regions. To accomplish this task, WPD datasets from different sources are combined through an optimal interpolation scheme. ~~The input data are described in Sect. 2.1, the technical description of the algorithm is presented in Sect. 2.2 and the generated WTC database in Sect. 2.3.~~

2.1 Input WPD observations

In the most recent version of the algorithm (GPD+), WPDs from the following sources are used as input: 1) tropospheric zenith total delays (ZTDs) computed at a dense GNSS network of stations distributed globally along the coastline; 2) total column water vapour (TCWV) products generated from measurements from passive imaging MWR on board environmental and meteorological Earth observation satellites; 3) along-track ~~WTC-WPD~~ (the ~~symmetric-absolute value~~ of ~~WPDWTC~~) measurements from the on-board MWR, before they become invalid when approaching the coast. The algorithm also provides

160 valid WTC estimates for offshore and open-ocean measurements for which invalid WTC are detected, provided WPD observations are available at those geographical locations. ~~In t~~This way, the algorithm attempts to eliminate measurements contaminated by heavy rain and ice, as well as faulty measurements due to, e.g., instrument malfunctioning.

2.1.1 WPD from GNSS-derived ZTD

Tropospheric propagation delays are a source of error in GNSS positioning as well, being therefore estimated, at each GNSS station, for each observation. The quantity computed at each station is the slant total delay (STD) between the satellite and the ground-based station. Provided *a priori* value for the zenith hydrostatic delay (ZHD or DTC in satellite altimetry terminology), computed from knowledge of surface atmospheric pressure either measured locally or NWM-derived meteorological data, and mapping functions for hydrostatic and wet components are known, the ZTD at station height can be computed with millimetre accuracy (Pany et al., 2001; Fernandes et al., 2013a, 2015). Mapping functions relate the delay in the station zenith direction, ZTD, with that in the actual satellite-station direction, STD. While the wet delay varies in time in an unpredictable way, the ZHD can be derived with millimetre accuracy from e.g. NWMs (Pany et al., 2001). Therefore, an *a posteriori* more accurate ZHD can be computed and subtracted from the estimated ZTD, yielding the wet delay in the zenith direction (zenith wet delay, ZWD or WPD in satellite altimetry terminology). ZHDs, computed with millimetre accuracy at station height from ZHDs at sea level derived from sea level pressure (SLP) fields from an NWM (e.g. [European Centre for Medium-Range Weather Forecasts ReAnalysis \(ERA\)](#) Interim or ECMWF operational [models](#)) and further reduced to station height using an adequate height reduction procedure, are used to derive WPD from GNSS (Fernandes et al., 2013a, 2015). The WPDs obtained this way are given at station height and therefore at a level different from that of interest in satellite altimetry, which is the mean sea level. Therefore, the height reduction of the WPD is required. This has been performed using an exponential decay function, empirically obtained by Kouba (2008), valid for WPD height reductions for heights below ~1000 m (Vieira et al., 2019b).

180 This summarises the methodology adopted by UPorto in the computation of WPD from GNSS measurements. A complete description of the methodology and its assessment can be found in Fernandes et al. (2013a, 2015) or Vieira et al. (2019b). Zenith total delays (ZTD) estimated at UPorto, along with those available online from international GNSS services (IGS (International GNSS Service), EPN (EUREF Permanent Network) and SuomiNet) and from several stations located at the German Bight, provided to UPorto by the Technische Universität Darmstadt (TUD) in the scope of ESA's Climate Change Initiative (CCI) project, have been used. More than 800 coastal (at distances from the coast less than 100 km) and offshore GNSS stations, with altitude below 1000 m, are being used at the time of writing. Figure 1 shows, ~~for the Envisat period,~~ the increase both in the number of GNSS stations and GNSS observations used as input in the GPD+ algorithm. The number of stations almost duplicates, in 2008.5, relatively to the number of stations in the beginning of the period and have been continuously increasing until present. [Figure 2 shows the location of the coastal and island GNSS stations used as input in the GPD+ and the standard deviation \(SD\) of the WTC field from ERA Interim for the along-track point of Envisat cycles 96-108 \(11/2010-11/2011\). WTC SD ranges from 1–15 cm and has a strong dependency with latitude. Maximum values of WTC SD can be seen in the tropical southern and eastern Asia, in the north of Australia, and around Mexico and southwest USA, due to](#)

variable precipitation determined by the monsoon regime (Vieira et al., 2019a). Over the polar regions, minimum WPD SD values are found (values < 3 cm).

195

2.1.2 WPD from scanning imaging MWR

The methodology developed by UPorto to calculate the WTC from TCWV products from passive imaging MWR on board Earth observation satellites is discussed in detail in Fernandes et al. (2013b, 2015). Due to their large spatial and temporal resolutions and spatial coverage, SI-MWR data increase the number of observations to use as input in GPD+ over the ocean, thus allowing the recovery of e.g. entire tracks for which the MWR-derive WTCs are missing due to instrument malfunctioning (i.e. where MWR- and GNSS-derived observations are not available). For this reason, their use improves the description of the WPD field. These Additionally, these data are of extreme importance ~~for use in the GPD+~~ since they provide the unique possibility of computing the WTC over open ocean for those RA missions that do not possess an MWR, like e.g. CryoSat-2 (CS-2). In fact, GPD+ is an upgrade from the GPD methodology, which was developed to compute the WTC only for coastal points, relying only on GNSS and valid on-board MWR measurements. Motivated by the need to compute an improved correction for CS-2, the SI-MWR data set was included and the focus of the correction extended to open ocean.~~In fact, GPD+ is an upgrade from the GPD methodology, which was developed to compute the WTC only for coastal points, thus relying only on GNSS and valid on-board MWR measurements.~~

200

205

TCWV datasets from 20 scanning imaging (SI) passive MWR (SI-MWR), available at NOAA Comprehensive Large Array-Data Stewardship System (CLASS) and at Remote Sensing Systems (RSS) have been selected. CLASS includes data from the AMSU-A (Advanced Microwave Sounding Unit-A) on board NOAA-16, -17, -18, -19, MetOp-A and MetOp-B satellites. RSS delivers datasets for several sensors, namely SSM/I (Special Sensor Microwave Imager) and SSM/IS (SSM/I Sounder) on board DMSP (Defense Meteorological Satellite Program) satellites (F08, F10, F11, F13, F14, ~~and~~ F16, F17 and, F18, respectively), WindSat aboard Coriolis, Tropical Rainfall Measuring Mission's (TRMM) radiometer TMI (TRMM Microwave Imager), Global Precipitation Measurement's (GPM) Microwave Imager (GMI), AMSR-E (Advanced Microwave Scanning Radiometer for EOS) on board AQUA and AMSR-2 in the Japanese Global Change Observation Mission – Water Satellite 1 (GCOM-W1). Two types of TCWV products have been used: Level-2 swath products in HDF-EOS2 format (near real time products, 14-15 orbital swaths per day available for each instrument) from all data sources except RSS, and Level-2 gridded products (two grids per day, each containing the ascending/descending passes) in binary format from RSS. Table 1 shows the availability of the TCWV products used as input in GPD+ and their main characteristics (spatial and temporal resolution and availability). Figure 3 shows the number of SI-MWR along time for each RA mission.

210

215

220

For the Envisat mission, for example, the number of SI-MWR increased from 4 to 11, from the beginning (05/2002) to the end (03/2012) of the mission, respectively.

225 The calculation of the path delay from TCWV can be performed knowing that the quotient between WPD and TCWV is modelled by a decreasing function of WPD of the type

$$\frac{WPD}{TCWV} = a_0 + a_1 TCWV + a_2 TCWV^2 + a_3 TCWV^3 \quad (3)$$

with constants $a_0 = 6.8544$, $a_1 = -0.4377$, $a_2 = 0.0714$, and $a_3 = -0.0038$, for TCWV in the right-hand side of the equation in centimetres (Stum et al., 2011).

230 It is known that, in addition to TCWV, WPD also depends on temperature. Expressions such as Eq. (3) account for an implicit modelling of this dependence. Fernandes et al. (2013b) have shown that this expression leads to similar results as those obtained by adopting formulae that make use of explicit values of atmospheric temperature given e.g. by an NWM, as the one adopted by Bevis et al. (1994). The authors show that after sensor inter-calibration, a crucial step to guarantee datasets consistency, the WTC derived from both methods are equivalent, with differences within ± 2 mm.

235 **2.1.3 WPD from along-track MWR**

The provenience of the MWR-derived WTC used as input in the GPD+ is the Radar Altimeter Database System (RADS) (Scharroo et al., 2012), except for Envisat, as this mission has been recently reprocessed, and SARAL before cycle 30 (for cycles 1 to 30, the MWR-derived WTC provided in the products from the Prototype for Expertise on AltiKa for Coastal, Hydrology and Ice (PEACHI) project (Valladeau et al., 2015), available through AVISO+, have been used). It is recalled that the WPD is the absolute value of the WTC, the quantity of interest in satellite altimetry. ~~We recall that the WTC is the symmetric of the wet path delay and the quantity of interest in satellite altimetry.~~ RA data necessary to compute the SLA datasets used to validate the GPD+ WTC are also extracted from RADS. For each RA mission, only valid MWR-derived WTC are input in the algorithm, therefore the correct identification of valid/invalid measurements is of crucial importance. Exception made for CryoSat-2 (for which, in the absence of an on-board MWR, a WTC is generated for all along-track altimeter points), GPD+ estimates a WTC for those points with an invalid MWR-derived WTC only. In this way, the valid observations from the on-board MWR are preserved.

Invalid measurements are usually detected using a set of flags, some of them provided in the products, as the radiometer flag for the surface type or the ice flag. If different from 0, these flags indicate invalidity due to land contamination or instrument malfunctioning, or ice, respectively, respectively. MWR-derived WTCs outside the range $-0.5 \text{ m} \leq \text{WTC} < 0.0 \text{ m}$, generally due to heavy rain or ice, are also discarded. A validity criterion based on the distance from coast is also applied: if the location of a certain MWR measurement is such that its distance from the coast is less than a threshold value, then this measurement is most certainly contaminated by land. Threshold values used in this criterion depend on the RA mission. Adopted values are based on the known characteristics of each instrument and on an independent assessment of the on-board MWR observations using GNSS-derived WPDs in the coastal zones (Vieira et al., 2019b). Results for ESA missions are alike, showing that land contamination occurs at distances from coast less than 30 km; the same threshold has been used for GFO and T/P. In relation to the remaining NASA missions, values of 15 km have been used for Jason-1/2/3. For SARAL, a threshold value of 15 km

was adopted. Also, noisy MWR measurements are discriminated using median filters based on statistical analysis of the differences to the NWM-derived WTC on the same along-track point and neighbouring points. Invalid measurements are detected if: 1) radiometer surface type flag is different from 0; 2) ice flag is different from 0; 3) do not satisfy the defined statistical criteria or are outside WTC limits, 4) are at a distance from coast less than the threshold established for that mission. Figure 2-4 shows all the along-track points flagged as invalid for Envisat cycle 12, which reach 29.5%. As it will be shown in Sect. 3 for Envisat, per cycle and on average, approximately 30% of the oceanic points have an invalid WTC value; for these points, an SLA value cannot be computed due to the invalidity of the WTC or of other corrections, or because certain criterion is not met (e.g., number of 18 Hz measurements to compute the 1 Hz values used less than the imposed minimum). For approximately 10% of all oceanic points (including the coastal zone), the WTC is the only correction that prevents the computation of the SLA. This is, on average, the percentage of points with a valid SLA value recovered by the GPD+ algorithm for a mission such as Envisat. For other missions, this percentage depends on instrument type, band of latitudes covered by the mission (which determines the amount of ice contamination) and instrument performance, and is summarised in the conclusions.~~For approximately 10% of all oceanic points, the WTC is the only correction that prevents the computation of the SLA. This is, on average, the percentage of points with a valid SLA value recovered by the GPD+ algorithm for a mission such as Envisat.~~

2.1.4 Radiometer Calibration

Global mean sea level is a valuable proxy to understand climate change and how it operates, since it includes the response from various components of the climate system. Also important in the analysis of trends in sea level change, which requires a 0.3 mm/yr error level set by the Global Ocean Observing System (GOOS), is the stability of the altimetry dataset. Therefore, the examination, and consequent accounting for, of drifts in the corrections, particularly in the WTC, is necessary to ensure that the corrections are stable in time and do not introduce spurious trends in the SLA.

~~Uncertainty in sea level rise quantification is required by the Global Ocean Observing System to be under 0.3 mm/year.~~ To ensure long-term stability of the GPD+ WTC, the large set of radiometers used in this study have been previously inter-calibrated through the inter-comparison of the various datasets. Data from the reference missions have been calibrated against those of the Special Sensor Microwave Imager (SSM/I) and the SSM/I Sounder (SSM/IS) by selecting matching points from each pair of missions operating simultaneously with a difference in time and location less than 45 minutes and 50 km, respectively (Fernandes et al., 2013b). The time-series of these matching points was used with a 3-parameter model to adjust offset (a), scale factor (b) and linear trend (c) for each mission (Fernandes and Lázaro, 2016):

$$Y = a + bX + c(T - T_0), \quad T_0 = 1992 \quad (4)$$

The remaining altimetry missions were then inter-calibrated to these calibrated datasets from the reference missions since orbits of most all remaining missions are sun-synchronous with different times for the Equator crossing than those of the SSM/I(S), with a small number of matchups mostly found at high latitudes, not representative of the WTC variability. For these missions, data were analysed at crossover points and the same adjustment parameters were obtained from the time-series. For the crossover analysis, only data with difference in time less than 180 minutes were used. As an example, the calibration parameters have been obtained for Envisat are $a=-6.82$ mm; $b=0.991$ and $c=-0.0028$ mm/yr, showing that the trend is negligible and indicating that the dataset is well aligned with the altimeter reference missions and with SSM/I and SSM/IS. The small offset and scale factor have the impact of making the correction more negative by 6-7 mm. The calibration parameters (offset, scale factor and linear trend) obtained for all satellite altimetry missions with an on-board MWR available in the GPD+ database are presented in Table 2.

2.1.5 WPD from NWM

Space-time collocated WTCs from NWM grids are adopted in the OA as first guess. Usually ~~two models from the European Centre for Medium range Weather Forecasts (ECMWF) are used: ReAnalysis (ERA) Interim~~ERA model, provided each 6 hours with $0.75^\circ \times 0.75^\circ$ spatial resolution, ~~is used for missions prior to 2004, and, For missions after this period, the~~ECMWF Operational Model (ECMWF Op., 6-hour time interval, $0.125^\circ \times 0.125^\circ$ spatial resolution) ~~is selected, for missions after this period. Since the ECMWF Op. has undergone several updates, not having the same accuracy over time, for all missions with data before 2004 (T/P, Jason-1, ERS-1, ERS-2, Envisat and GFO) ERA Interim is used in GPD+, while for the most recent missions the ECMWF Op. model is adopted.~~ Therefore, in the absence of observations to improve the first guess, a WTC estimate from ERA Interim or ECMWF Op. is output from GPD+. This is normally the case for the northernmost latitudes. In addition, to reduce data discontinuities, output values solely based on model data are adjusted to the valid MWR measurements of each cycle by solving for the mean difference, of the order of a few millimetres, between the two datasets for all points with a valid MWR-derived WTC.

2.2 Algorithm description

The GPD+ algorithm is based on objective analysis and estimates the wet path delay, given measurements from different sources of the variable under study at a restricted number of data points. The statistics of the field are estimated in the form of a correlation function and of the measurement errors associated with each type of observation. The expected error associated to this estimate is also derived. The technique for the objective analysis is fully described in Bretherton et al. (1976).

The algorithm has been originally implemented to calculate the WTC in the coastal zone, where the retrieval of the wet path delay from on-board MWR measurements become invalid. Later, it has evolved to provide the correction also over open ocean, providing the correction during, for example, instrument malfunctioning, and inland waters.

For the altimetry missions carrying an on-board MWR (all but CryoSat-2), a GPD+ WTC estimate is calculated for all along-track points with an MWR-derived WTC deemed as invalid, using valid WTC observations from different sources at the nearby location and within a time interval, defined by the spatial and temporal radiuses of influence used in the computation. For all satellite missions but CryoSat-2 and for each along-track point deemed as invalid, a WTC estimate is calculated from valid WTC observations from different sources at the nearby location and within a time interval, defined by the spatial and temporal radiuses of influence used in the computation. In the current GPD+ version, these radiuses have been set equal to the correlation

spatial and temporal scales. Whilst the spatial correlation scale varies spatially, both with longitude and latitude (Fernandes and Lázaro, 2016), the temporal correlation scale has been set to 100 minutes (Bossler et al., 2007). For the CryoSat-2 mission, since it does not carry a passive microwave radiometer, a GPD+ WTC estimate is computed for every along-track point using third-party data (WTC observations, other than those from the on-board MWRs) only. The location and time of each along-track are those provided in the GDR products present in RADS. Due to the temporal difference between adjacent satellite tracks, in practice only along-track valid on-board MWR measurements from the track to which the point of estimation belongs are used.

Regarding the accuracy of the observations, a constant value of 0.5 cm has been set for the white noise of the GNSS- and MWR-derived wet path delays, while for the SI-MWR observations a value between 0.7 cm and 1.1 cm, depending on the mission, has been used (Fernandes et al., 2013b).

The procedure for finding a good estimate of the WTC starts with the definition of the first guess or *a priori* value for the field. In the current version of the algorithm, the first guess is the space-time collocated NWM-derived wet path delay from ERA Interim or ECMWF-Op, the most suitable depending on purpose and time period. Therefore, in the absence of observations, the GPD+ WTC equals the NWM-derived WTC. In the presence of observations, its input number is limited to 15 in order to decrease computational burden; the chosen observations are those for which the statistical weights are larger, meaning that for these measurements the differences in acquisition time and distance to the point where the estimate is being calculated are the smallest.

The estimates for those missions that embark an MWR rely on the valid MWR-derived WPD values. Therefore, one of the core competencies of the GPD+ methodology is its ability to detect corrupted WTC values, which is achieved through the definition of improved criteria for their detection. Measurements flagged as invalid are those that: - have the radiometer surface type flag set as 1; - are contaminated by ice; - are contaminated by rain; - are outside the range [-0.5 m, 0.0 m]; have mission-dependent flags (e.g., radiometer along-track averaging flag for Envisat) set as 1; - do not satisfy several statistical criteria based on the differences between adjacent measurements and between MWR and NWM values; - are at distances from coast less than 15 or 30 km, depending on being a reference and SARAL or ESA mission.

A general Gaussian space-time correlation function of the form

$$G(r, \Delta t) = e^{-\frac{r^2}{c^2}} \cdot e^{-\frac{\Delta t^2}{T^2}} \quad (5)$$

where r and Δt represent the distance and the time interval between acquisitions of each pair of points, and C and T are the spatial and temporal correlation scales, respectively, has been adopted to account for the spatial and temporal variability.

A diagram showing the workflow of the GPD+ algorithm is shown in Fig. 35.

355 2.3 GPD+ WTC files description and nomenclature

As the impact of the correction is mainly in ocean studies, in the current version, the final GPD+ WTCs are continuous products over the ocean and coastal regions. To prevent the loss of points when interpolating to 20 Hz points, in addition to ocean points, the closest point over land is included, provided it is within a distance less than 50 km from the ocean. This guarantees that observations over ocean necessary to compute the WTC for this location are still available within the radiuses of influence centred on the point. The WTC estimated for the closest points over land are also estimated at sea level.~~To prevent the loss of points when interpolating to 20 Hz points, in addition to ocean points, the closest land point is included, provided it is within a distance less than 50 km from the ocean.~~ For Envisat, as this mission has been recently reprocessed (Version 3.0), the GPD+ WTC covers the whole range of latitudes and surfaces, including land. Corrections are currently publicly available for ten RA missions: T/P, Jason-1, Jason-2, Jason-3, GFO, ERS-1, ERS-2, Envisat, SARAL and CryoSat-2. Figure 4-6 gives an example of the GPD+ WTC for Envisat's cycle 12, showing global coverage (top panel) and over ocean regions with valid sea level anomaly values (bottom panel). As stated above, the correction has its main impact over the ocean since it is meant to be used to improve satellite altimetry. Over non-oceanic surfaces, the correction has been set equal to the ECMWF ERA Interim or Operational models, depending on the mission, as previously explained (Sect. 2.1.5). As already done for Envisat, future versions of the correction will cover all surface types for all missions. In addition, over non-oceanic regions where WPD observations exist (e.g. from MWR over large lakes or from GNSS), new estimates will be obtained based on available measurements.

The GPD+ WTC products, which content is described in Table 23, are provided for each cycle of the mentioned altimetric missions. For the time and location of each altimeter measurement, specified by the variables 'time_01' in UTC seconds since 2000-01-01 00:00:00.0 and 'geodetic lat_01' and 'lon_01' in degrees as given in each GDR file, the GPD+ wet tropospheric correction, in metres, and its associated validity flag, fields 'GPD_wet_tropo_cor_01' and 'GPD_wet_tropo_cor_qual_01' respectively, are provided at 1 Hz. The sign convention adopted is that the WTC should be added to the range measured by the altimeter to correct it for the range delay. The data-quality flag can take the following values:

- 0: the MWR-derived WTC is valid and, in this case, the GPD+ correction is equal to the MWR-derived WTC, after applying calibration factors, therefore preserving the high accuracy of these data;
- 1: the invalid MWR-derived WTC has been replaced by a valid GPD+ estimate based on observations;
- 2: no observations were available for the computation and the GPD+ estimate is the first guess (i.e., ERA Interim for TOPEX/Poseidon, ERS-1, ERS-2, Envisat, Jason-1 or ECMWF Op. for OSTM/Jason-2, Jason-3, Cryosat-2, SARAL/AltiKa) with possible small bias applied.

- 3: GPD + estimate is outside the valid range ([-0.5, 0.0]), and either the value -0.5 or 0.0 was attributed to the output value (in the most recent implementation this never occurs, as these are replaced by the NWM values).

By using this flag, a knowledgeable user can select the data most suitable for a given application: a continuous correction e.g. for coastal studies, solely the valid measurements for the on-board MWR (e.g. for calibration purposes or global climate studies) or exclude the points solely based on NWM values.

NetCDF files include self-documenting variables and common attributes.

390 The nomenclature selected for the GPD+ dataset is:

`< MISSION>_c<CYCLE_NUMBER>_gpd.nc`

where <MISSION> is two-letter code that depends on the mission (see Table 34) and <CYCLE_NUMBER> is a three-digit number indicating the cycle number of <MISSION>. In all cases, the RADS cycle number convention has been adopted. In cases such as Jason-1 geodetic phase (phase c), cycle numbers are different from those adopted by AVISO. For CryoSat-2, sub-cycle numbers of 27 or 29 days are used according to RADS convention. The availability of GPD+ WTC for each mission is presented in Table 3-4 (Fernandes et al., 2019).

3 Results and Discussion

Results—The results here provided have been obtained in the scope of several ESA-funded research projects and present new scientific findings that have not been published before. For Envisat, the GPD+ WTC was computed for inclusion in the newly reprocessed Envisat Geophysical Data Records (GDR) V3.0 in the ambit of the ESA second Envisat Altimetry Full Mission Reprocessing (FMR).

Results concerning the remaining RA missions are summarised in the conclusions. For more details—results concerning the remaining satellite altimetry missions, the reader is advised to consult Fernandes and Lázaro (2018) for Sentinel-3, Fernandes and Lázaro (2016) for Cryosat-2 and GFO, and Fernandes et al. (2015) for T/P, Jason-1 and -2 and ESA missions, however the latter results were obtained with a previous version of GPD+, the so-called GPD algorithm.

3.1 GPD+ WTC for Envisat Mission

Results for Envisat cover the period May 2002 to April 2012, cycles 6 to 113, which corresponds to the whole Envisat FMR V3.0 dataset released in July 2018 (ESA, 2019). The GPD+ WTC is here compared ~~to~~ with the ECMWF Reanalysis WTC (ERA Interim, ~~GDR—field mod_wet_tropo_cor_reanalysis_01~~) and with the WTC ~~present in the AVISO CORSSH L2P products in July 2019 (AVISO, 2017) derived from the on-board MWR (field 'rad_wet_tropo_cor_sst_gam_01').~~ ~~The latter dataset is usually called Composite Correction since, as GPD+, also combines original MWR values with those from models, in the regions where the former are invalid (Mereier, 2004; Mereier et al., 2010, both present).~~ The main difference between GPD+ and the Composite WTCs is that the first estimates the new WTC values from observations (whenever available) while the second uses only NWM derived WTCs, previously adjusted to the closest valid MWR in the FMR GDRs.

415 ~~This FMR follows the first Envisat Altimetry reprocessing Version (V2.1) completed in 2012 (ESA, 2018).~~ The Envisat V3.0 reprocessed data have been improved, comparatively to the previous version, in many aspects, among which is an increased availability of the data acquired by the MWR, particularly at the beginning of the mission.

In the estimation process, the ERA Interim WTC was selected as first guess, being therefore the adopted values in the absence of measurements, as those occurring over land. ~~Anomalies in this field have been found, with the field out of limits in a set of points, most of them concentrated on certain passes. This is due to the fact that this correction has been computed from 3D model fields at the altimeter measurement altitude. Therefore, whenever the altimeter-derived surface height is not set (Not a Number value, NaN), the corresponding model-derived WTC will also be NaN. As our goal is to be able to provide continuous WTC, without data gaps, this field is unsuitable for use in the GPD+ estimations.~~
420 ~~Anomalies in this field have been found, with the field out of limits in a set of points, most of them concentrated on certain passes, making it unsuitable for use in the GPD+ estimations.~~ ~~To be able to use the ERA Interim WTC~~For this reason, abnormal values present in the products were replaced by those computed from ERA Interim single layer fields of TCWV and 2-metre temperature, with the formulation used by Fernandes and Lázaro (2016).
425

The MWR-based correction used in the generation of ~~these files~~the GPD+ WTC products is the ('rad_wet_tropo_cor_sst_gam_01' GDR field); ~~is~~ hereafter called 'on-board MWR-derived WTC'. Figures ~~5-7 and 8~~ shows the GPD+ WTC for some Envisat tracks, ~~with different WTC variability conditions~~, exemplifying several issues commonly encountered in the on-board MWR-derived WTC that no longer exist in the GPD+ WTC: unavailability of the correction (Fig. 7a); correction contaminated by ice (Fig. 7b and Fig. 8a, at latitudes above $\pm 60^\circ$); existence of outliers (red points over open ocean at latitudes 30°S - 40°S in Fig. 8a); and correction contaminated due to land proximity (red points around coastal regions in all panels except Fig. 7a). It is important to refer that the corrections are shown only for points for which a valid SLA value can be computed after recovering the WTC, as explained in what follows.
430
435

Figure ~~6-9~~ summarizes ~~the results~~, for the whole Envisat period (cycles 06 to 113), ~~interesting results~~. The percentage of points, for each Envisat cycle, with a rejected MWR-derived WTC, for which a GPD+ estimate has been computed are represented in pink and are seen to be around 30%. ~~Figure 4 shows an example of the geographical location of these invalid MWR-derived WTCs for Envisat Cycle 12. For this cycle, the percentage of ocean points with invalid WTC is 29.5% and the corresponding number when only points with valid SLA are selected is 10.9%. By way of example, for the same cycle, the percentage of points recovered due to land, ice and rain contamination, this latter also including outliers, is 8.9%, 17.4% and 3.2%, respectively.~~ The corresponding percentage of points for which a valid SLA value could be computed after the estimation of the WTC by the GPD+ is shown in green. The number of points with valid SLA values (in grey) per cycle is also represented. This figure allows us to show that the GPD+ algorithm leads to the recovery of approximately 10% of the points with valid SLA value. In some cycles this value can reach 20% or more, most of these points are located at high latitudes and in coastal regions. Keeping in mind that ESA missions are near-polar missions with an inclination of $\sim 98.5^\circ$, they have the great advantage, when compared to the reference missions, of acquiring measurements at high latitudes. The recovery of data in these regions, besides along the coastal regions, can be considered one of the greatest advantages of the GPD+ methodology.
440
445

The given figures show that for around 20% of the altimeter measurements, an SLA value could not be computed due to a reason other than the invalidity of the WTC. This means that if in future ~~FRM-FMR~~ the issues that prevent the SLA computation are totally or partially solved, the percentage of data recovery will increase up to a maximum of 30% when the GPD+ WTC is used. Despite being provided continuously, the GPD+ WTC has its largest impact over ocean.

GNSS data cannot be considered independent from the GPD+ WTC, since they have been used in their computation. Therefore, these data are not adequate to use in the GPD+ validation. However, the analysis of the root mean square (RMS) value of the WTC differences, function of distance from coast, can be valuable to inspect the correction in coastal regions, where the methodology is committed to ameliorate the WTC. For this assessment, GNSS-derived WTC have been computed at a network of 60 GNSS stations using the methodology explained in Vieira et al. (2019b). This network has a good geographical distribution and covers regions around the world with different atmospheric variability conditions. This data set consists of WTC measurements at each station location for the whole period of observations available for that station, allowing a non-collocated comparison with WTC estimations at MWR points. Differences between these GNSS-derived WTC and the on-board MWR and the GPD+ WTC retrievals, respectively, have been computed and analysed for the whole Envisat mission.

~~Only GPD+ estimates retrieved using observations are selected.~~ For the acquisition instant of each MWR-derived WTC, a GNSS-derived WTC is ~~computed/interpolated,~~ at the station location, ~~for the same instant using interpolation in time and is further reduced to sea level;~~ at the same acquisition epoch and location ~~of each MWR-derived WTC,~~ the GPD+ WTC is also available, being the ~~latter two~~ collocated both in time and space ~~with each other~~ and over ocean. For each pair of WTCs (MWR and GNSS-derived WTCs and GPD+ and GNSS-derived WTCs, relative to the same instant), the distance from coast of each altimeter point is computed. This process is repeated for each GNSS station with surrounded altimetry measurements and then the whole set of stations is considered, ~~in order to~~ obtain representative results for the whole globe. Differences are binned into 5-km intervals and the RMS values computed function of distance from coast. The results are shown in Fig. 710, for distances up to 65 km from the coast, where red and grey bars represent the number of measurements used to compute the RMS of the differences GNSS-MWR and GNSS-GPD+, respectively. The number of differences is not the same ~~in for~~ each case, ~~since the number of invalid MWR-derived WTCs increases as the tracks approach coast, being discarded from the analysis, while the same along-track points have valid WTC estimates from GPD+.~~ ~~While in the second case only~~ For the comparison GNSS-GPD+, ~~only~~ WTC retrieved from the observations have been selected (~~i.e.~~ those estimated from the model where discarded); ~~for the comparison GNSS-MWR, in the first case only~~ valid MWR values and those ~~that would be~~ rejected solely based on the criteria of distance from coast were ~~kept selected~~ (otherwise the invalid measurements ~~due to e.g. ice or rain contamination~~ would overestimate the results). ~~As expected~~ Consequently, the number of GNSS-MWR differences is generally smaller than the number of GNSS-GPD+ differences. ~~Figure 7 therefore shows that the GPD+ methodology recovers the WTC not only along the coastal areas, but also offshore.~~

The increase in the RMS value of the GNSS-MWR differences in the closest 25 km of the coast, seen in Fig. 710, is a clear indication ~~of~~ of the loss of accuracy of MWR-derived WTCs in this coastal strip. This also shows that when all rejection criteria except the one ~~concerned-related~~ with the distance from coast are applied, land contamination ~~is still present~~ exists, and ~~that~~

~~this criterion is therefore necessary to set up a criterion based on distance from coast. Therefore, all MWR-derived WTCs within distances from coast lesser than this threshold value are flagged as invalid in the GPD+ methodology (even if they are set as valid in the GDR) and not used as observations. Consequently, this threshold value can be useful in forthcoming GPD+ versions to estimate the WTCs for all points within this distance from coast. The decrease in the number of GNSS-MWR differences indicates, in turn, the existence of invalid MWR-derived WTC, not used in these statistics. On the contrary Figure 10 shows that t~~ the RMS of the differences GNSS-GPD+ decreases when approaching coast. Generally, where the stations and the number of differences generally increase, indicating that the GPD+ WTCs estimates are valid up to the coastline and that these WTC values are recovered at all along-track points without valid MWR-derived WTCs. Moreover, Fig. 10 shows that the GPD+ methodology recovers the WTC not only along the coastal areas, but also offshore.

For other missions, results have been presented in Vieira et al. (2019b) and in Fernandes and Lázaro (2018) and are summarised here. For the 2-band radiometers, land contamination on the MWR observations occurs for points at distances from coast smaller than 25-30 km (ERS-1 and ERS-2), 20-25 km (Sentinel-3) and 15-20 km (GFO and SARAL), the latter in agreement with the smaller radiometer footprint of the SARAL MWR. Similar analysis shows that land contamination is observed up to 25-30 km from the coast for T/P and Jason-1 and up to 20-25 km for Jason-2 and Jason-3. These numbers are function both of the instrument footprint size and of the efficiency of the criteria used to detect valid/invalid MWR observations, since in these plots only MWR values that passed all validation criteria, except for the distance from coast, have been used. In summary, for each mission, these analyses show the distances from coast up to which the MWR observations are contaminated by land and must be discarded. Moreover, they also show that GPD+ is efficient in removing this effect.

3.2 Performance assessment ~~Accuracy assessment~~ of the Envisat GPD+ WTC

Water vapour content can be accurately obtained by radio sounding data that could ideally be employed to validate the GPD+ estimates. Despite having high vertical resolution, radiosonde measurements are distributed only over limited areas, i.e., regions where stations are located, do not cover oceanic regions and are very scarce over the Southern Hemisphere (Ye et al., 2017). Therefore, their low temporal and spatial resolutions have reduced their use as a validation tool in the context of satellite altimetry.

For this reason, the GPD+ products have been ~~validated~~ assessed through various SLA variance statistical analyses, ~~assessing~~ analysing simultaneously the impact of the correction on sea level variability. The reasoning for adopting this analysis is that the larger the variance reduction in the SLA signal when using a certain WTC, the better is the correction, i.e., the larger is the reduction in the SLA error, and closer to a pure oceanic signal is the SLA dataset that uses that correction. Therefore, three SLA datasets of collocated along-track points were derived using the same standard corrections (Sect. 1) but the WTC, which can be the ~~GPD+, the Composite correction present in AVISO CorSSH L2P products (Comp)MWR-derived, or the GPD+ or the ERA Interim WTCs.~~ The criteria to select valid SLA are those recommended in the literature and adopted in the standard RADS processing (Scharroo et al., 2012) and include: application of thresholds for all involved fields (satellite orbit above

reference ellipsoid, altimeter range, all range and geophysical corrections), altimeter ice and rain flag (whenever set) and SLA within $\pm 2\text{m}$.

In the comparisons with the ERA Interim, all points with valid SLA have been selected, including points over ocean, coastal and polar regions. However, in the comparisons with the on-board MWR, only points for which the MWR-derived WTC is available and within the -50 cm - 0 cm range are used. Therefore, in the latter case, points with WTCs from the on-board MWR which values are outside this range or are absent, have been discarded from the analyses. For Envisat cycle 12 (Fig. 4), these points are represented in dark green and correspond mainly to entire tracks for which no MWR-derived WTCs are available. Consequently, the number of points used in the WTC comparisons between GPD+ and ERA and GPD+ and MWR is different, however quite similar for both comparisons as it can be seen in Fig.11 below.

Differences between each pair of SLA data sets are computed along track and at crossovers and the weighted variance estimated for the ~~time span of period spanning~~ the whole Envisat period, with latitude-dependent weights. Variance differences have been calculated in such a way that negative values represent an improvement in the description of the SLA field when the GPD+ WTC is used for its generation. For the computation of the crossovers, only measurements with a temporal difference less than 10 days were used. Besides the temporal analysis, the variance differences, both calculated along-track and at crossovers, are also mapped globally for the analysis of their spatial distribution. In this latter case, the variances of the SLA differences are gridded onto 4-degree spatial resolution cells. Along-track SLA variance differences are also computed as function of latitude and distance from coast, where the variance for the whole Envisat period is computed over bins of latitude and distance from coast. Sub-section 3.2.1 shows the results obtained from the global analysis. Sub-section 3.2.2 shows the results zoomed into three different geographical domains: North American and European coasts, selected due the existence of the great quantity of GNSS stations, and Indonesia region, a challenging region in terms of coastal satellite altimetry.

3.2.1 Global Analysis

Figure 8-11 illustrates the ~~obtained~~ results obtained for the period of the whole Envisat mission. From this figure, it is observed that the GPD+ WTC for Envisat represents, in general, a significant improvement when compared to the other WTCs selected for this validation assessment. In these comparisons, all points with valid SLA have been selected. For those points with the Composite WTC outside limits or absent, the ERA Interim WTC value has been assumed for this correction.

Usually the SLA variance reduction is analysed at crossover locations, however since oceanic variability with periods lower than 10 days is neglected when doing this analysis, whilst preserved in the along-track differences, both diagnostics are considered complementary. Figure 11 shows the results for both diagnoses: variance differences calculated along-track are shown in yellow, while variance differences at crossovers are represented in blue.

Using the GPD+ WTC instead of the ~~Comp-MWR-derived~~ WTC (Fig. 8a11a) leads, in the along-track analysis, leads to an improvement in the variance of the oceanic signal of 0.35 cm^2 in average, this improvement increasing in the second half of the period, where values of 2 cm^2 can be reached in some cycles. For the GPD-MWR comparison, the SLA reduction is more noticeable in the along-track analysis than in the crossover analysis. Smaller variance differences are expected in this later

analysis, since the GPD+ generally equals the MWR-derived WTC in open ocean, where most crossovers are located. Adopting the GPD+ WTC instead of the ERA Interim ~~model~~ one (Fig. ~~8b11c~~) leads to a reduction in SLA variance which, in average, is in the range of 1 and 2 cm², for the analysis along the tracks, reaching a maximum value of 3 cm² in the analysis at crossovers. Therefore, it is expected that the GPD+ WTC leads to a reduction in the SLA variance over open ocean too. For both comparisons, the SLA reduction is more noticeable in the along-track analysis than in the crossover analysis. Usually the SLA variance reduction is analysed at crossover locations, however since oceanic variability with periods lower than 10 days is neglected when doing this analysis, whilst preserved in the along-track differences, both diagnostics are considered complementary. Figures 11b and 11d show the number of crossovers (in blue) and along-track pairs (yellow) used, per cycle, in the comparison of the GPD+ with the MWR-derived and ERA WTCs, respectively. A large amount of Envisat data was lost in the period corresponding to cycles 94 and 95, since a new orbit configuration (30-day repeat cycle) for the mission was implemented in October 2010, corresponding to a change from Envisat Phase b to Phase c.

Figure 9-12 shows the reduction in SLA variance globally, after being spatially averaged and gridded onto 4-degree spatial resolution cells, estimated at crossovers for the differences GPD+ and ~~Comp~~ MWR-derived WTCs, and GPD+ and ERA WTCs, on top and bottom plots, respectively. In these plots, blueish colours represent an improvement in the SLA dataset by reducing the SLA variance. The improvement of the GPD+ WTC over the model WTC (Fig. 129b) is clear, with maximum values of variance reduction in the tropical oceans, particularly over the Pacific Ocean. The improvement over the Southern Ocean and around the coast of Antarctica shows that the model WTC is not able to capture the full variability of the WPD field yet. Regarding the comparison with the ~~Comp~~ WTC (Figure 9a12a shows that the GPD+ and the MWR-derived WTCs are equal over the eastern oceanic basins (SLA variance close to zero, represented by the green colour) as expected, since the GPD+ preserves the valid MWR-derived WTC over open ocean.), However, despite the SLA improvement when using GPD+ WTCs being smaller than that when the ERA WTCs are used, it although the SLA improvement when using GPD+ WTC is smaller than the previous one, it can be emphasized that the improvement is global, therefore not limited to the coastal regions, being clear over e.g. the regions where the western boundary currents flow. Therefore, the use of third-party, mainly SI-MWR, data can help the description of the WPD field. Over the Southern Ocean, for latitudes 80°S-60°S, some degradation is visible when the GPD+ is used. This could probably be due to the existence of ice contamination in the radiometer-derived (both along-track and image) WTCs. However, it is recalled that, over this region, the MWR-derived WTC is usually missing or out of range, and that these points, for which a GPD+ estimate would be computed otherwise, have been removed from the analysis. Therefore, it must be emphasized that these results for the comparison GPD+ and MWR-derived WTCs provides underestimated results for the GPD+.

SLA variance differences have also been analysed as function of latitude and distance from coast and the results are shown in Fig. 4013. Both the differences between GPD+ and ERA WTCs ~~or~~ and GPD+ and ~~Comp~~ MWR-derived WTCs are represented. The variance of the SLA dataset is reduced when GPD+ is used instead of the ~~other WTCs~~ ERA WTC for all latitudes (Fig. 40a13a). The improvement of the GPD+ WTC with respect to the model one, with an average value of 1.3 cm² is maximum

over latitudes where maximum atmospheric water content can be found, namely over the subtropical ocean and over latitudes where the western-boundary currents flow, particularly in the northern hemisphere where the variance reduction surpluses 2 cm². As expected, the improvement is smaller for the comparison with the ~~Comp-MWR-derived~~ WTC, since this analysis includes open-ocean points where both corrections are equal. Leading to an improvement in the SLA variance of 0.4-32 cm² in average, the GPD+ WTC has its best performance against the ~~Comp~~-WTC from the radiometer in the extratropical ocean, especially in the northern one. The increase in the reduction of the SLA variance at these latitudes is associated to a better description of the WPD field in the coastal regions northwards of the regions where the western boundary currents flow (off Newfoundland and in the Sea of Okhotsk), as can be concluded from the maps showing the reduction in SLA variance for the difference GPD+ and ~~Comp-MWR-derived~~ WTCs, computed along-track and spatially averaged at each 4-degree cell (not shown). The SLA dataset is also improved over the coastal regions when the GPD+ WTC is applied (Fig. 40b13b). The improvement over the ERA WTC is, in average, 0.77 cm² in the 30 km closest to land, increasing to ~1.4 cm² for larger distances. This means that a better description of both the WTC and SLA fields is obtained over open ocean when the GPD+ WTC is adopted (cf. Fig. 12). The improvement over the ~~Comp~~-WTC from the on-board MWR is larger in the nearest 50-20 km to the coast, where the reduction in variance can reach 3.3 cm² (average value is 2.0 cm²), varies is, in average, 0.8 cm². As the distance to shore increases, the reduction in variance decreases, although still negative and around -0.5-60 cm² in average. This result is expected, since the number of invalid MWR-derived WTCs decrease offshore and so does the number of Comp estimates and therefore the GPD+ WTCs equal those retrieved from the MWR measurements.

~~On the opposite, the improvement over the model correction increases with distance from coast due to the improvement in the description of the WPD field over open ocean (cf. Fig. 9). The improvement obtained with when the GPD+ methodology in is applied to the coastal areas due to the increase in the number of points with valid SLA value is unfortunately not completely evident in the presented se depicted results, since the MWR-derived WTC for those part of the points for which this correction is that do not possess a valid MWR derived correction missing or outside limits have not been, for in the analyses. For these points, if available, the MWR-derived WTCs are expected to be significantly worse than the GPD+ one, which a GPD+ estimate is computed, are discarded from the analysis.~~

3.2.2 Coastal Analysis

This section shows zoomed-in results for three different regions: North American and European coasts, and Indonesia region.

The first two regions have been selected due to the great quantity of GNSS stations available along the coast (shown by the red dots in Fig. 2), while the third has been selected since it is recognised as being quite challenging for satellite altimetry. The results have been obtained for the whole period of the Envisat mission and all along-track points within the geographic limits have been considered. As already described in the previous section, points with MWR-derived WTC out of the range -50 cm - 0 cm and those for which the WTC is not defined in the altimeter products are rejected from the comparisons with the on-board MWR, while in the comparisons with ERA all points with valid SLA are selected.

Results are illustrated in Fig. 14. Left panels show the SLA variance difference (in cm^2) function of distance from coast calculated along the satellite tracks, where negative variance differences represent an improvement in the description of the SLA field when the GPD+ WTC is used. Right panels show the spatial distribution of the weighted SLA variance differences (in cm^2) computed along the satellite tracks, after being spatially averaged and gridded onto 4-degree spatial resolution cells.

620 In these latter plots, blueish colours represent an improvement in the SLA dataset (reduction in the SLA variance) when the GPD+ WTC is used.

All the regions show that the SLA variance is reduced along the coasts when the GPD+ WTC is used rather than the MWR- (in green) or the ERA-derived (in blue) WTCs. For the North American coast (Fig. 14a, left panel), the improvement is clear up to 100 km off the coast. For distances up to 40 km off the coast, the reduction in SLA variance is, on average, 8.7 cm^2 , being $\sim 3.4 \text{ cm}^2$ when averaged for distances between 40-100 km off the coast. For larger distances, the differences tend to zero, since the GPD+ preserves the valid MWR-derived WTC and therefore both corrections are equal. The comparison with the ERA-derived WTC shows an averaged SLA variance difference of -1.2 cm^2 (GPD+ reducing the variance) for the whole range of distances. The right panel of Fig. 14a shows that the reduction in SLA variance, when the GPD+ correction is used instead of the ERA-derived one, is larger along the eastern coast, where the WTC variability is larger (cf. Fig. 2), and that the improvement is not limited to the coastal zone, but is also clear over open ocean. This result can be extended to the three selected regions.

625 For the European region (Fig. 14b, left panel), an improvement of 1.5 cm^2 is, on average, obtained for the comparison GPD+ and MWR-derived WTCs for the 20 km closest to the coast. For larger distances, and up to 100 km off the coast, the averaged reduction in SLA variance is 0.67 cm^2 . The comparison with the ERA-derived WTC shows an SLA variance difference of -1.2 cm^2 (GPD+ reducing the variance), on average, for the whole range of distances. SLA variance reduction is notorious over the Mediterranean region (Fig. 14b, right panel).

630 For the Indonesia region, the improvement of the GPD+ WTC with respect to the MWR-derived one is mainly achieved in the 20 km closest to the coast, where the SLA variance reduction is, on average, 1.4 cm^2 . The use of GPD+ WTC instead of ERA-derived WTC leads to an improvement that, on average, is of the order of 2.2 cm^2 for the whole range of distance from coast.

635 This reduction is observable over almost the whole region, being larger in its northern part.

The results obtained for the comparison with the ERA WTC are a clear indication that current NWM do not correctly represent the WTC field variability yet. This result can also be extracted from Fig. 7 and Fig. 8, where it is seen that the NWM-derived WTC does not exhibit the small spatial scales as well as the MWR-derived, and consequently, GPD+ WTCs.

640 Once again, it is worth noticing that, in these results, the improvement obtained when the GPD+ methodology is applied to coastal areas is underestimated, since the MWR-derived WTCs for those points for which this correction is missing or outside limits have not been used in the performed analyses. For these points, the MWR-derived WTC, if available, would probably be contaminated by land and would degrade the MWR-derived dataset.

645

54 Data Availability

650 The GPD+ WTCs are freely available in NetCDF format at the UPorto's Satellite Altimetry repository https://doi.org/10.23831/FCUP_UPORTO_GPDPlus_v1.0 (Fernandes et al., 2019) and at the AVISO (Archiving, Validation and Interpretation of Satellite Oceanographic data) webpage (<https://www.aviso.altimetry.fr/en/data/products/auxiliary-products/gpd-wet-tropospheric-correction.html>).

65 Conclusions

655 The wet tropospheric correction (WTC) is still considered an important source of error in satellite altimetry, particularly in coastal and polar regions, where the retrieval of the wet path delays from the microwave radiometer (MWR) measurements on board the altimetry missions leads to invalid values. During the data processing aiming at deriving the sea level anomaly, altimeter measurements are discarded if the WTC is absent, which is frequent in coastal and polar regions. In the last years, a huge effort has been made to develop methodologies capable of computing WTC estimates where the correction is absent, while keeping the high-accuracy of MWR-derived WTC values. A few methodologies emerged, among which the GPD and its most-updated version GPD+ have proven to be the most effective in reducing the SLA variability due to non-ocean phenomena, simultaneously leading to the recovery of a significant number of measurements.

This paper describes the GPD+ WTC database and exemplifies the results using as input the Envisat FMR V3.0. The GPD+ WTC equals the MWR-derived WTC whenever this latter is valid, thus preserving its accuracy. For those MWR-derived WTCs detected by the algorithm as ~~invalid~~anomalous, a new estimate and its associated mapping error are computed. The GPD+ algorithm has been trained to detect land, ice, and outlier-contaminated measurements, besides those identified in the GDR data already. On top of preserving the accuracy of the WTC derived from the on-board MWR measurements, the GPD+ algorithm guarantees the continuity and consistency of the output WTC globally and, in particular, in the coastal zone.

Prior studies using a previous GPD+ version (e.g., GPD algorithm cf. Fernandes et al. (2015)) show that the GPD WTC led to a significant improvement of the SLA dataset for T/P and ESA-funded missions, since these, particularly the latter, had ~~an on-board MWRs~~ which retrieval algorithms ~~were unable to deal with coastal and ice contaminated measurements~~output very noisy values in coastal and ice contaminated regions. For these missions, the GPD WTC was proven to be the preferred WTC to be used in the definition of the SLA field, when compared to the baseline MWR one, the model-derived one and the AVISO reference composite correction, provided in their products ([Legeais et al., 2018](#)). The main advantage of the methodology when applied to the T/P mission is the correction of several TOPEX/Poseidon Microwave Radiometer (TMR) anomalies present in the second part of the mission, particularly noticeable in the Indian Ocean, which would otherwise seriously affect the calculation of the mean sea level at regional scales (Fernandes et al., 2015).

The GPD+ WTCs for GFO and CryoSat-2 missions have been described in Fernandes and Lázaro (2016). Despite the MWR on board GFO mission being considered a stable and accurate instrument, it had periods of malfunctioning, particularly in the last years of the mission. In addition to improving the derived SLA dataset, by reducing the error associated with non-pure

oceanic signal, the GPD+ recovers the WTC for the periods during which the GFO MWR was defective. For CryoSat-2 mission, without an on-board MWR and therefore without a WTC relying on observations, the GPD+ is computed for all along-track points. GPD+ WTC thus replaces the NWM-derived WTC that otherwise would have to be used instead. For this mission, the exploitation of third-party data has been proven to be very effective. As the results in this paper show, the NWM-

Products available for Jason missions already possess a coastally improved WTC (Brown, 2010). Still, although small, some improvement, particularly at high latitudes and mainly for Jason-1 can be achieved when the GPD+ correction is used in the generation of the SLA dataset (Fernandes et al., 2015). The current version of the correction (GPD+) for the reference missions leads to more accurate retrievals than before, due to several improvements (e.g. the inclusion of WPD third-party observations from imaging radiometers and a better screening for anomalous MWR-derived WTCs). Due to the fact that, contrary to Jason missions, T/P products do not possess a coastal enhanced WTC, the improvements reached by GPD+ are more significant for T/P than for Jason. For all other RA with 2-band MWRs (ERS-1, ERS-2, Sentinel-3, SARAL and GFO), GPD+ proves to be a significant improvement over NWM, MWR and the AVISO composite WTC, reducing the SLA variance (both along-track, at crossovers, function of distance from coast and function of latitude) by 1-2 cm² (Fernandes and Lázaro, 2016, 2018).

Many authors have also proven the positive impact of the GPD+ corrections, particularly in coastal studies, e.g. Handoko et al. (2017) in the Indonesia region and Dinardo et al. (2018, 2020) in the German Bight.

Taken as a whole, the GPD+ algorithm possesses the advantage of being able to compute the WTC at a considerable number of along-track points with an invalid/inexistent MWR-derived WTC, therefore leading to the recovery of the SLA signal at these points. The percentage of recovered points when GPD+ is applied in place of the baseline MWR-derived WTC depends on instrument type, band of latitudes covered by the mission (which determines the extent of ice contamination) and instrument performance. For all ESA missions (ERS-1, ERS-2, Envisat, Sentinel-3) and SARAL, possessing 2-band radiometers and measuring up to latitudes $\pm 81.2^\circ$, the percentage of recover data is similar to that of Envisat, in the range of 7% - 15% of the SLA valid points of each cycle. For the reference missions, measuring only up to $\pm 66.7^\circ$ and already possessing an improved WTC near the coast (all except T/P), this percentage is smaller, from 2 to 4%. For T/P, these values are from 4% to 7%, larger in the second half of the mission. For GFO, measuring up to $\pm 72.0^\circ$, the percentage is similar to that of TP. Exceptions occur for various missions over periods of instrument malfunction, when the percentage of recovered points can be considerably larger, up to 100%, as it happens for Envisat and GFO.

Moreover, the GPD+ WTC is a continuous correction in the ocean/land interface region, as well as in the polar regions. The scientific novelty and practical significance for the common satellite altimetry user is that the GPD-corrected SLA dataset can be used for coastal applications, constituting a major step forward for satellite altimetry to become a tool for coastal management.

Despite significant efforts made in the past to improve the WPD calculation at GNSS-station height and the sea-level reduction of the correction to use in satellite altimetry over ocean, the unpredictable way the WPD varies with altitude is still a factor constraining the precise GNSS data reduction procedure, since all other data are provided at sea level. Therefore, the modelling

715 of the 4D variability of the WPD field is under research at UPorto (Vieira et al., 2019c). It is expected that a better knowledge
of the WTC variability will improve the GPD+ WTCs aiming at a larger reduction of the sea level variance due to non-oceanic
signals, since the whole GNSS data processing upstream to the GPD+ computation is also performed at UPorto.
Upcoming developments include: i) the inclusion of an ameliorate modelling of the WTC vertical variability (Vieira et al.,
2019c), leading to a better consistency of the various datasets combined in the OA procedure; ii) the extension of the corrections
720 to all surface types with new estimates over all regions where observations exist, e.g. large lakes and rivers where valid MWR
and GNSS can be exploited; iii) and, for the older missions, the replacement of the ERA Interim model by ERA5, the most
recent reanalysis by ECMWF (Vieira et al., 2019d).

Author Contributions.

MJF and CL developed the methodology and the code. All authors performed the [simulationsanalyses](#). CL prepared the
725 manuscript with contributions from all co-authors. All authors have read and approved the final paper.

Competing Interests.

The authors declare that they have no conflict of interest.

Acknowledgements.

The results here provided for Envisat ~~FRM-FMR~~ V3.0 were obtained in the scope of the ESA funded project CLS-SCO-17-
730 0034,
ENVISAT RA-2 LEVEL 1B ESL AND PROTOTYPE MAINTENANCE SUPPORT, Subcontract to ESA/Contract N°
4000110859/14/I-AM. The authors thank Radar Altimeter Database System (RADS) for providing the GPD+ input altimeter
data for all missions except Envisat [and SARAL up to cycle 30](#), Aviso+ (<https://www.aviso.altimetry.fr/>), ~~as part of the Ssalto~~
~~ground processing segment~~, for the production and distribution of ~~CorSSH-L2P SARAL PEACHI altimeter~~ products [up to](#)
735 [cycle 30](#), the European Centre for Medium-Range Weather Forecasts (ECMWF) for making both the ECMWF operational
and the ERA Interim models available, and all institutions providing the water vapour products used in this study: National
Oceanic and Atmospheric Administration (NOAA) – Comprehensive Large Array-Data Stewardship System (CLASS) and
Remote Sensing Systems. SSM/I and SSMIS data are produced by Remote Sensing Systems and sponsored by the NASA
Earth Science MEaSUREs Program and are available at www.remss.com.

740 **Financial Support.**

Telmo Vieira is supported by the Fundação para a Ciência e a Tecnologia (FCT) through the PhD grant SFRH/BD/135671/2018, funded by the European Social Fund and by Ministério da Ciência, Tecnologia e Ensino Superior (MCTES). This research was also supported by Centro Interdisciplinar de Investigação Marinha e Ambiental (CIIMAR) through the project with reference UID/Multi/04423/2019.

745 **References**

Askne, J. and Nordius, H.: Estimation of Tropospheric Delay for Microwaves From Surface Weather Data, *Radio Sci.*, 22(3), 379–386, doi: 10.1029/RS022i003p00379, 1987.

~~[AVISO: Along track Level 2+ \(L2P\) SLA Product Handbook, SALP MU P EA 23150 CLS, 1 rev 0, 2017.](#)~~ [Bevis, M., Businger, S., Chiswell, S., Herring, T.A., Anthes, R.A., Rocken, C., Ware, R.H.: GPS Meteorology – Mapping Zenith Wet delays onto precipitable water. *Journal of Applied Meteorology*, 33, 379-386, doi: 10.1175/1520-0450\(1994\)033<0379:GMMZWD>2.0.CO;2, 1994.](#)

Bosser, P. Bock, O., Pelon, J., Thom, C.: An improved mean-gravity model for GPS hydrostatic delay calibration, *IEEE Geosci. Rem. Sens. Letters*, 4(1), 3–7, doi: 10.1109/LGRS.2006.881725, 2007.

755 Bretherton, F P., Davis, R. E. and Fandry, C. B.: A technique for objective analysis and design of oceanographic experiment applied to MODE-73, *Deep-Sea Res.*, 23, 559–582, doi: 10.1016/0011-7471(76)90001-2, 1976.

Brown, S.: A novel near-land radiometer wet path-delay retrieval algorithm: Application to the Jason-2/OSTM advanced microwave radiometer, *IEEE Trans. Geosci. Remote Sens.*, 48, 1986–1992, doi: 10.1109/TGRS.2009.2037220, 2010.

760 Chelton, D. B., Ries, J. C., Haines, B. J., Fu, L. L., Callahan, P. S.: Satellite Altimetry. In *Satellite Altimetry and Earth Sciences: A Handbook of Techniques and Applications*; Fu, L.L., Cazenave, A., Eds.; Academic: San Diego, CA, USA; Volume 69, 1–131, 2001.

Cipollini, P., Benveniste, J., Birol, F., Fernandes, M. J., Obligis, E., Passaro, M., Strub, P. T., Valladeau, G., Vignudelli, S., Wilkin J.: Satellite altimetry in coastal regions. In D. Stammer and A. Cazenave, (Eds.), *Satellite Altimetry Over Oceans and Land Surfaces*, 343–380, CRC Press. ISBN: 9781498743457, 2017.

765 Dinardo, S., Fenoglio-Marc, L., Buchhaupt, C., Becker, M., Scharroo, R., Fernandes, M. J., Benveniste, J.: Coastal SAR and PLRM altimetry in German Bight and West Baltic Sea. *Advances in Space Research*, 62(6), 1371-1404. doi:10.1016/j.asr.2017.12.018, 2018.

- 770 [Dinardo, S., Fenoglio-Marc, L., Becker, M., Scharroo, R., Fernandes, M. J., Staneva, J., Grayek, S., Benveniste, J.: A RIP-based SAR Retracker and its application in North East Atlantic with Sentinel-3, *Advances in Space Research*, In press, doi:https://doi.org/10.1016/j.asr.2020.06.004, 2020.](https://doi.org/10.1016/j.asr.2020.06.004)
- Dousa, J. and Elias, M.: An improved model for calculating tropospheric wet delay, *Geophys. Res. Lett.*, 41, 4389–4397, doi:10.1002/2014GL060271, 2014.
- 775 [Escudier, P., Ablain, M., Amarouche, L., Carrère, L., Couhert, A., Dibarboure, G., Dorandeu, J., Dubois, P., Mallet, A., Mercier, F., Picard, B., Richard, J., Steunou, N., Thibaut, P., Rio, M.-H., and Tran, N.: *Satellite radar altimetry: principle, accuracy & precision*, in: *Satellite Altimetry Over Oceans and Land Surfaces*, edited by: Stammer, D. and Cazenave, A., CRC Press Taylor & Francis, London, UK, 670 pp, doi:10.1201/9781315151779, 2017](https://doi.org/10.1201/9781315151779)
- European Space Agency (ESA) (2018), RA2 Products and Algorithms, webpage <https://earth.esa.int/web/sppa/mission-performance/esa-missions/envisat/ra2/products-and-algorithms/products-information>, accessed July 2019.
- European Space Agency (ESA) (2019), Envisat Altimetry Full Mission Reprocessing V3.0, webpage <https://earth.esa.int/web/guest/content/-/article/envisat-altimetry-v3-0-full-mission-reprocessing>, accessed July 2019.
- 780 [Fernandes, M. J., Lázaro, C.: GPD+ Wet Tropospheric Corrections for CryoSat-2 and GFO Altimetry Missions, *Remote Sens.* 2016, 8\(10\), 851, doi: 10.3390/rs8100851, 2016.](https://doi.org/10.3390/rs8100851)
- Fernandes, M. J., Lázaro, C.: Independent assessment of Sentinel-3A wet tropospheric correction over the open and coastal ocean, *Remote Sens.*, 10(3), 484. doi:10.3390/rs10030484, 2018.
- 785 [Fernandes, M. J., Lázaro, C., Ablain, M., Pires, N.: Improved wet path delays for all ESA and reference altimetric missions, *Remote Sens. Environ.*, 169, 50–74, doi: 10.1016/j.rse.2015.07.023, 2015.](https://doi.org/10.1016/j.rse.2015.07.023)
- Fernandes, M. J., Lázaro, C., Nunes, A. N., Scharroo, R.: Atmospheric Corrections for Altimetry Studies over Inland Water, *Remote Sens.*, 6(6), 4952-4997. doi:10.3390/rs6064952, 2014.
- 790 [Fernandes, M. J., Lázaro, C., Vieira, E., Vieira, T.: UPorto GPD+ Wet Tropospheric Correction. Dataset available at: https://doi.org/10.23831/FCUP_UPORTO_GPDPlus_v1.0 \(last access: 16 September 2019\), 2019.](https://doi.org/10.23831/FCUP_UPORTO_GPDPlus_v1.0)
- Fernandes, M. J., Nunes, A. N., and Lázaro, C.: Analysis and Inter-Calibration of Wet Path Delay Datasets to Compute the Wet Tropospheric Correction for CryoSat-2 over Ocean, *Remote Sens.*, 5(10), 4977-5005. doi:10.3390/rs5104977, 2013b.
- Fernandes, M. J., Pires, N., Lázaro, C., Nunes, A. L.: Tropospheric delays from GNSS for application in coastal altimetry, *Adv. Space Res.*, 51(8), 1352–1368, doi: 10.1016/j.asr.2012.04.025, 2013a.
- 795 [Fernandes, M. J., Barbosa, S., Lázaro, C.: Impact of Altimeter Data Processing on Sea Level Studies. *Sensors*, 6\(3\), 131-163. doi:10.3390/s6030131, 2006.](https://doi.org/10.3390/s6030131)

- Handoko, E., Fernandes, M. J., Lázaro, C.: Assessment of Altimetric Range and Geophysical Corrections and Mean Sea Surface Models—Impacts on Sea Level Variability around the Indonesian Seas. *Remote Sens.*, 9(2), 102. doi:10.3390/rs9020102, 2017.
- 800 Kouba, J.: Implementation and testing of the gridded vienna mapping function 1 (VMF1), *J. Geod.*, 82, doi: 10.1007/s00190-007-0170-0, 193–205, 2008.
- Legeais, J.-F., Ablain, M., Zawadzki, L., Zuo, H., Johannessen, J. A., Scharffenberg, M. G., Fenoglio-Marc, L., Fernandes, M. J., Andersen, O. B., Rudenko, S., Cipollini, P., Quartly, G. D., Passaro, M., Cazenave, A., and Benveniste, J.: An improved and homogeneous altimeter sea level record from the ESA Climate Change Initiative, *Earth Syst. Sci. Data*, 10, 281–
- 805 301, <https://doi.org/10.5194/essd-10-281-2018>, 2018.
- Mercier, F.: Amélioration de la correction de troposphère humide en zone côtière. Rapport Gocina, CLS-DOS-NT-04-086, 2003.
- Mercier, F., Rosmorduc, V., Carrere, L., Thibaut, P.: Coastal and Hydrology Altimetry Product (PISTACH) Handbook, CLS-DOS-NT-10-246, Issue 1.0, CNES, 2010.
- 810 Pany, T., Pesec, P. and Stangl, G.: Atmospheric GPS slant path delays and ray tracing through numerical weather models, a comparison, *Phys. Chem. Earth PT A*, 26(3), 183–188, doi: 10.1016/S1464-1895(01)00044-8, 2001.
- Quartly, G. D., Legeais, J., Ablain, M., Zawadzki, L., Fernandes, M. J., Rudenko, S., Carrère, L., García, P. N., Cipollini, P., Andersen, O. B., Poisson, J. C., Mbajon Njiche, S., Cazenave, A., Benveniste, J.: A new phase in the production of quality-controlled sea level data. *Earth Syst. Sci Data*, 9(2), 557-572. doi:10.5194/essd-9-557-2017, 2017.
- 815 [S. Rudenko, K. Neumayer, D. Dettmering, S. Esselborn, T. Schöne and J. Raimondo, "Improvements in Precise Orbits of Altimetry Satellites and Their Impact on Mean Sea Level Monitoring." in IEEE Transactions on Geoscience and Remote Sensing, vol. 55, no. 6, pp. 3382-3395, June 2017, doi: 10.1109/TGRS.2017.2670061.](#)
- Scharroo, R., Leuliette, E. W., Lillibridge, J. L., Byrne, D., Naeije, M. C., Mitchum, G. T.: RADS: Consistent multi-mission
- 820 products, Proceedings of the 20 Years of Progress in Radar Altimetry Symposium, Venice, Italy, 20–28 September 2012.
- Steunou, N., Picot, N., Sengenès, P., Noubel, J., Frery, M.L.: AltiKa Radiometer: Instrument Description and In-Flight Performance, *Mar. Geod.*, 38:sup1, 43–61, DOI: 10.1080/01490419.2015.1006381, 2015.
- Stum, J., Sicard, P., Carrere, L. Lambin, J.: Using Objective Analysis of Scanning Radiometer Measurements to Compute the Water Vapor Path Delay for Altimetry, *IEEE Trans. Geosci. Remote Sens.*, 49, 9, 3211–3224, doi:
- 825 [10.1109/TGRS.2011.2104967](#), 2011.

Valladeau, G., Thibaut, P., Picard, B., Poisson, J. C., Tran, N., Picot, N., & Guillot, A.: Using SARAL/AltiKa to Improve Ka-band Altimeter Measurements for Coastal Zones. Hydrology and Ice: The PEACHI Prototype, Marine Geodesy, 38:sup1, 124-142, DOI:10.1080/01490419.2015.1020176, 2015.

830 Vieira, E., Lázaro, C., Fernandes, M. J.: Spatio-temporal variability of the wet component of the troposphere – Application to Satellite Altimetry, *Advances in Space Research*, 63(5), 1737-1753. doi: 10.1016/j.asr.2018.11.015, 2019a.

Vieira, T., Fernandes, M. J., Lázaro, C.: Independent Assessment of On-Board Microwave Radiometer Measurements in Coastal Zones Using Tropospheric Delays from GNSS, *IEEE Trans. Geosci. Remote Sens.*, 57, 1804–1816, doi: 10.1109/TGRS.2018.2869258, 2019b.

835 Vieira, T.; Fernandes, M.J.; Lázaro, C. Modelling the Altitude Dependence of the Wet Path Delay for Coastal Altimetry Using 3-D Fields from ERA5. *Remote Sens.* 2019, 11, 2973.
~~Vieira, T., Fernandes, M. J., Lázaro, C.: Modelling the altitude dependence of the Wet Path Delay for coastal altimetry using 3-D parameters from ERA5. *Remote Sens.* To be submitted, 2019c.~~

Vieira, T., Fernandes, M. J., Lázaro, C.: Impact of the new ERA5 Reanalysis in the Computation of Radar Altimeter Wet Path
840 Delays. *IEEE Trans. Geosci. Remote Sens.* doi: 10.1109/TGRS.2019.2929737, 2019d.

Vignudelli, S., Cipollini, P., Gommenginger, C., Snaith, H. M., Coelho, E., Fernandes, J., Gomez-Henri, J., Martin-Puig, C., Woodworth, P. L., Dinardo, S., Benveniste, J. J.: The COASTALT Project: Towards an Operational Use of Satellite Altimetry in the Coastal Zone, *American Geophysical Union, Fall Meeting 2009*, abstract id. OS22A-02, 2009.

Ye, S., Xia, P., and Cai, C.: Optimization of GPS water vapor tomography technique with radiosonde and COSMIC historical
845 data, *Ann. Geophys.*, 34, 789–799, doi:10.5194/angeo-34-789-2016, 2016.

850

855

Table 1. Total Column Water Vapour (TCWV) availability ~~(Fernandes et al., 2016)~~. **For gridded products, two grids per day are made available, each grid comprising the ascending/descending passes. For the swath products, 14-15 orbital swaths per day are available for each instrument. For these latter products, the value provided for the spatial resolution is that of the central pixel (maximum value for pixel size is 130 km).**

Satellite/Sensor	Spatial Res	Temporal Res.	Availability
<u>DMSP-F08/SSM/I</u>	<u>0.25° × 0.25°</u>	<u>2 grids/day</u>	<u>July 1987–December 1991</u>
DMSP-F10/SSM/I	<u>0.25° × 0.25°</u>	<u>2 grids/day</u>	December 1990–November 1997
DMSP-F11/SSM/I	<u>0.25° × 0.25°</u>	<u>2 grids/day</u>	November <u>December</u> 1991–May 2000
DMSP-F13/SSM/I	<u>0.25° × 0.25°</u>	<u>2 grids/day</u>	March–May 1995–November 2009
DMSP-F14/SSM/I	<u>0.25° × 0.25°</u>	<u>2 grids/day</u>	May 1997–August 2008
DMSP-F16/SSM/IS	<u>0.25° × 0.25°</u>	<u>2 grids/day</u>	since October 2003
DMSP-F17/SSM/IS	<u>0.25° × 0.25°</u>	<u>2 grids/day</u>	since December 2006
<u>DMSP-F18/SSM/IS</u>	<u>0.25° × 0.25°</u>	<u>2 grids/day</u>	<u>since October 2009</u>
NOAA-15/AMSU-A	<u>50 km</u>	<u>14-15 orbital swaths per day</u>	since July 2003
NOAA-16/AMSU-A	<u>50 km</u>	<u>14-15 orbital swaths per day</u>	July 2003–June 2014
NOAA-17/AMSU-A	<u>50 km</u>	<u>14-15 orbital swaths per day</u>	July 2003–April 2013
NOAA-18/AMSU-A	<u>50 km</u>	<u>14-15 orbital swaths per day</u>	since August 2005
NOAA-19/AMSU-A	<u>50 km</u>	<u>available on an orbital basis</u>	since May 2009
MetOp-A/AMSU-A	<u>50 km</u>	<u>14-15 orbital swaths per day</u>	since May 2007
MetOp-B/AMSU-A	<u>50 km</u>	<u>14-15 orbital swaths per day</u>	since April 2013
AQUA/AMSR-E	<u>0.25° × 0.25°</u>	<u>2 grids/day</u>	May 2002–October 2011
GCOM-W1/AMSR-2	<u>0.25° × 0.25°</u>	<u>2 grids/day</u>	since May 2012
TRMM/TMI	<u>0.25° × 0.25°</u>	<u>2 grids/day</u>	December 1997–March 2015
Coriolis/WindSat	<u>0.25° × 0.25°</u>	<u>2 grids/day</u>	since February 2003
<u>GMI</u>	<u>0.25° × 0.25°</u>	<u>2 grids/day</u>	<u>since April 2014</u>

865

870

Table 2. Calibration parameters (offset, scale factor and linear trend) obtained for all RA missions with an on-board MWR included in the GPD+ database (Fernandes et al., 2019). For Jason-3 (J3) and SARAL (SA) missions, no parameter for the linear trend has been computed due to the short length of their datasets. For explanation on the mission codes, please refer to Table 4.

875

<u>Satellite Altimetry</u>	<u>offset (a) (mm)</u>	<u>scale factor (b)</u>	<u>linear trend (c) (mm/year)</u>
<u>mission</u>			
<u>TP</u>	<u>-8.05</u>	<u>0.978</u>	<u>0.150</u>
<u>J1</u>	<u>-5.09</u>	<u>0.987</u>	<u>-0.049</u>
<u>J2</u>	<u>-6.25</u>	<u>0.980</u>	<u>-0.178</u>
<u>J3</u>	<u>-9.44</u>	<u>0.992</u>	<u>0.000</u>
<u>E1</u>	<u>-12.04</u>	<u>0.964</u>	<u>0.169</u>
<u>E2</u>	<u>-12.28</u>	<u>0.958</u>	<u>0.050</u>
<u>EN</u>	<u>-6.82</u>	<u>0.991</u>	<u>-0.0028</u>
<u>GFO</u>	<u>4.71</u>	<u>0.993</u>	<u>0.0153</u>
<u>SA</u>	<u>-3.70</u>	<u>0.992</u>	<u>0.000</u>

880

885

890

Table 23. Data content in each GPD+ WTC NetCDF file, for the time and location of each altimetry-RA mission measurement (Fernandes et al., 2019).

Variable	Description
time_01	time of measurement, UTC seconds since 2000-01-01 00:00:00.0
lat_01	latitude of measurement, as in the GDR file
lon_01	longitude of measurement, as in the GDR file
GPD_wet_tropo_cor_01	GPD+ wet tropospheric correction (metres)
GPD_wet_tropo_cor_qual_01	validity flag of the GPD+ estimate: 0-valid, 1-invalid

895

Table 34. Mission Code used in the name of the GPD+ Datasets (Fernandes et al., 2019) and their availability.

Mission Code	Mission	Start Time	End Period
TP	TOPEX/Poseidon	1992/ 07 <u>09</u> (cycle 1)	2005/ 08 <u>10</u> (cycle 481)
J1	Jason-1	2002/01 (cycle 1)	2012/03 (cycle 374*)
J2	OSTM/Jason-2	2008/ 05 <u>07</u> (cycle 1)	2018 <u>2019</u> / 06 <u>10</u> (cycle 353 <u>383</u>)
J3	Jason-3	2016/02 (cycle 1)	2018 <u>2020</u> / 05 <u>01</u> (cycle 084 <u>145</u>)
E1	ERS-1	1991/08 (phase A, cycle 1)	1996/ 04 <u>06</u> to phase g, cycles 156* or 53**
E2	ERS-2	1995/ 04 <u>05</u> (cycle 1)	2011/05 (cycle 167)
EN	Envisat	2002/ 04 <u>05</u> (cycle 16)	2012/03 (cycle 113)

GFO	GEOSAT Follow-On	2000/01 (cycle 37)	2008/09 (cycle 223)
C2	CryoSat-2	2010/07 (sub-cycle 4)	20 <u>20</u> / <u>18</u> / <u>06</u> / <u>30</u> <u>01</u> (sub-cycle <u>106</u> <u>126</u>)
SA	SARAL/AltiKa	2013/03 (cycle 1)	2016/ <u>01</u> <u>07</u> (cycle <u>30</u> <u>35</u>)

* RADS convention

** AVISO convention

900

905

910

915

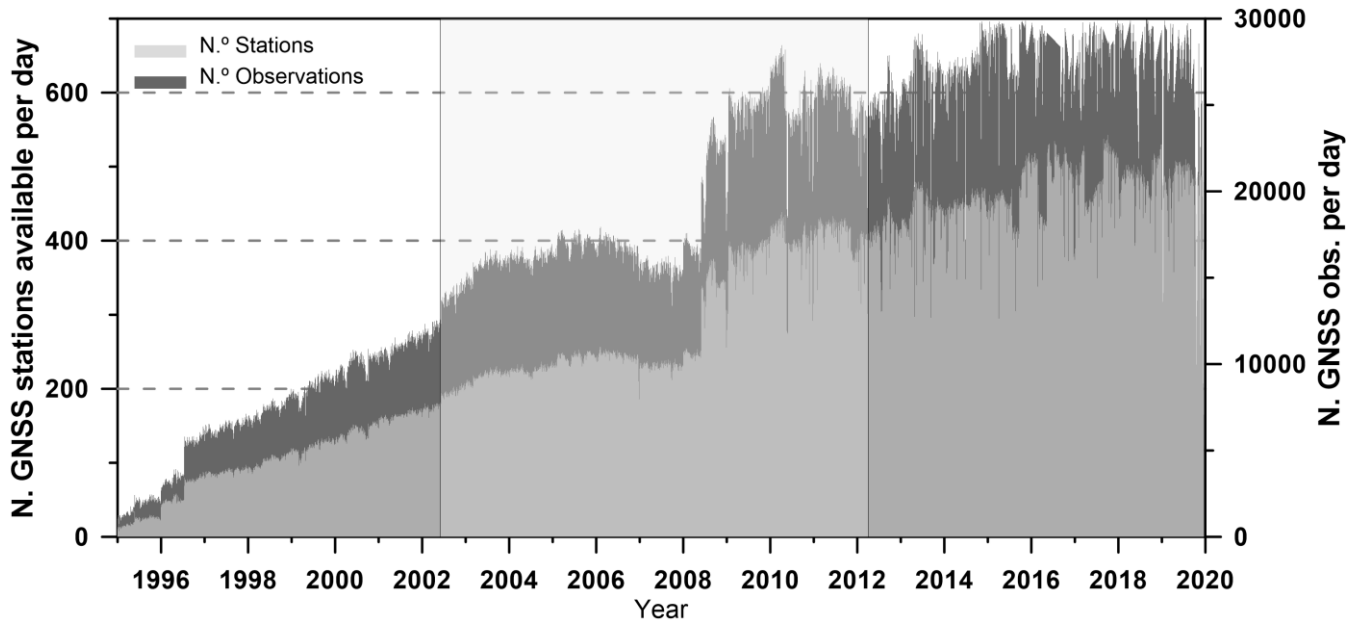


Figure 1 Number of GNSS stations used in the GPD+ over time (light grey) and number of available GNSS observations per day (dark grey), for the whole RA era. -Envisat period (5/2002-3/2020) is shown by the shaded rectangle. All GNSS stations are at a distance from coast less than 100 km.

920

925

930

935

940

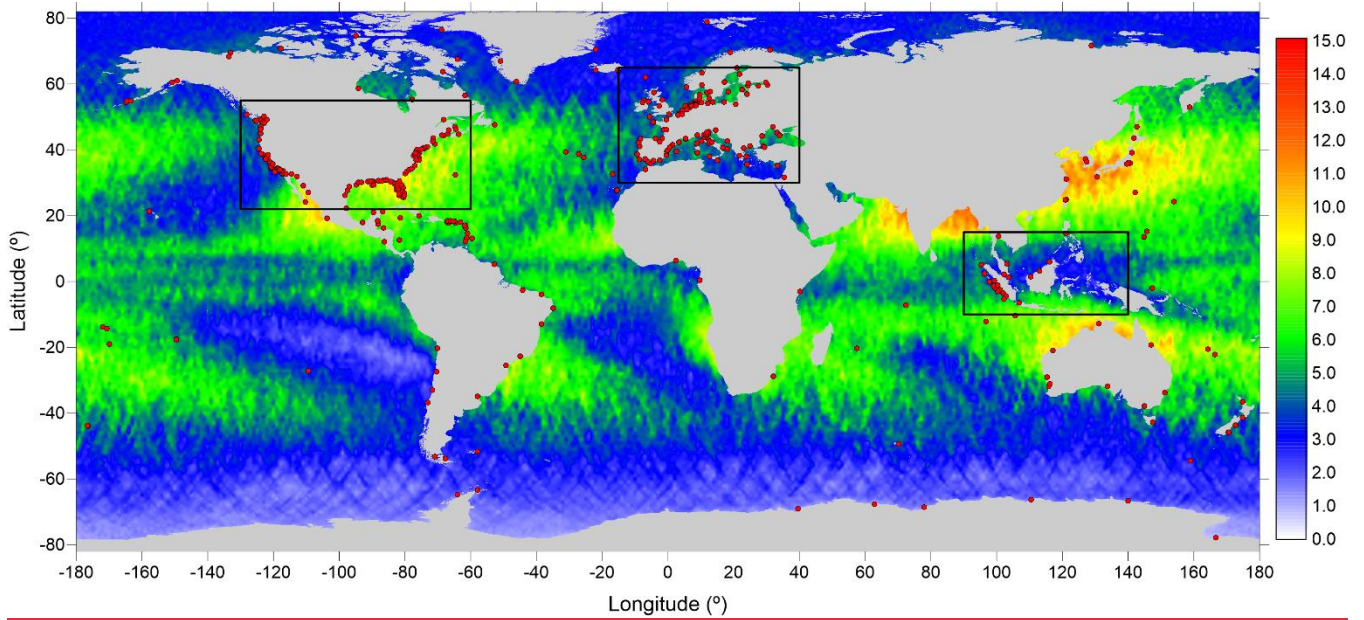


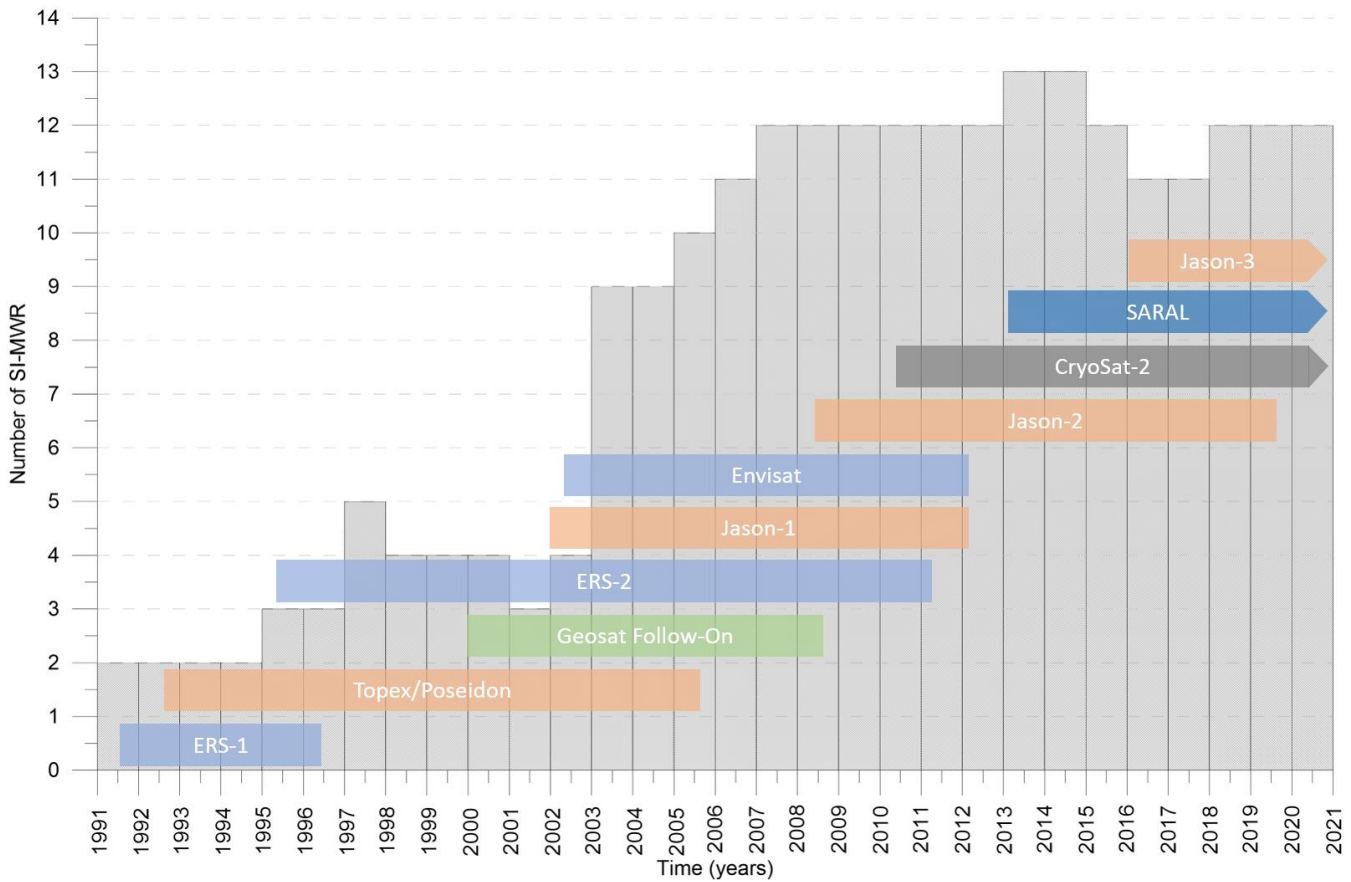
Figure 2 Location of the coastal and island GNSS stations used in the GPD+ (red dots). Background image shows the standard deviation of the WTC field, in centimetres, computed using ERA Interim extracted for Envisat along-track points for the period November 2010 -November 2011 (cycles 96 to 108). The black rectangles show the regions selected to perform the coastal assessment of the GPD+ WTCs (North American and European coasts and Indonesia region).

945

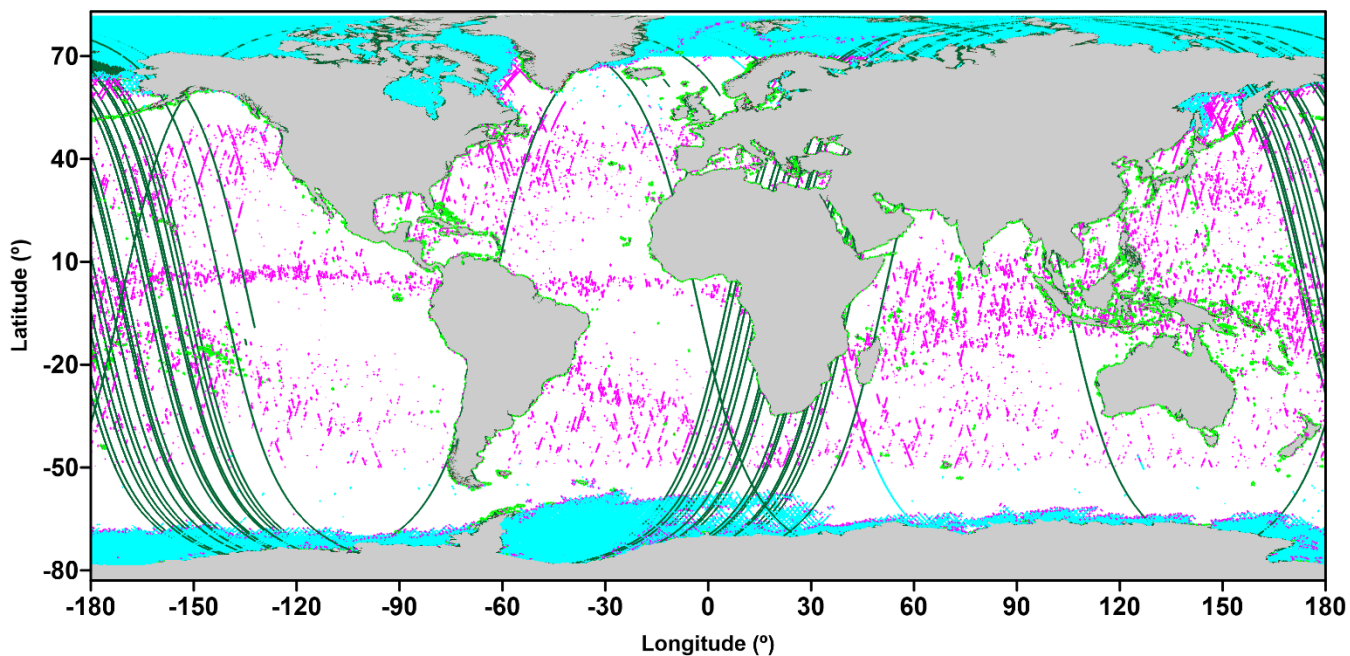
950

955

960



970 **Figure 3 Number of SI-MWR used in the GPD+ along time and period covered by each RA mission. SARAL, CryoSat-2 and Jason-3 missions are currently operational RA missions.**



985

Figure 2-4 Invalid MWR-derived WTC for Envisat cycle 12: ● correction contaminated due to ice, ● correction contaminated due to rain and outliers; ● points flagged as coastal, may possess a correction contaminated by land; ● no available MWR-derived WTC value (the “fill value” is given). A note must be made that there are several points with available MWR-derived field but with an invalid value and without any error flag, that are detected and flagged by the GPD+ algorithm.

990

995

1000

1005

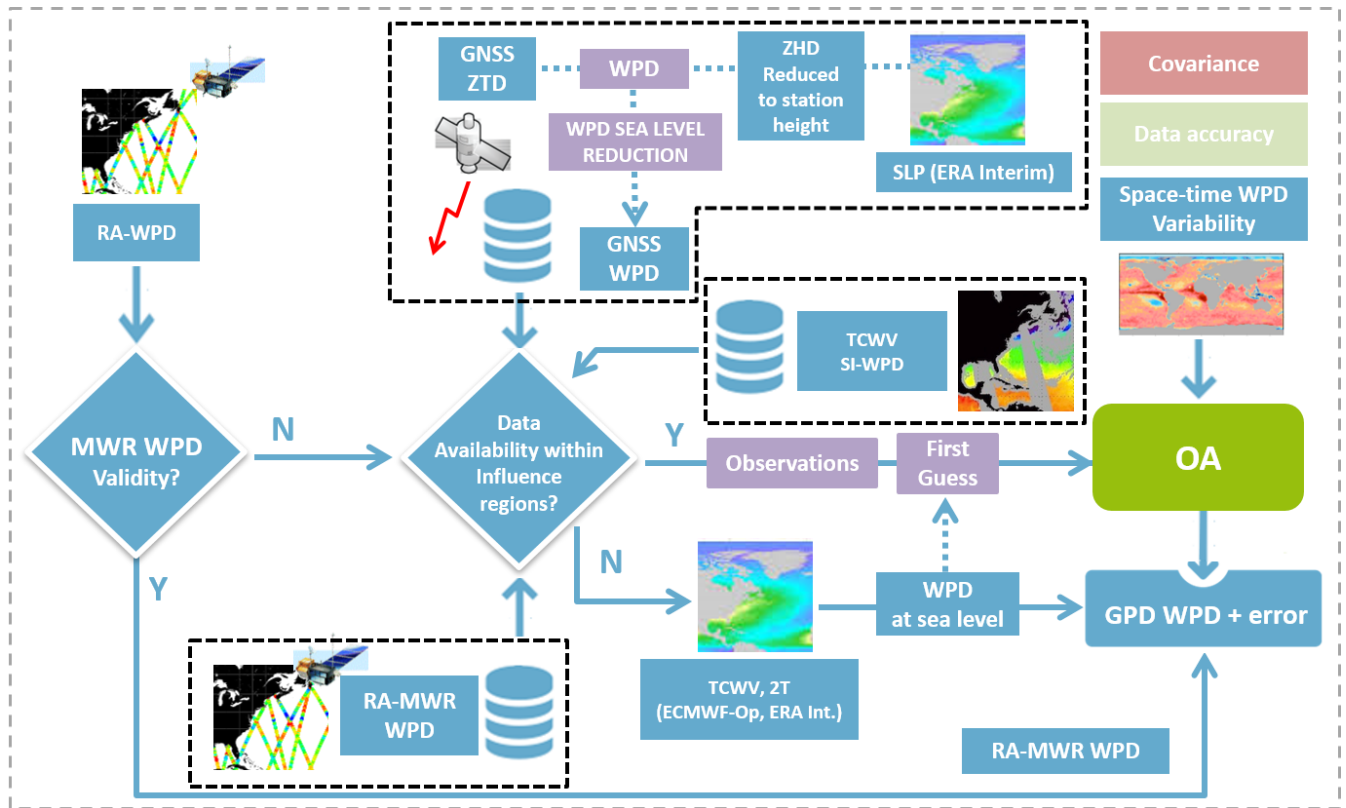
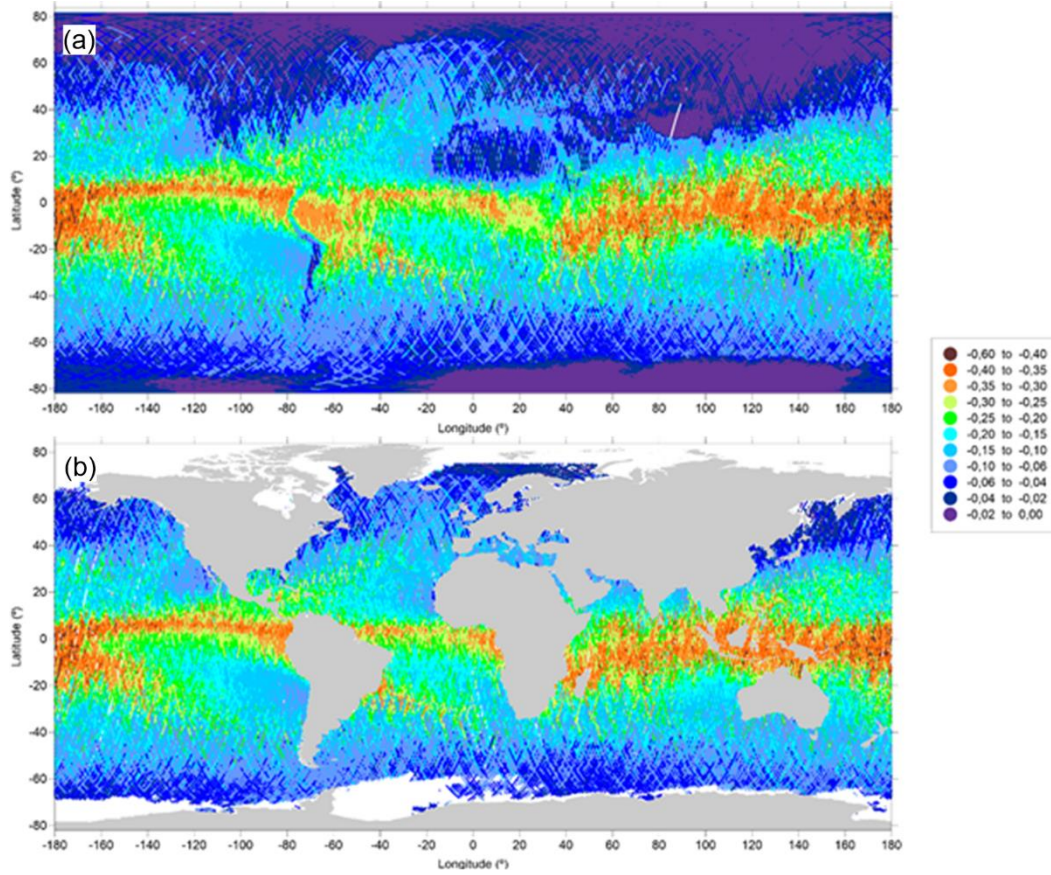


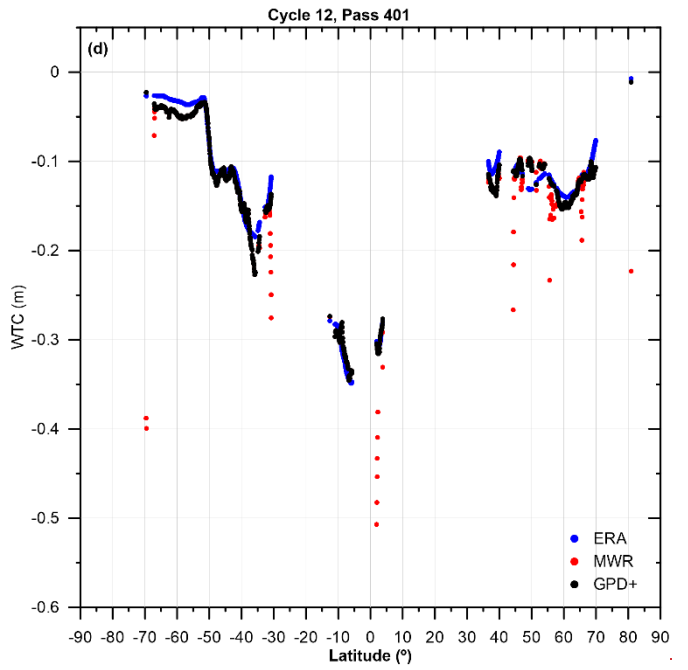
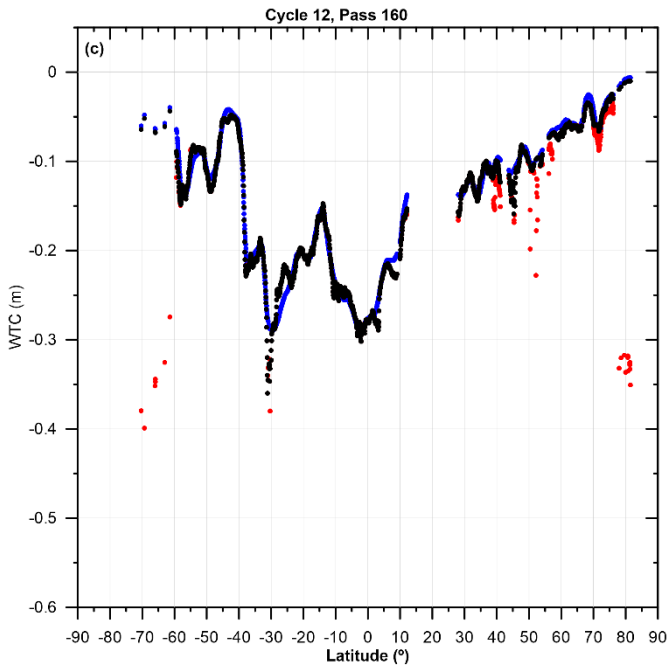
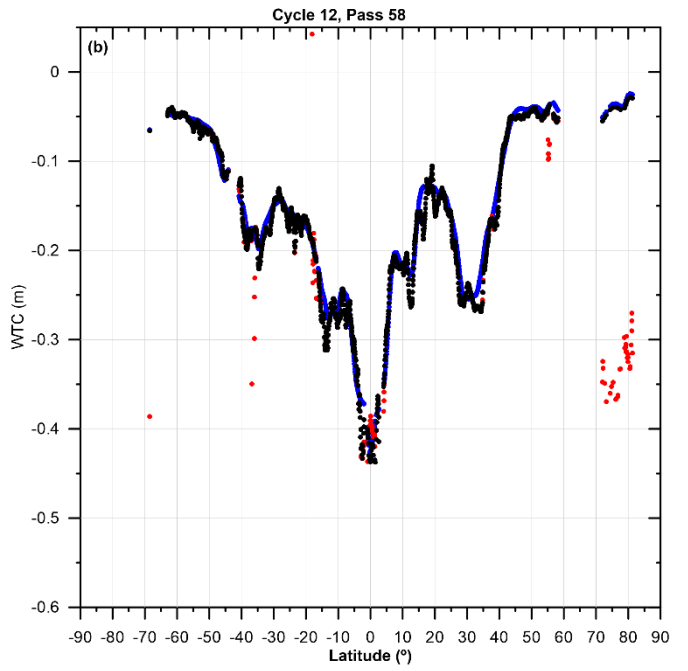
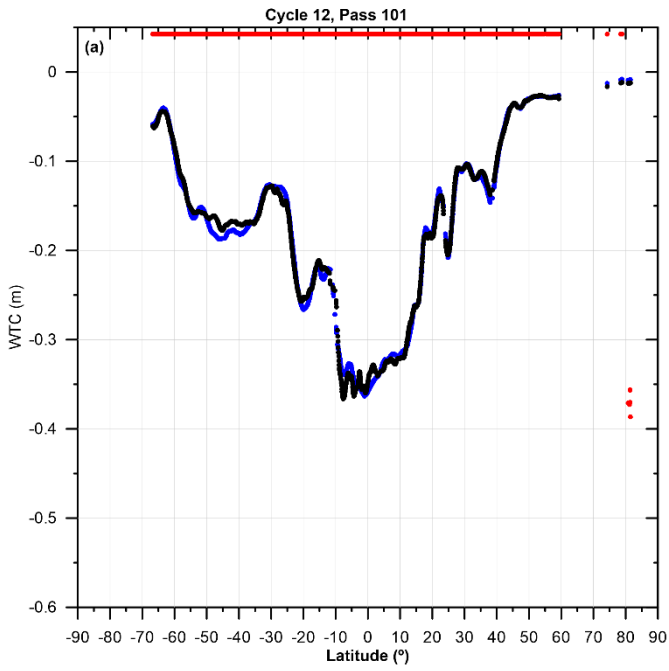
Figure 3-5 Fluxogram of the GPD+ algorithm.

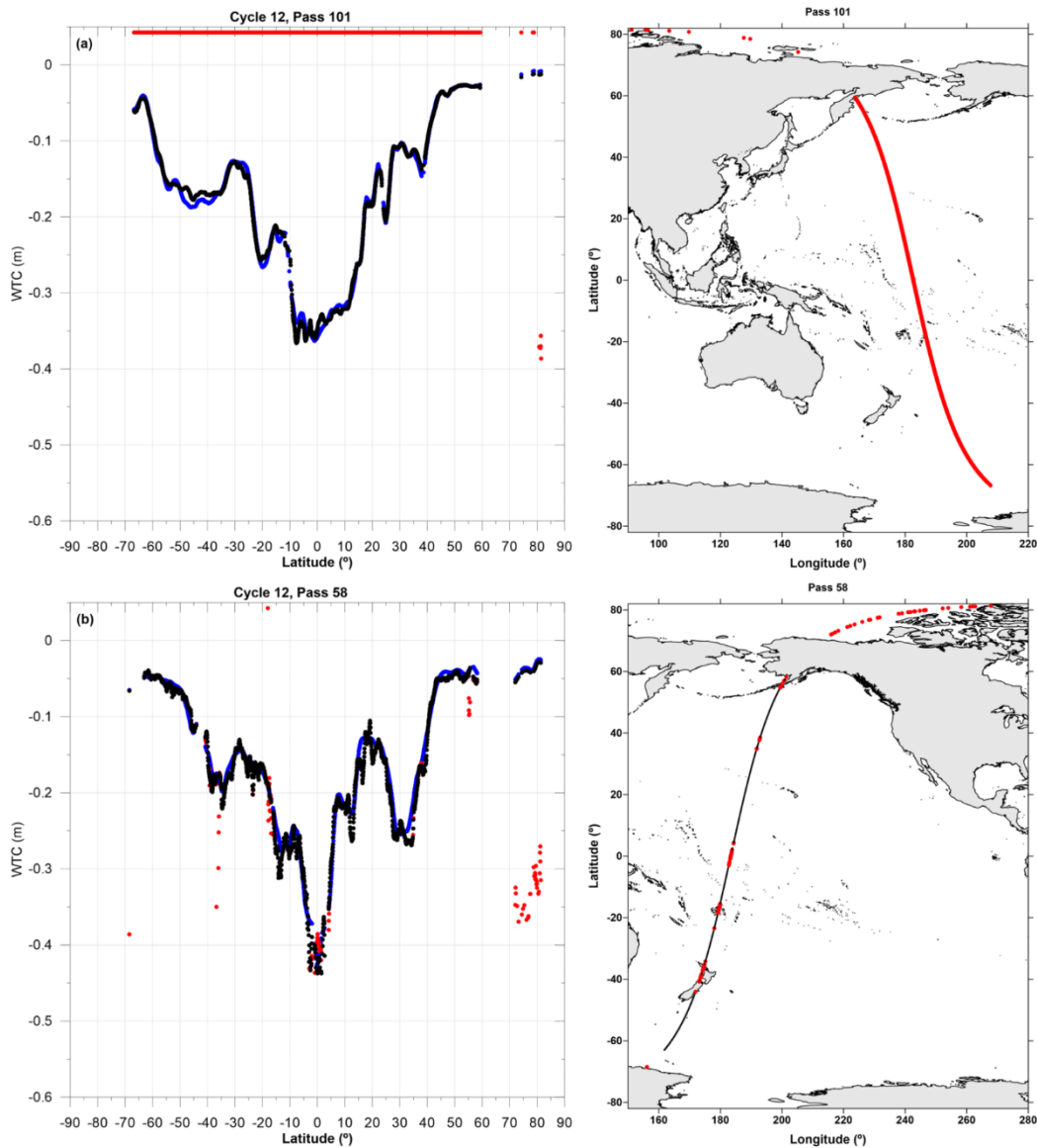
1010

1015



1025 **Figure 4-6** GPD+ WTC, in metres, for Envisat cycle 012: (a) global coverage and (b) correction over oceanic regions with valid SLA.

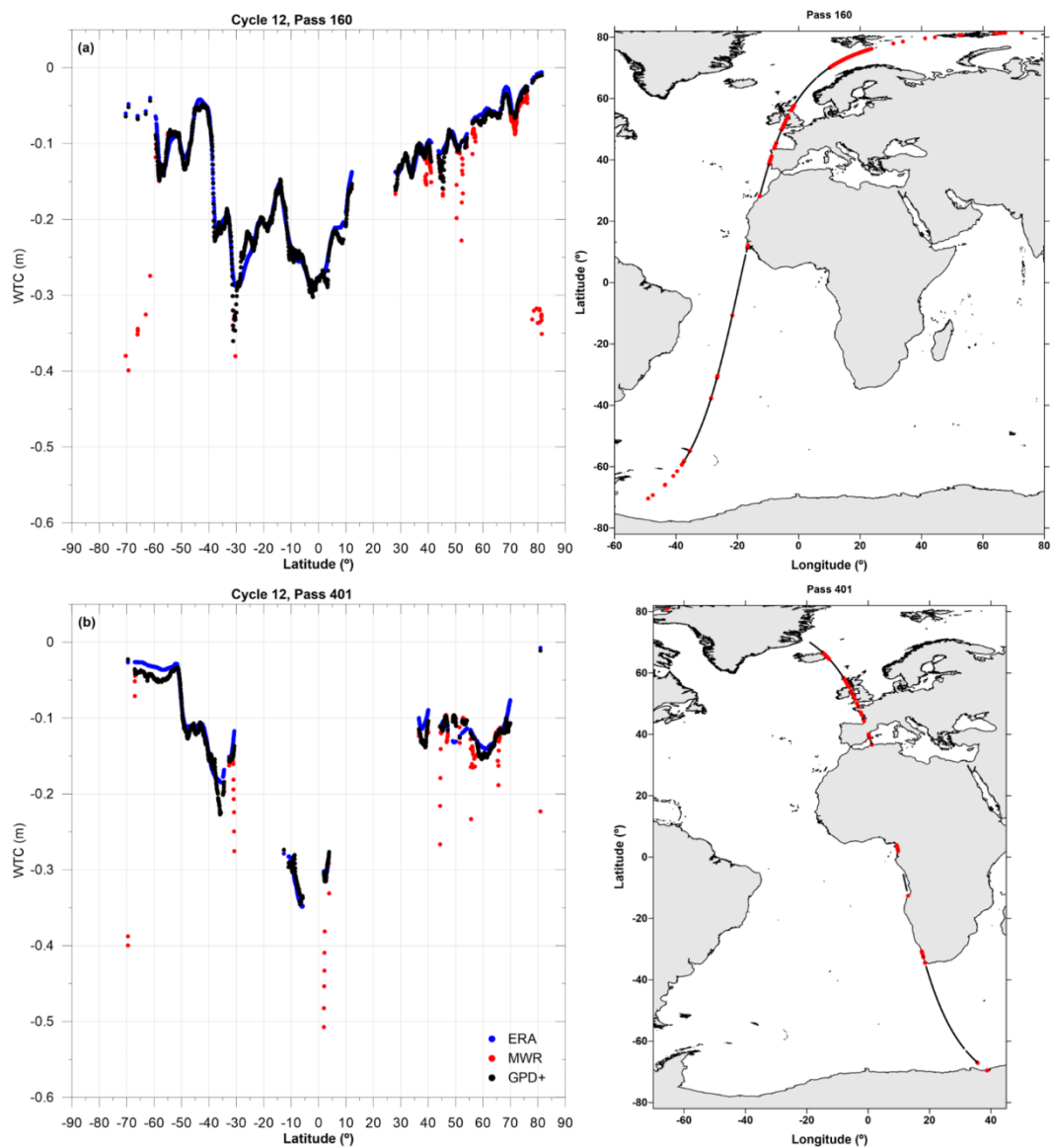




1040

Figure 5-7 **Left:** GPD+ WTC (black) for some Envisat tracks, exemplifying several issues commonly encountered in the on-board MWR-derived WTC (red) that no longer exist in the GPD+ WTC: (a) unavailability of the correction (Cycle 12, pass 101); (b) correction contaminated by ice and rain (see red points around the Equator) (Cycle 12, pass 58); (c) existence of outliers (Cycle 12, pass 160); (d) correction contaminated by land proximity (Cycle 12, Pass 401). In the top-left plot it is possible to see the improvement in the description of the WTC signal in terms of small spatial scales when compared to the ERA Interim WTC (in blue). In these plots, the corrections are shown in metres only for points with valid SLA values. **Right: Geographical coverage of the Envisat tracks shown in the left panels (longitude is given in the 0°-360° range to show the entire track). Along-track points with a GPD+ estimate are shown in red, while point where the GPD+ kept the MWR-derived WTC are shown in black.**

1045



1055 **Figure 8** Same as Fig. 7 for Envisat tracks 160 and 401 (Cycle 12) showing: (a) the existence of outliers (red points located over ocean between latitudes 30°S and 40°S); (b) contamination by land proximity.

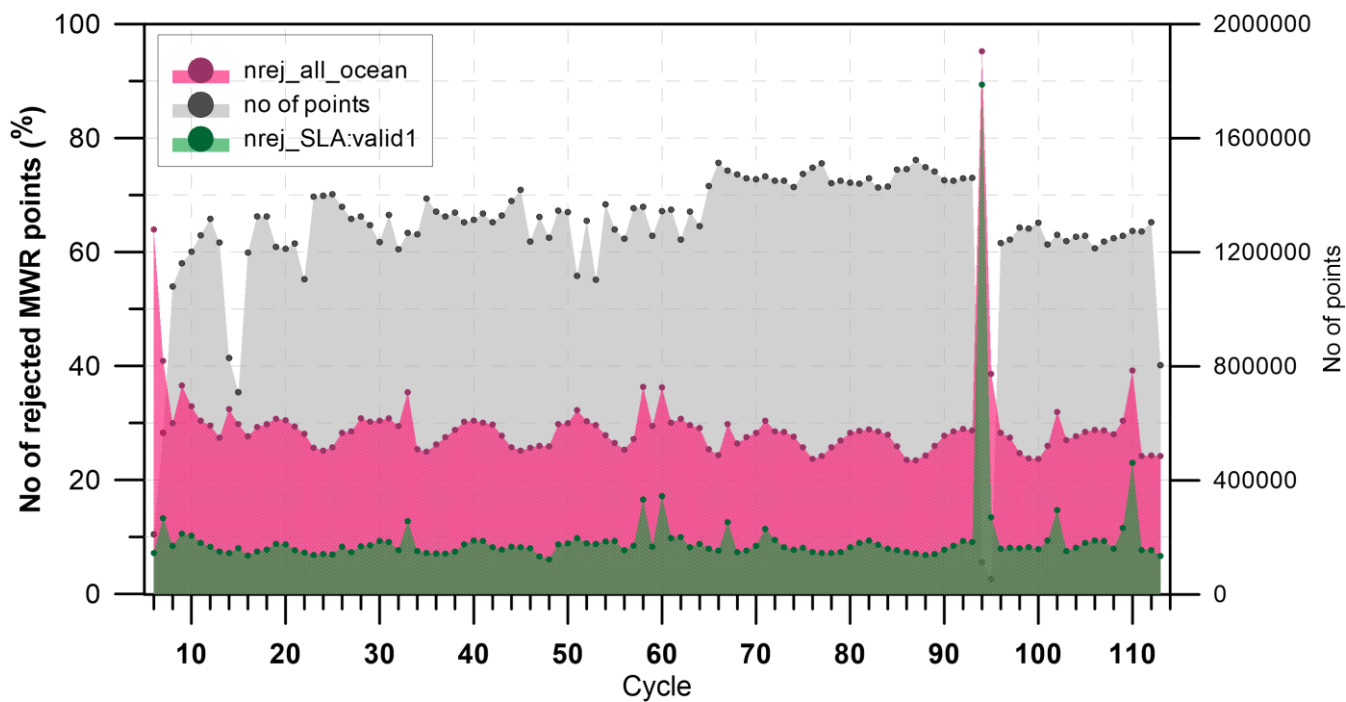
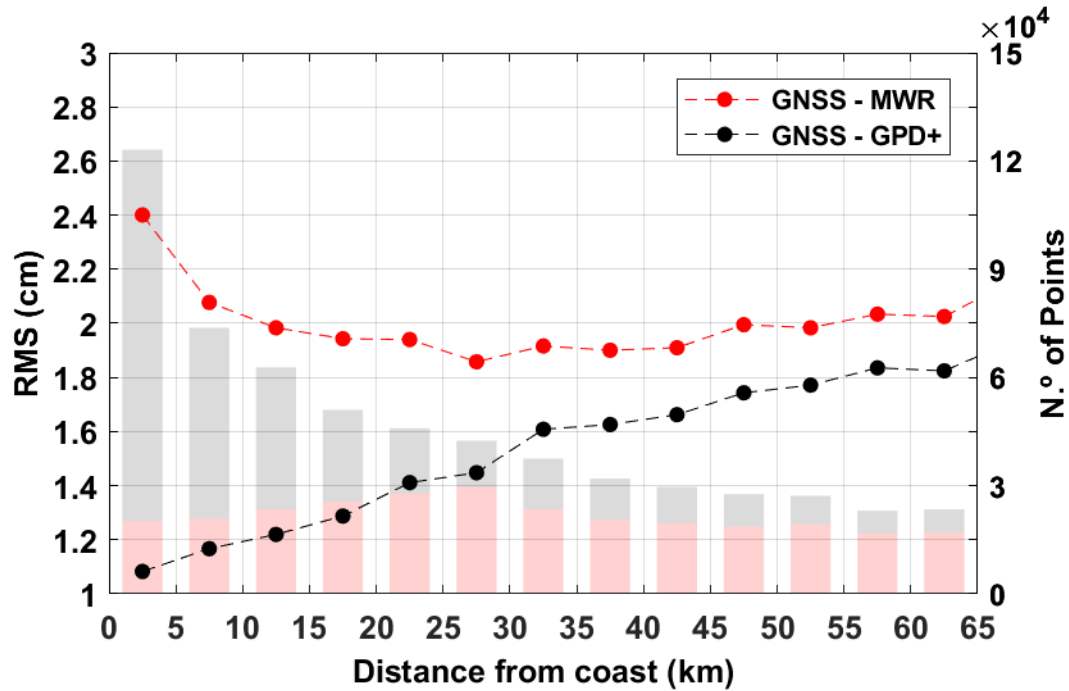


Figure 6-9 Summary, for the whole Envisat period, of the percentage of points: (pink) with a rejected MWR-derived WTC, for which a GPD+ estimate has been computed; (green) for which a valid SLA value could be computed after the estimation of the WTC by the GPD+. Also shown in grey is the number of points with valid SLA values per cycle.

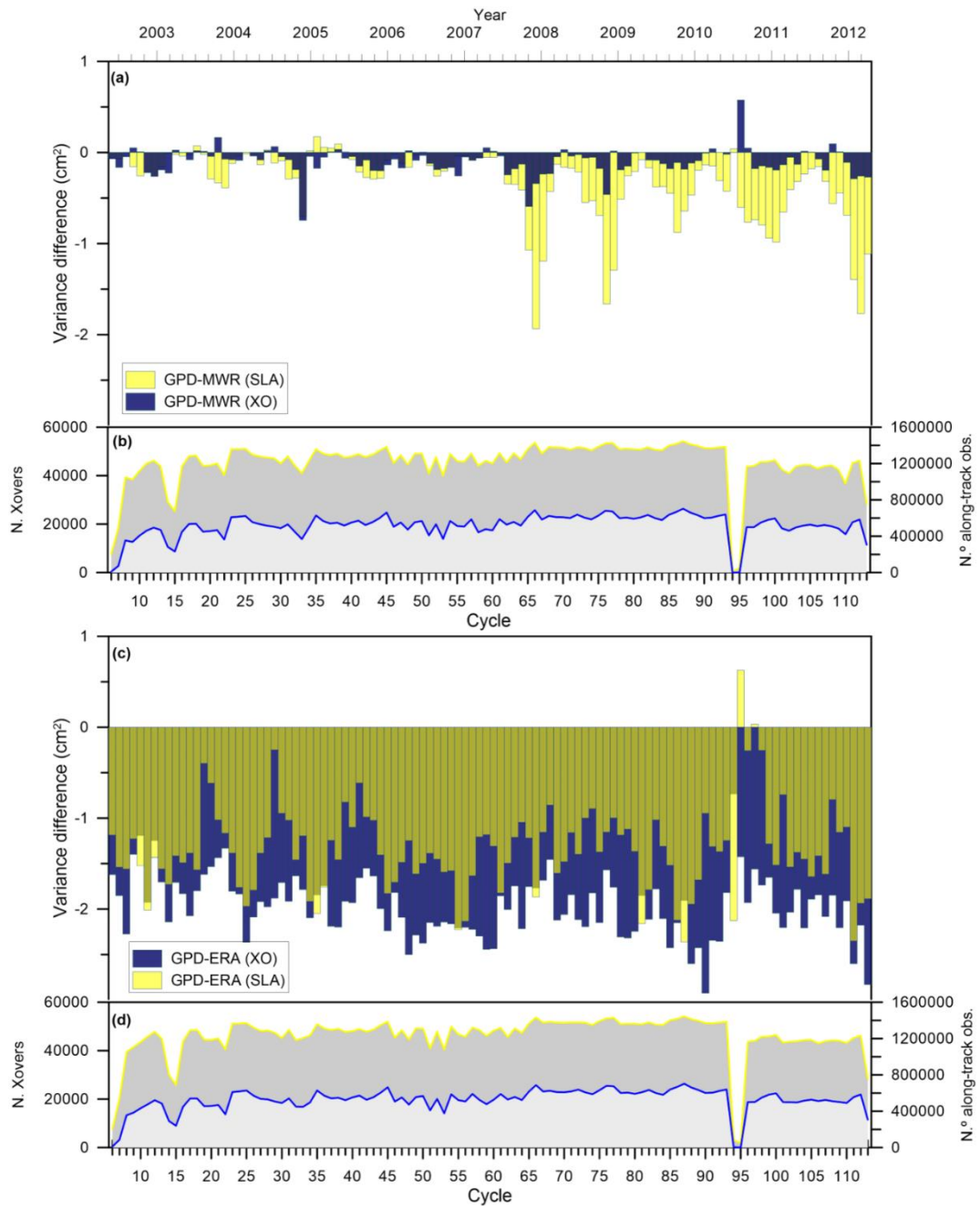


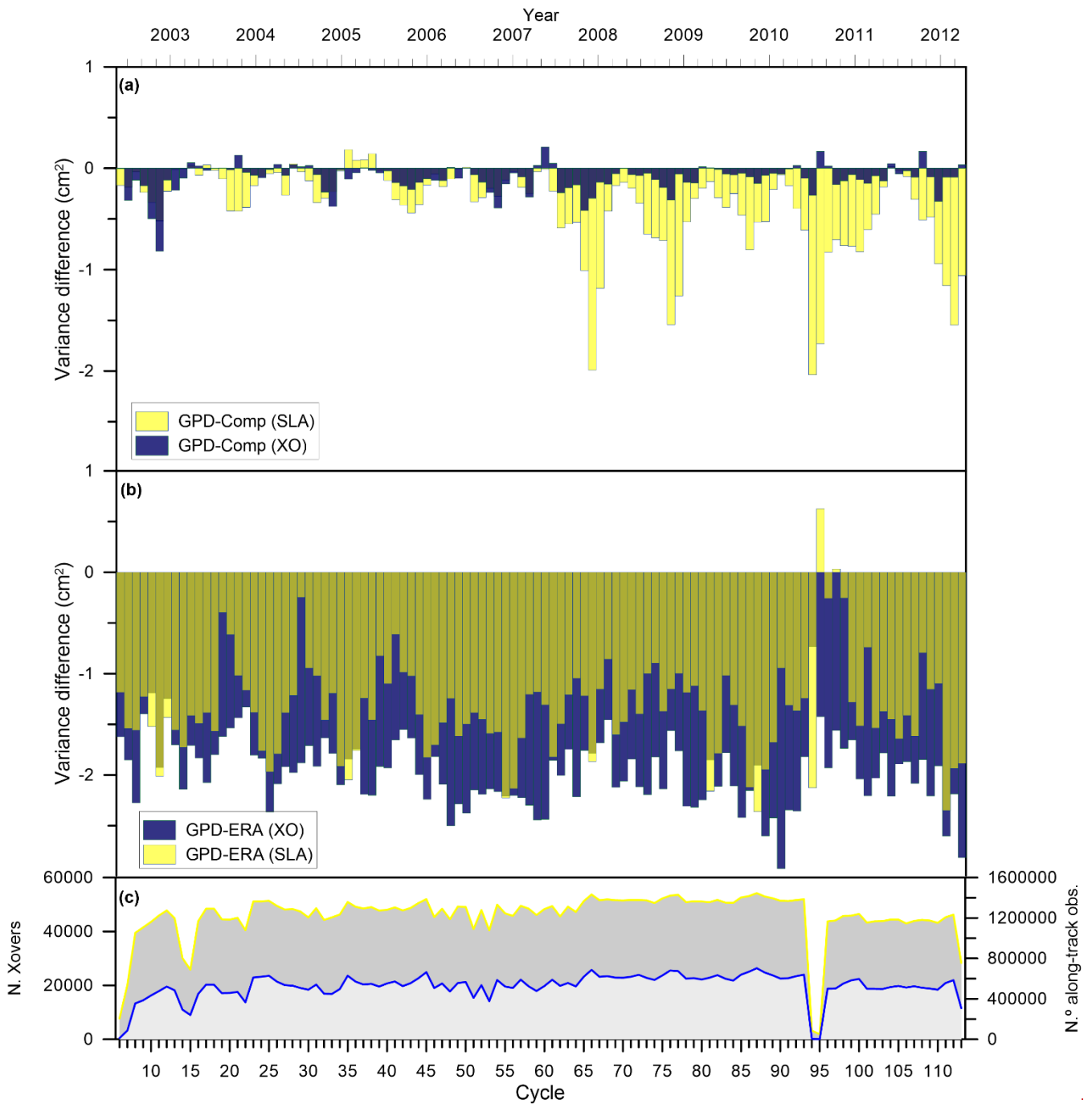
1085

Figure 7-10 RMS (in cm) of WTC differences (left axis) and number of altimetry measurements used (right axis) for the Envisat mission, function of distance from coast. Red bars represent the number of measurements used to compute the RMS of the differences GNSS-MWR, while grey bars represent the number of points used to compute the RMS of the differences GNSS-GPD+. In the comparison GNSS – MWR only valid MWR-derived observations have been used.

1090

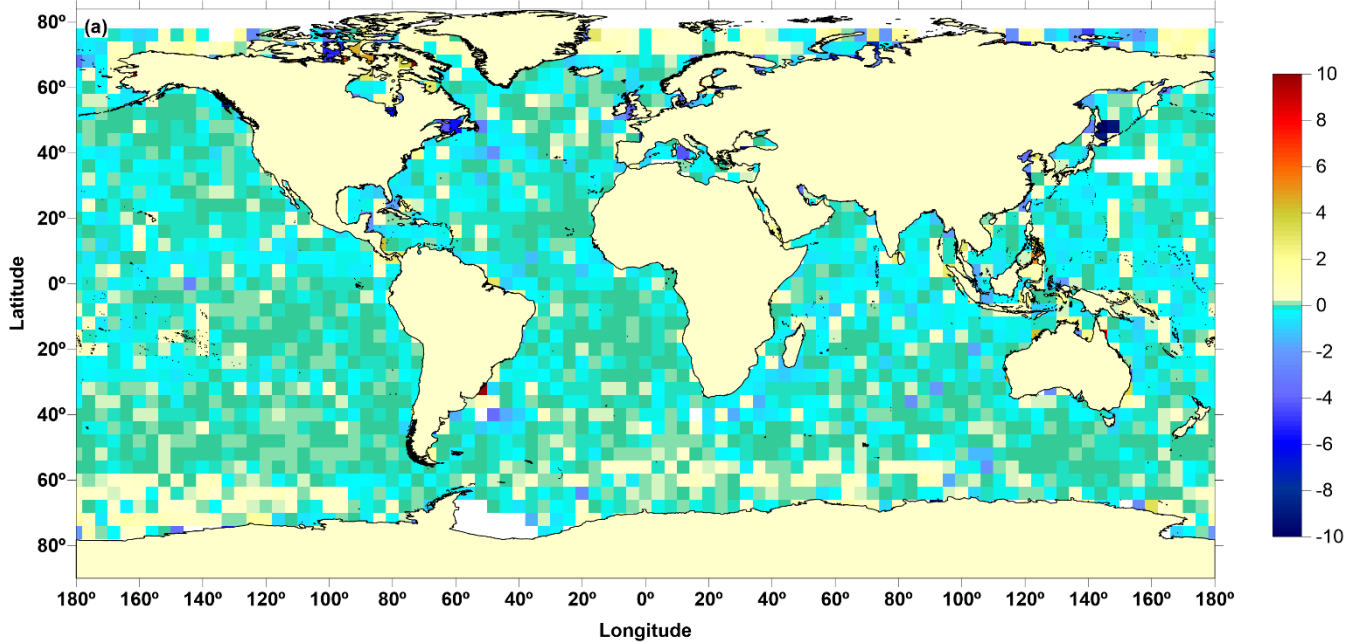
1095



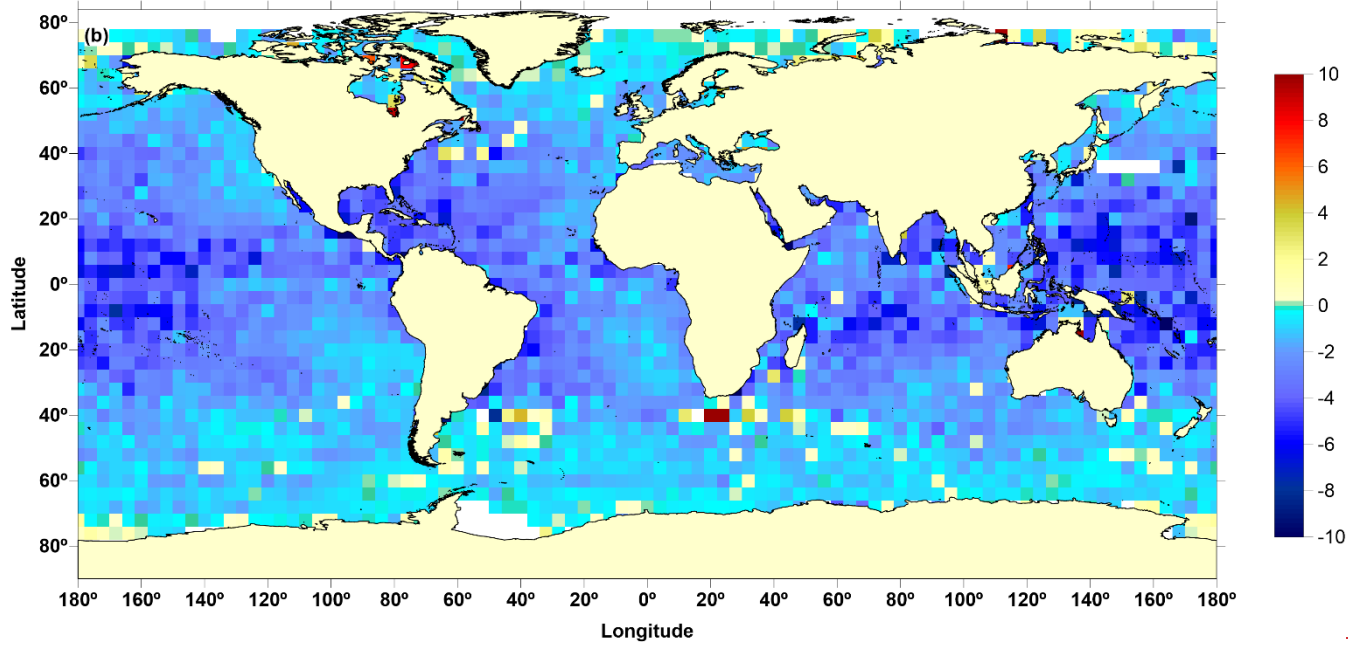


1105 **Figure 8-11** Temporal evolution of weighted SLA variance differences (cm^2) along satellite tracks (yellow) and at crossovers (blue) between (a) GPD+ and the CompositeMWR-derived WTCs and (b) between GPD+ and ERA Interim WTCs. Bottom plots (b) and (c) shows the number of crossovers (“N. Xovers”, blue) and the number of along-track (yellow) pairs used, per cycle, in the GPD-MWR and GPD-ERA analyses, respectively. To facilitate the analysis, both cycle number (bottom x-axis) and time (year, top x-axis) are used.

Variance difference at XO: GPD-COMP



Variance difference at XO: GPD-ERA



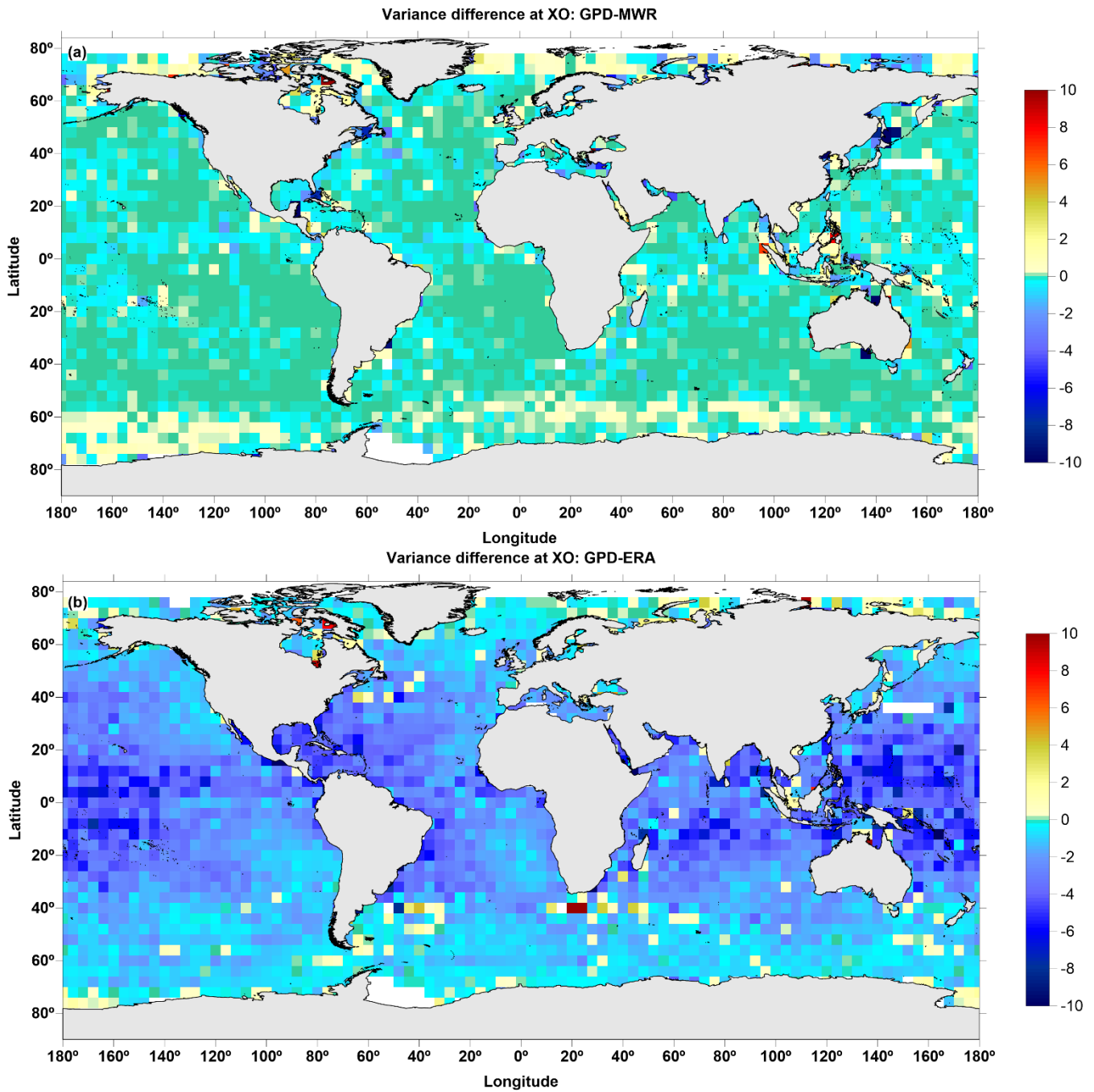
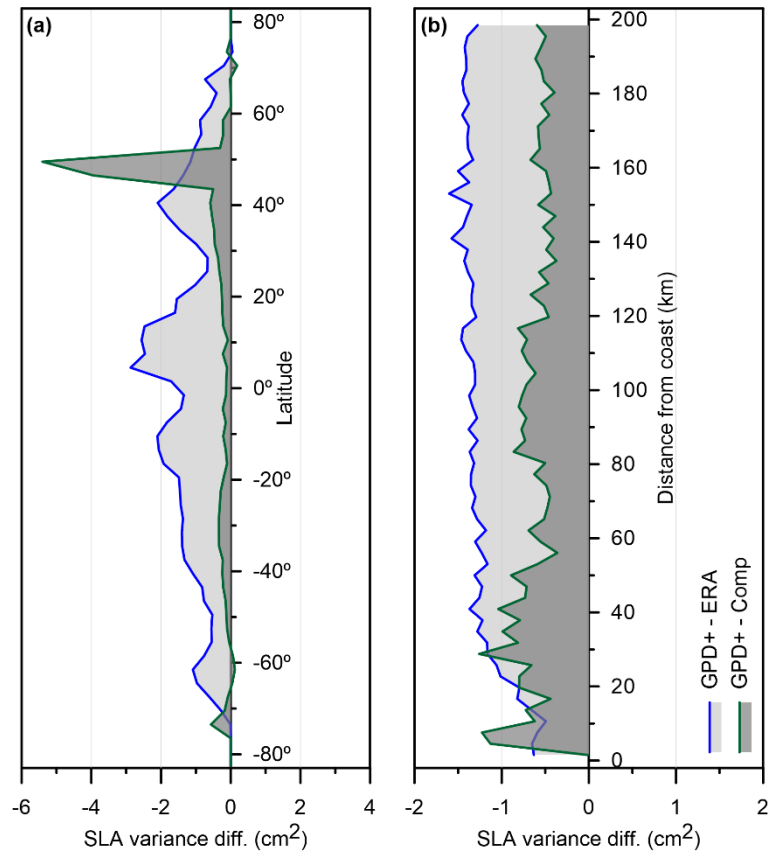
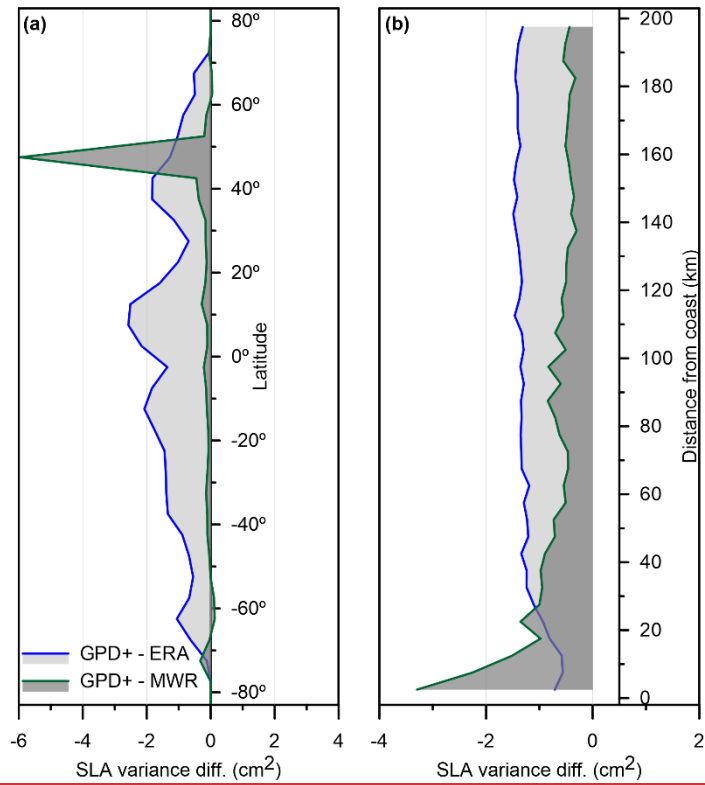


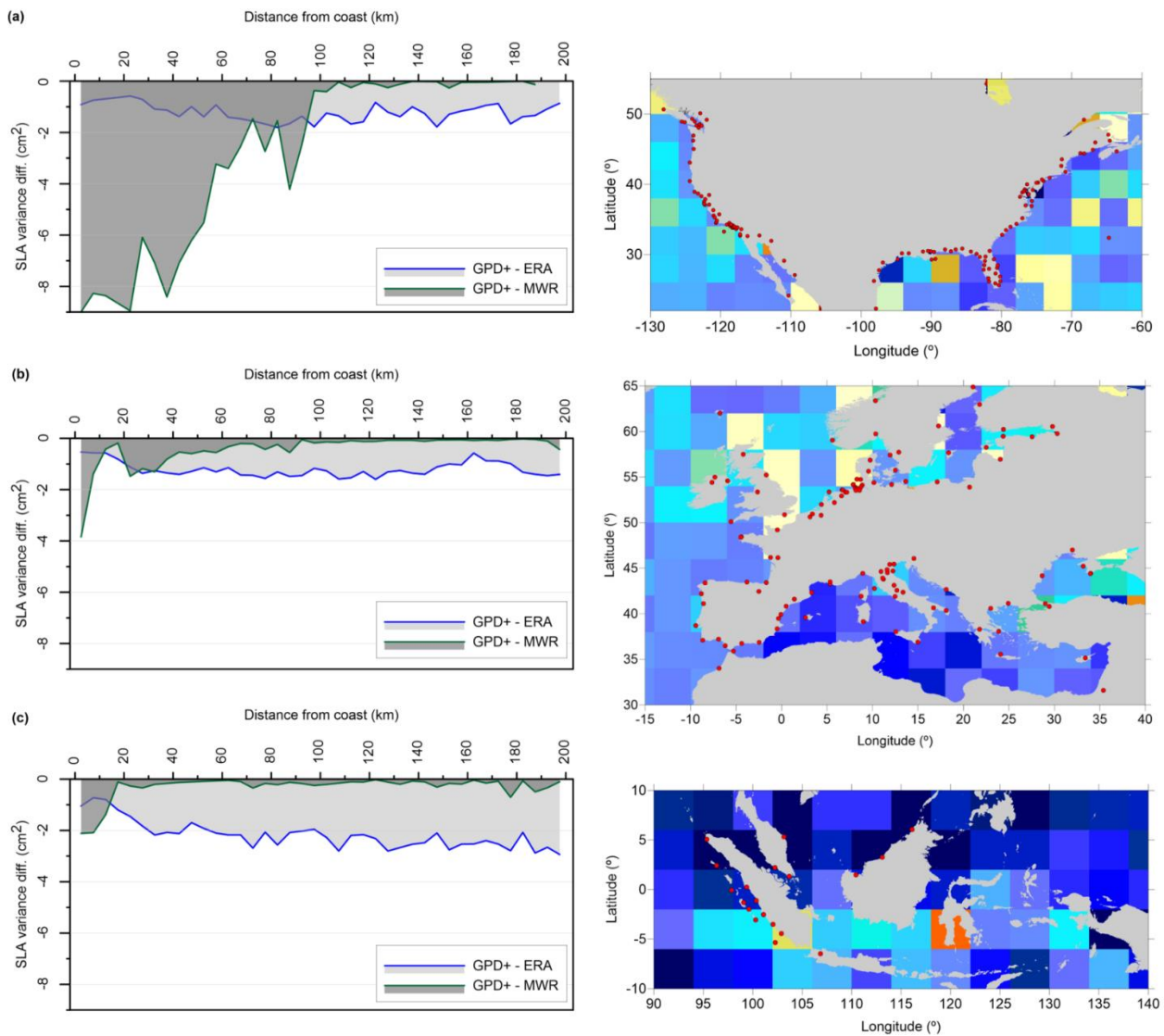
Figure 9-12 Spatial distribution of the weighted SLA variance differences (in cm^2) at crossovers (XO) between (a) GPD+ and the Composite-MWR-derived WTCs and (b) GPD+ and the ERA Interim WTCs for the whole Envisat period (cycles 006 to 113). The green colour represents SLA variance differences around zero. Pixels with no data are shown in white.

115





120 **Figure 10-13** Variance differences (cm²) of SLA versus latitude (a) and distance from coast (b) between GPD+ and ERA Interim WTCs (blue) and GPD+ and the Composite-MWR-derived WTCs (green) for Envisat cycles 006 to 113.



125 **Figure 14** Variance differences (cm^2) of SLA function of distance from coast (left) between GPD+ and ERA Interim WTCs (blue) and GPD+ and MWR-derived WTCs (green) for the whole Envisat period (cycles 006 to 113) for North American coast (a), European coast (b) and Indonesia region (c). In the plot for the North American coast, the y-axis has been clipped to -9 cm^2 (minimum value is around -13 cm^2). Right panels show the spatial distribution of the weighted SLA variance differences (in cm^2), computed along the satellite tracks, between GPD+ and ERA Interim WTCs. The green colour represents SLA variance differences around zero. The GNSS stations used in the computation of the GPD+ WTC are represented as red dots.

130